University of Alberta

Functional Characterization of Variants of the Copper Transporter, ATP7B

by

Taha Mohammad Maan Deeb

A thesis submitted to the Faculty of Graduate Studies and Research
in partial fulfillment of the requirements for the degree of

Master of Science

in

Medical Sciences-Medical Genetics

Edmonton, Alberta

Fall 2008

Library and Archives Canada

Published Heritage Branch

395 Wellington Street
Ottawa ON K1A 0N4
Canada

Bibliothèque et Archives Canada

Direction du Patrimoine de l'édition

395, rue Wellington
Ottawa ON K1A 0N4
Canada

Your file Votre référence
ISBN: 978-0-494-47200-2
Our file Notre référence
ISBN: 978-0-494-47200-2

NOTICE:
The author has granted a non-exclusive license allowing Library and Archives Canada to reproduce, publish, archive, preserve, conserve, communicate to the public by telecommunication or on the Internet, loan, distribute and sell theses worldwide, for commercial or non-commercial purposes, in microform, paper, electronic and/or any other formats.

The author retains copyright ownership and moral rights in this thesis. Neither the thesis nor substantial extracts from it may be printed or otherwise reproduced without the author's permission.

AVIS:
L'auteur a accordé une licence non exclusive permettant à la Bibliothèque et Archives Canada de reproduire, publier, archiver, sauvegarder, conserver, transmettre au public par télécommunication ou par l'Internet, prêter, distribuer et vendre des thèses partout dans le monde, à des fins commerciales ou autres, sur support microforme, papier, électronique et/ou autres formats.

L'auteur conserve la propriété du droit d'auteur et des droits moraux qui protège cette thèse. Ni la thèse ni des extraits substantiels de celle-ci ne doivent être imprimés ou autrement reproduits sans son autorisation.

In compliance with the Canadian Privacy Act some supporting forms may have been removed from this thesis.

While these forms may be included in the document page count, their removal does not represent any loss of content from the thesis.

Conformément à la loi canadienne sur la protection de la vie privée, quelques formulaires secondaires ont été enlevés de cette thèse.

Bien que ces formulaires aient inclus dans la pagination, il n'y aura aucun contenu manquant.

Canada

ABSTRACT

ATP7B is a P-type ATPase required for copper homeostasis. In 1993, our laboratory discovered that defects in ATP7B cause Wilson disease (WND). Treatment of WND is effective, particularly when provided in the early stages of the disease. Mutation analysis is an important tool for reliable diagnosis of this clinically variable disease. Our laboratory has documented 518 ATP7B variants; (http://www.medicalgenetics.med.ualberta.ca/wilson/index.php) however, only 50 have been functionally characterized. Functional studies are important for discriminating between normal and disease causing variants.

In my studies, a yeast model was used to study 21 ATP7B variants. I developed a 96-well plate version of the Fet3p (orthologue of human ceruloplasmin) oxidase assay that is more sensitive and time-efficient. The ATP7B variants were further analyzed using computational programs developed to distinguish normal from disease causing variants. These programs (PolyPhen, SIFT, and Align GVGD) use amino acid conservation and biochemical properties. PolyPhen and SIFT are useful tools for developing a hierarchical plan for selecting variants to be analyzed in future functional assays.

ACKNOWLEDGEMENTS

This thesis owes its existence to the help, support, and inspiration of many people. In the first place, I would like to express my sincere appreciation and full gratitude to my supervisor Dr. Diane Cox. I am indebted to my supervisor for her constant encouragement and enthusiasm for scientific discovery. She allowed me to follow my own research path in order to become an independent and critical thinker.

I would like to thank the past and present members of the Cox Lab, who made the lab an enjoyable place to work. I am grateful for all that I have learned from every Cox lab member. I would especially like to thank Dr. Gina Macintyre for all her intellectual contributions, friendship and generous support. I also thank Susan Kenney from The Applied Genomics Centre (TAGC) for DNA sequence analysis.

I would like to address my full recognition to my committee Dr. Moira Glerum and Dr. Michael Walter for all their time, suggestions and scientific contributions. I would also like to thank everyone in the Department of Medical Genetics, many of whom have become good friends. Special thanks to Dr. Susan Andrew laboratory for using the 96-well plate reader.

I thank all of the patients and their families who provided samples for our studies.

I would like to thank my family, specially my wife Amany, for without her support, encouragement and confidence in my abilities, I would not have accomplished this goal. I owe special gratitude to my parents for continuous and unconditional support.

Finally, I would like to dedicate this thesis to the most wonderful gift I had in this life.

To my son Adam Taha Deeb

TABLE OF CONTENTS

CHAPTER 1: INTRODUCTION 1

1. Physiological Aspects of Copper 1
   1.1. Physiological Importance of Copper 1
   1.2. Copper Uptake 2
   1.3. Copper Homeostasis 3
   1.4. Copper Toxicity 4
2. Wilson Diseases 5
   2.1. Genetics 6
   2.2. Diagnosis 9
   2.3. Treatment 10
3. Copper Transporter, ATP7B 11
   3.1 ATP7B: a P1-ATPase 11
   3.2 Role of ATP7B Domains 12
      3.2.1 Role of N-terminal Metal Binding Domain 13
      3.2.2 Role of ATP7B Transmembrane Domain 16
      3.2.3 Role of ATP7B loop 17
      3.2.4 Role of C-terminal Region 18
   3.3 Transport Mechanism of ATP7B 19
4. ATP7B Functional Assays 20
   4.2 Yeast Complementation Assay 22
   4.1 Localization and Other ATP7B Assays 23
5. Genetic Variations and Prediction Programs 24

5.1 Amino Acid Properties 26
5.2 Protein Structure Properties 27
5.3 Evolutionary Properties 28
5.3.1 PolyPhen 28
5.3.2 SIFT 29
6. Aim of the Project 31
CHAPTER 2: FUNCTIONAL ASSESSMENT OF ATP7B VARIANTS 32
1. Introduction 31
2. Materials and Methods 32
2.1 Growth of Bacteria and Yeast 32
2.2 Construction of *ATP7B* cDNA Variants 33
2.3 Yeast Expression Vectors 36
3.4 Yeast Strain and Transformation 36
3.5 Southern Blotting 37
3.6 Yeast Complementation Assay 40
3.7 Fet3p Oxidase Assay 41
3.8 Western Blotting 42
3.9 ATP7B Modeling Analysis 43
3. Results 44
3.1 Construction of ATP7B Variants 47
3.2 Yeast Growth Assay 47
3.3 Fet3p Oxidase Assay 47
3.4 ATP7B Modeling Analysis 48
4. Discussion 67
CHAPTER 3: COMPUTATIONAL ANALYSIS OF ATP7B MISSENSE VARIANTS 73
1. Introductions 72
2. Materials and Methods 73
2.1. Prediction Programs Used 73

2.1.1. PolyPhen 73
2.1.2. SIFT 74
2.1.3. Align GVGD 74
2.2. Functional Data Used 75
3. Results78
3.1-Comparing prediction scores using defective ATP7B missense variants 78
3.2 Analysis of prediction scores of functionally normal ATP7B variants 79
3.3 Analysis of suspected non disease causing variants in PolyPhen, SIFT, and Align GVGD 84
4. Discussion 87
CHAPTER 4: CONCLUSIONS AND FUTURE DIRECTIONS 92

LIST OF TABLES

Table 2.1: List of ATP7B mutagenic primers 35
Table 2.2: Functional characterization of ATP7B single copy variants 56
Table 2.3: Functional characterization of ATP7B multiple and unknown copy number variants 57
Table 2.4: Summary of functional characterization of selected ATP7B variants 65
Table 2.5: Analysis of the biochemical changes of ATP7B missense variants studied in yeast transport assay 66
Table 3.1: List of proteins used for the multiple sequence alignment in the selected prediction programs 77
Table3.2: Comparison of prediction programs using functionally defective ATP7B variants 80
Table 3.3: Summary of functionally defective ATP7B variants analyzed in the selected prediction programs 82
Table 3.4: Prediction scores of ATP7B variants that are indicated as normal variants in functional assays 83
Table 3.5: Analysis of suspected non disease causing variants in PolyPhen, SIFT and Align GVGD 85
Table 3.6: Summary of the prediction scores of 29 suspected non-disease causing ATP7B variants 86

LIST OF FIGURES

Figure 1.1: Copper distribution in the body 5
Figure 2.1: *ATP7B* integration into the yeast genome 39
Figure 2.2: ATP7B model showing variants analyzed in this thesis 45
Figure 2.3: Southern blot analysis of selected ATP7B variants for information using radioactive and DIG-labeled probe. 47
Figure 2.4: Yeast growth assay 50, 51, 52
Figure 2.5: Oxidase activity of ATP7B control variants 53
Figure 2.6: Oxidase assay of ATP7B variants 54, 55
Figure 2.7: Analysis of R616Q and A604P using Chimera software 58
Figure 2.8: Western blot analysis and band analysis of ATP7B variants using MemPrep Kit 59
Figure 2.9: Western blot analysis of ATP7B variants using MemPrep Kit 60
Figure 2.10: Western blot analysis of hydrophilic and hydrophobic membrane fractions using MempKit for information on cross reactive component 61
Figure 2.11: Western blot analysis of selected ATP7B variants using modified protocol for protein extraction 62
Figure 2.12: Western blot analysis of selected ATP7B variants using modified protocol for protein extraction 63
Figure 2.13: Western blot analysis of selected ATP7B variants using modified protocol for protein extraction 64

LIST OF SYMBOLS AND ABBREVIATIONS.

-Cu	low copper media
+Cu	high copper media
3D	3-dimensional
BCS	bathocuproine disulfonic acid
bp	base pair
CCS	copper chaperone for superoxide dismutase
cDNA	complementary DNA
Cp	ceruloplasmin
C-terminal	carboxy-terminal
Cu	copper
CuBD	copper-binding domain
Cu/Zn-SOD1	copper/zinc-superoxidase dismutase
Cys	cysteine
DNA	deoxyribonucleic acid
DTT	dithiothreitol
ECL	enhanced chemiluminescence
ER	endoplasmic reticulum
Fe	iron
H-bond	hydrogen-bond
hrs	hours
kb	kilo base
kDa	kilo Dalton
KF ring	Kayser-Fleischer ring
LB	Luria Bertani
MBS	metal-binding site
MNK	Menkes disease
mRNA	messenger RNA
MT	metallothionein
Multi-copy	multiple copy
N-ATP7B	N-terminal domain of ATP7B
NCBI	National Center for Biotechnology Information
N-terminal	amino-terminal
PAGE	polyacrylamide gel electrophoresis
PCR	polymerase chain reaction
PM	plasma membrane
pPD	p-phenylenediamine dihydrochloride substrate
RNA	ribonucleic acid
ROS	reactive oxygen species
rpm	rotations per minute
RT-PCR	reverse transcriptase PCR

S. cerevisiae	*Saccharomyces cerevisiae*
SD medium	synthetic dextrose medium
SDS	sodium dodecyl sulphate
SSC	standard sodium citrate
TBS	Tris-buffered saline
TGN	*trans*-Golgi network
TM	transmembrane
WND	Wilson disease
Zn	zinc

CHAPTER 1

INTRODUCTION

1. Physiological Aspects of Copper

1.1. Physiological Importance of Copper

Copper is a vital trace element for all living organisms. It is required for essential physiological activities including: free radical detoxification, cellular respiration, neurotransmitter biosynthesis, iron transport, and others. Copper is an indispensable cofactor for several enzymes including: dopamine-β-hydroxylase, tyrosinase, lysyl oxidase, peptidylglycine-α -amidating monooxygenase, superoxide dismutase, cytochrome c-oxidase, and ceruloplasmin. The physiological importance of copper is reflected by the deleterious consequences obtained when copper transporters have impaired function. Menkes disease (OMIM 309400) is a fatal childhood disorder caused by mutations in *ATP7A* (Vulpe et al., 1993a; Kaler, 1998). *ATP7A* is a gene that encodes a Cu-ATPase expressed in several tissues, mainly the intestine. ATP7A inactivation causes copper deficiency due to disrupted delivery of copper from the intestine. Patients with Menkes disease suffer from developmental and neurological impairment as well as other symptoms including: connective tissue abnormalities, loss of pigmentation, and tortuosity of blood vessels (Kaler, 1998; Tumer and Horn, 1998; Kodama and Murata, 1999; Kodama et al., 1999).

Inactivation of another copper transporter, ATP7B, leads to Wilson disease (WND) (Bull et al., 1993). ATP7B is a homologue of ATP7A that is involved in the secretory pathway of copper transport. Wilson disease patients suffer from copper

accumulation in the liver, brain, and other tissues. These two diseases demonstrate that copper homeostasis is tightly controlled in living organisms. Copper accumulation (WND) and copper deficiency (Menkes disease) are associated with deleterious consequences (Gitlin, 2003; Ferenci, 2005).

1.2. Copper Uptake

The average daily intake of copper is around 2 mg. Most of this copper is absorbed in the small intestine, mainly the duodenum. The apical parts of the intestinal cells contain a copper transporter that is thought to import copper from the lumen of the intestine into the cytoplasm of the enterocyte. Studies using mice have shown that the high affinity copper transporter, Ctr1, is located on the apical part of the intestinal cells during the suckling period (Kuo et al., 2006). Adult mice had their Ctr1 localized to other cytoplasmic compartments within the endothelial cells. Therefore, Ctr1 is involved in copper transport and possibly copper regulation. Inactivation of Ctr1 in mice blocks copper absorption into the blood and results in copper deficiency in various tissues. However, this inactivation does not prevent copper from accumulating in the intestinal cells. These observations suggest that other mechanisms are involved in the apical uptake of copper (Nose et al., 2006). DMT1 (divalent metal transporter 1) is a candidate protein for the intestinal uptake of copper. Studies have shown that dietary iron is absorbed by the intestinal cells through DMT1 (Anderson and Frazer, 2005). Knocking down expression of DMT1 in cultured cells decreased copper uptake by these cells (Arnesano et al., 2002). However, the role of DMT1 on copper transport in tissues has not been examined. Another candidate for the copper uptake into the enterocytes could

be the ATP-driven copper transport system detected in the brush-border of the intestine (Knopfel et al., 2005). The nature of this system is still under investigation. Copper could be imported into the intestinal cells by pinocytosis. Mann et al postulated that suckling mice could absorb their dietary copper through pinocytosis at the distal part of the small intestine (Mann et al., 1979).

Copper absorbed by the intestine is delivered to the various organs through the blood. This process involves exporting of copper from the enterocytes to the blood vessels. Copper enters the enterocytes, then is carried by chaperones to the specific intracellular destinations. ATOX1, antioxidant protein 1, is a copper chaperone required for the excretion pathway (Hamza et al., 2003). Copper is exported from the enterocytes into the blood by ATP7A in a process that involves trafficking of the transporter towards the baso-lateral membrane (Petris et al., 1996; Monty et al., 2005).

1.3. Copper Homeostasis

The liver plays a central role in copper homeostasis. It is responsible for the export of excess copper out of the body. The export of copper from the liver is mediated by the copper-transporting ATPase, ATP7B.

Copper enters hepatocytes through the high affinity copper transporter CTR1, as noted above. In the cytosol, copper binds to specific chaperones that direct it to various intracellular destinations. Copper chaperone of superoxide dismutase (CCS) delivers copper to superoxide dismutase (SOD1) that is involved in free radical detoxification (Culotta et al., 1997). The second copper destination involves cytochrome-c oxidase (COX). Several proteins, including COX17, have been reported to be involved in copper

delivery to the mitochondria (Punter and Glerum, 2003; Prohaska and Gybina, 2004). The third important destination of copper is the secretory pathway. ATOX1 delivers copper to ATP7B, a Cu-ATPase that is localized to the trans-Golgi network (TGN) (Hamza et al., 2003). ATP7B then transports copper to the lumen of the Golgi network. In the lumen, copper is incorporated into ceruloplasmin (CP) which is a copper dependent ferroxidase. CP is then secreted into the blood. Although CP carries more than 90% of copper in the plasma it does not seem to play an essential role in copper transport (Meyer et al., 2001). CP is involved in various functions including: oxidation of organic amines, iron(II) oxidation and the regulation of cellular iron levels, free radical scavenging and other antioxidant processes (Healy and Tipton, 2007).

Excess copper in the liver is excreted into the bile. In the hepatocyte, ATP7B traffics from the TGN to cytoplasmic vesicles in response to high copper concentrations in the cytoplasm (Forbes and Cox, 2000). These vesicles, containing excess copper, fuse with the bile canaliculi membrane releasing copper to the bile ducts (Hamza et al., 1999). The excess copper is then eliminated from the body through feces.

1.4. Copper Toxicity

Copper is a transition metal that is able to release or accept an electron easily. Copper in the intestinal lumen and blood is thought to be in its oxidized form (Knopfel and Solioz, 2002). However, within the cell it is in the reduced Cu (I) form. Copper is considered a potential potent cytotoxin when allowed to accumulate in excess inside the cell. Copper can react with poorly reactive oxygen species (ROS) to produce highly reactive radicals. ROS are involved in various diseases including cancer,

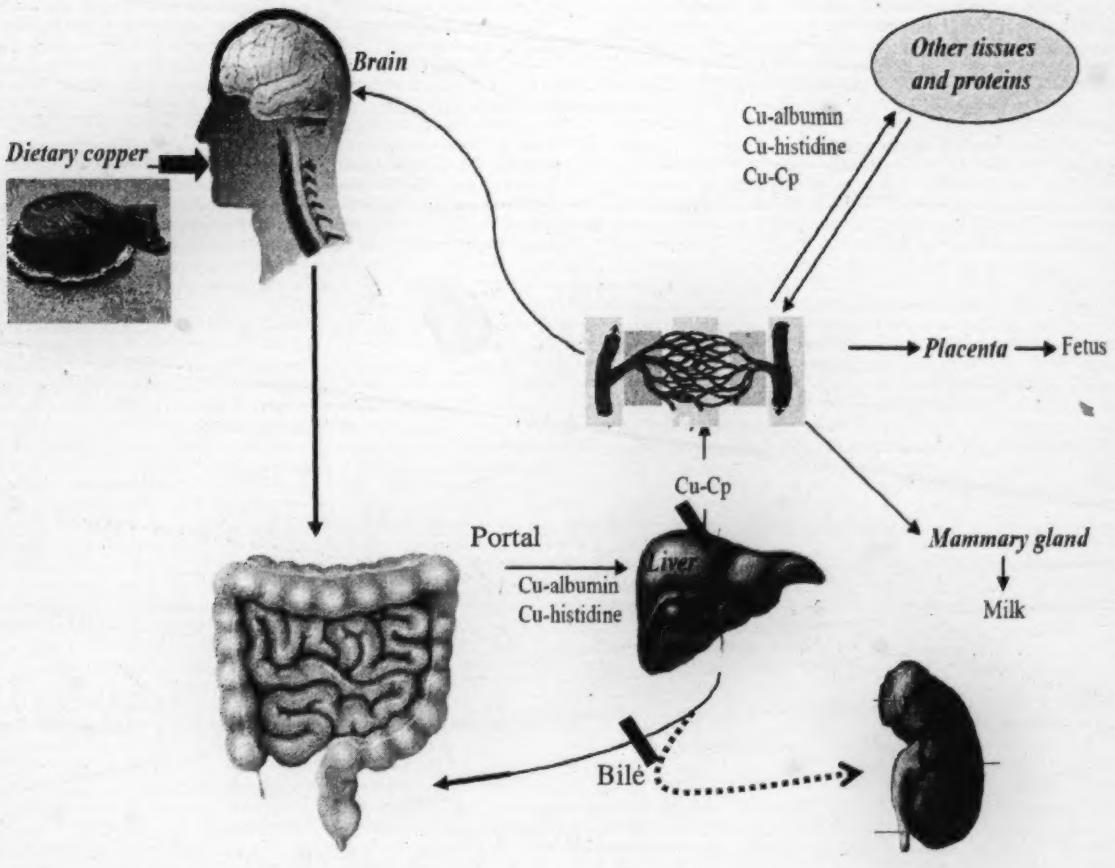

Adapted from Mercer, Nature Genetics 2003

Figure 1.1 Copper distribution in the body.

neurodegeneration, and aging (Halliwell and Gutteridge, 1990). Studies have shown that trace amounts of Copper can catalyze the generation of hydroxyl radicals from hydrogen peroxide via the Fenton reaction; reviewed in (Halliwell and Gutteridge, 1984; Tapiero et al., 2003). Hydroxyl radicals are toxic free radicals involved in peroxidation of lipid membranes, cleavage of DNA and RNA molecules, and oxidation of proteins; reviewed in (Halliwell and Gutteridge, 1990; Pena et al., 1999). Furthermore, copper can replace other metal cofactors. Thus, it can potentially disturb a wide range of biological activities.

2. Wilson Disease

Wilson Disease (WND) is a hereditary liver disorder with neurological manifestations as first described by Kinnear Wilson (Wilson, 1912). It is an autosomal recessive disorder with an incidence of 1 in 30,000 worldwide. In 1948, the etiology of the disease was identified. Tissues from patients with WND were found to be overloaded with copper reviewed in (Brewer and Yuzbasiyan-Gurkan, 1992). WND presents with various symptoms. Although the hepatic form is the most common phenotype of the disease (Kitzberger et al., 2005), other manifestations such as progressive neurological disorder and psychiatric illness are also common (Roberts and Cox, 2006). These symptoms could appear at any time between 3 and 65 years.

Liver disease is the most common presentation of patients with WND. It involves acute, sub acute, as well as chronic liver conditions. In most case, WND patients develop hepatic injury that gradually progresses into cirrhosis if left untreated (Scheinberg and Sternlieb, 1984). Hemolytic anemia is rarely associated with WND

(Roberts and Schilsky, 2003). Neurological presentation is characterized by Parkinsonian disturbances and movement disorders as well as rigid dystonia. The most common symptoms recognized are speech defects, hand tremors and gait disturbances; reviewed in (Roberts and Cox, 2006). A hallmark of the disorder is the Kayser-Fleischer (KF) ring, formed from deposition of copper in the Descemet membrane of the cornea. KF ring is the most common ocular presentation of WND patients. It is found in 90-95% of patients with neurological symptoms (Steindl et al., 1998). Psychiatric symptoms range from behavioral abnormalities and personality changes to psychosis. Wilson disease patients presented with psychiatric features are usually misdiagnosed in the first stages of the diseases.

WND also has specific biochemical signs. Copper in serum is bound to albumin and can be transferred into tissues. Most WND patients have reduced levels of serum CP (Scheinberg and Gitlin, 1952). However, non-CP serum copper is elevated. The effect of decreased holo-CP in the serum was shown to have minor importance on copper homeostasis, but affects the transport of iron (Shim and Harris, 2003). Livers of WND patients are usually overloaded with copper, as biliary Cu excretion is impaired. In the liver, copper is incorporated into the CP. Excess copper remains in the liver and leads to serious liver injury. Excess copper in plasma leads to accumulation in other tissues, especially kidney and brain. Excess plasma copper is eliminated through urine, and urinary copper is increased in most patients.

2.1. Genetics

The gene causing WND, *ATP7B*, was identified in 1993 by two independent groups (Bull et al., 1993; Tanzi et al., 1993). *ATP7B* is located on chromosome 13q14.3 (Bowcock et al., 1987; Bowcock et al., 1988; Yuzbasiyan-Gurkan et al., 1988), spans 80 kb of genomic DNA, and includes 21 exons. ATP7B is expressed mainly in the liver, kidney, and slightly in the placenta, heart, brain, lungs, muscles, and pancreas (Bull et al., 1993). An alternative splice variant of ATP7B was identified in brain tissues. The alternative splice variant was missing exons 5 and 11 (Tanzi et al., 1993). Further analysis identified another brain splice variant that lacks a combination of exons including: exon 17; exon 13; exon 6, 7, and 8; and exon 12. These variants were also detected in kidney and placenta (Petrukhin et al., 1994). In 1998, an interesting ATP7B alternative splicing variant was identified in the pineal gland. This variant lacks exons 1, 2, 3, 4, 5, 6, and 7 and uses a promoter in intron 8 to produce a 665 amino acid polypeptide designated as pineal night-specific ATPase (PINA) (Li et al., 1998). Although PINA loses the N-terminal metal binding domain and the first four transmembrane domains it was reported to limit restoration of transport activity in yeast (Borjigin et al., 1999). Further studies to explore the function of PINA are required to confirm these observation

Mutational analyses of WND patients and their relatives have identified more than 518 distinctive variants as reported in the WND mutation database (http://www.medicalgenetics.med.ualberta.ca/wilson/index.php). Most of these variants are probable disease-causing variants (379 out of 518 variants). The remaining variants are reported as possible normal variants. The molecular analysis of ATP7B in affected individuals has shown that most patients are compound heterozygtes (Figus et al., 1995;

Thomas et al., 1995; Loudianos et al., 1996; Loudianos et al., 1998; Loudianos et al., 1999b). There are only a few mutations occurring at a high frequency in a given population. For example, p.H1069Q, the most common mutation in WND patients of European origin, is found in 70% of WND Polish patients (Czlonkowska et al., 1997), and 60% of the Austrian population (Maier-Dobersberger et al., 1997). On the other hand, R778L is the most common WND mutation detected in Asian populations, accounting for 37.9% of mutations in Korean patients (Kim et al., 1998) and 45.6% in Han Chinese WND patients (Liu et al., 2004).

Phenotypic variation and mutational analysis have raised questions on the genotype-phenotype correlations in WND patients. The wide range of phenotypes presented by WND patients is an integration of several factors, both including genetic and environmental. However, there are few phenotypes that can be explained as a consequence of a specific mutation only. For example, mutations that are known to cause abolition of ATP7B function are usually associated with hepatic disease, and the age of onset can be as early as 3 years. On the other hand, patients with less severe mutations have an age of onset around 15 years and they mainly present with neurological abnormalities (Thomas et al., 1995; Wu et al., 2001). Studies have shown that p.H1069Q, the common Caucasian mutation, causes WND that presents with neurological symptoms and a later age of onset (Figus et al., 1995; Czlonkowska et al., 1997; Shah et al., 1997a; Sham et al., 1997; Stapelbroek et al., 2004). However, most of the mutations identified in ATP7B fail to explain the variable age of onset, clinical presentation, and other biochemical features observed in WND patients. The marked phenotypic variations observed between related WND patients suggest that additional

genetic and environmental factors contribute to the course of the disease (Riordan and Williams, 2001; Panagiotakaki et al., 2004).

2.2. Diagnosis

Wilson disease is a highly variable disorder in its clinical presentation. There is no specific combination of clinical and biochemical features that is definitive of Wilson disease in all patients. Therefore, diagnosing WND is often difficult and some times delayed. The major clinical symptoms used in diagnosing WND are KF rings and low serum CP. However, KF rings are not found in all WND patients especially those with hepatic presentations (Gow et al., 2000). Low serum Cp is another hallmark of WND. The challenge with CP is that it is elevated as a response to inflammation and high estrogen levels in the blood making it an unsuitable sole tool to diagnose WND (Steindl et al., 1997; Ferenci, 2004). More than 15% of WND patients have a normal range of serum CP (Cauza et al., 1997; Steindl et al., 1997; Yuce et al., 1999). Urinary copper can assist in the diagnosis of WND. Affected individuals tend to have elevated urinary copper. However, urinary copper might be increased as a consequence of other liver injuries including extensive hepato-cellular necrosis. On the other hand, some WND patients have normal urinary Cu excretion in the early stages (Gow et al., 2000; Ferenci et al., 2003). Hepatic copper is a sign for the diagnosis of WND. Hepatic biopsy is used to quantify the hepatic copper content, which is a useful diagnostic tool as well as for assessing the degree and type of histological injury. Normal hepatic copper usually excludes the diagnosis of WND except in presymptomatic relatives of patients. In contrast, neither KF rings nor elevated liver copper is individually sufficient to confirm

the diagnosis of WND, because either of these parameters occur in any disorder with impaired biliary excretion (Gollan and Gollan, 1998; Schilsky, 2002).

2.3. Treatment

The treatment of WND focuses on reestablishing copper homeostasis and preventing copper from accumulating in certain tissues. According to the American Association for the Study of Liver Diseases (AASLD) practice guidelines, the treatment of symptomatic WND patients should include copper chelation mainly with D-penicillamine (Walshe, 1956). WND patients are effectively treated with copper chelator agents if early diagnosis is confirmed (Schilsky, 2002; Roberts and Schilsky, 2003). The copper chelators remove excess copper from the blood, and to a lesser extent from liver. Some chelators might have other effects such as: induce metallothioneins in tissues and/or interfere with copper absorption (Roberts and Cox, 1998; Fatemi and Sarkar, 2002). Trientine is an alternative copper chelator that has similar effectiveness. These medications are sometimes accompanied by sideroblastic anemia and bone marrow suppression. Thus, WND patients are monitored consistently during treatment (Walshe, 1982; Brewer et al., 2003; Roberts and Cox, 2006).

Zinc acetate (Zn treatment) is a safe and effective treatment for a long-term maintenance. Zn inhibits copper absorption from the gastrointestinal tract. Zn induces metallothioneins in enterocytes. These metallothioneins have a great affinity for copper and sequester it inside the intestinal cells. The endothelial cells are sloughed off as a part of the normal regeneration of the intestine and copper will be excreted with fecal materials (Brewer et al., 1998). Zn treatment is recommended for WND patients that

have already maintained the normal copper level through chelation treatment (Schilsky, 2002).

WND patients could develop advanced liver failure with decompensated cirrhosis as a consequence of delayed diagnosis, poor compliance with treatment, and or rapid, fulminant hepatitis. Death is almost certain without hepatic transplantation in such patients. Studies have shown that liver transplantation restores copper to the normal levels in a period of 6 months (Schumacher et al., 1997). Recurrence of Cu-associated liver damage has not been reported in WND patients (Langner and Denk, 2004). However, reliable and early diagnosis can avoid this extreme treatment.

3. Copper transporter, ATP7B

3.1. ATP7B: a P_1-ATPase

ATPases are enzymes that catalyze the conversion of adenosine tri-phosphate (ATP) into adenosine di-phosphate (ADP) and inorganic phosphorous (P_i), releasing energy. The energy is used to drive essential cellular processes. Some of the ATPase enzymes are integrated into the membranes and are involved in the transport of various metabolites across the membrane. P-type ATPase is one of the three major classes of ion transporting ATPases. This class is characterized by the formation of a phosphorylated intermediate as part of the transport cycle. P-type ATPases include most of the membrane ion transporters, for example sodium potassium pump, sarco-endoplasmic reticulum Ca^{++} ATPase, as well as other cation pumps. The other two classes of ion transporting ATPase are more related to each other. F-type ATPases are characterized by a multi subunit structure and the lack of a phosphorylated intermediate. Members of

this class are located in the inner membrane of mitochondria and chloroplast. V-type ATPase is the vacuolar ATPase that uses energy released from ATP hydrolysis to pump protons across the membrane of vacuoles, lysosomes and other cellular organelles. V-type ATPases lacks the phosphorylated intermediate and are involved in the pH homeostasis and acidification of certain organelles.

The P-type ATPases contain the four amino acid motif (DKTG) next to the aspartate residue. This aspartate is phosphorylated during the reaction cycle. Members of the P- type ATPases are classified into subfamilies. ATP7B is a P type ATPase that utilizes ATP to transport copper through the membrane. ATP7B shares common features with other P type ATPases such as: ATP7A (Menkes protein) (Chelly et al., 1993; Mercer et al., 1993; Vulpe et al., 1993b), CopA (bacterial copper transporter) (Rensing et al., 2000), ZntA (bacterial zinc transporter) (Rensing et al., 1997). These proteins form type 1 P-ATPases (P_1-ATPase). This subfamily is distinguished from other P- ATPases for having common features including: eight transmembrane domains instead of six, N-terminal cytoplasmic metal binding domain, and a Cys-Pro-Cys (CPC) motif in the transmembrane six domains.

3.2. Role of ATP7B Domains

ATP7B is a large integral membrane protein with eight transmembrane domains forming the transporter channel. ATP7B translocates copper from the cytosol across the cellular membranes using energy liberated from ATP hydrolysis. ATP7B binds copper from the cytosol, delivers it to the transmembrane portion of the transporter, and then releases it at the other side of the membrane. This whole process requires distinct

functional properties that are reflected in the architecture of the protein. The major bulk of ATP7B, including its key domains, is located in the cytoplasm. Several key functional domains can be identified in the structure of ATP7B including: N-terminal metal binding domains (MBD), transmembrane domains (Tm), ATP-binding (ABD) and phosphorylation domains (Ph), and C-terminal domains (C-ter).

3.2.1. Role of N-terminal Metal Binding Domain (MBD)

The N terminal part of ATP7B is a large cytosolic portion of the protein that contains more than 600 residues. It includes six repetitive sequences; each containing the conserved motif GMT/HCXXC. Each of the sequences folds into an individual metal binding domain (MBD) that binds one copper ion in its reduced Cu (I) form. The six domains are joined together via linker sequences to form the cytoplasmic N-terminal region of the protein. Copper ion is coordinated on each MBD via two cysteine residues contained in the individual CXXC motif (DiDonato et al., 1997; Lutsenko et al., 1997). These motifs can bind other metals such as zinc (DiDonato et al., 2002) and lead (Qian et al., 2005). However, the functional consequence of binding the different metals is still under investigation.

MBDs are essential for ATP7B function. Studies have shown that mutating the six MBDs results in a non-functional transporter (Cater et al., 2004). The first four MBD are characteristic of mammalian ATPases and are involved in regulatory functions. There are enough data suggesting that MBD1 to 4 are not critical for the transport of copper. The deletion of MBD1 to 4 did not affect the affinity of the transporter for copper (Forbes et al., 1999). However, this deletion stimulates copper-dependent

catalytic phosphorylation, as studied in insect cells (Huster and Lutsenko, 2003). Tsivkovski et al demonstrated that the N-terminus interacts with the ATP-binding domain and that this interaction is weakened by copper binding (Tsivkovskii et al., 2001). These results suggest that MBD 1 to 4 play an auto-inhibitory role through interacting with the ATP-binding domain (ABD) and preventing ATP hydrolysis (Huster and Lutsenko, 2003). When MBD1 to 4 are loaded with copper, the ABD is free to bind ATP and the catalytic activity of the transporter is restored.

MBD5 and 6 are the nearest to the transmembrane region of the protein. These two MBDs are required for normal ATP7B function. Their effect might be in controlling the transporter conformation or donating copper to the intramembrane copper binding sites. Mutating the cysteine residues, the copper coordinating residues, in the CXXC motif of MBD5 or 6 decreases the affinity of the transmembrane domain for copper (Huster and Lutsenko, 2003). Rice et al also showed that in the bacterial copper transporter, CopA, the MBD of the N-terminus interact with the intramembrane domains (Rice et al., 2006). These observations suggest that copper binding to MBD5 and 6 favors subsequent copper binding to the transmembrane portion of ATP7B. Copper binding to the isolated MBDs did not affect their structure. Achila et al detected small rearrangements in the vicinity of the metal binding site (Achila et al., 2006). A complete 3D structure of ATP7B is still not available. Thus, the effect of copper binding on the overall conformation of ATP7B is still unclear.

ATP7B function involves the interaction with various proteins. Failure to interact properly with these proteins impairs ATP7B function and could result in diseases. There are three proteins that are known to interact with the N-terminal binding

domains of ATP7B. ATOX1 is a cytosolic metallochaperone that passes copper to ATP7B at the membrane of the trans Golgi network (Hamza et al., 1999). Cu(I)-ATOX1 forms a complex with MBD2 and MBD4 of the N-terminus (Achila et al., 2006). The consequence of this interaction is discussed earlier in this chapter. COMMD1 (MURR1) is a protein recently associated with copper accumulation in Bedlington terriers. The deficiency in COMMD1 contributes to copper toxicosis, a canine disorder that shares many pathophysiological features with WND. The interaction of ATP7B and COMMD1 supports the role of COMMD1 in copper homeostasis and suggests that these two proteins cooperate to facilitate the excretion of excess copper through the bile canaculi (Tao et al., 2003). Recent studies have revealed that COMMD1 is involved in a variety of other cellular processes including hypoxia-inducible factor 1 (van de Sluis et al., 2007) and nuclear factor κB (NF-κB) signaling pathways (Ganesh et al., 2003). Lim et al in 2006 identified an additional protein that interacts with the N-terminal region of ATP7B using a yeast two-hybrid approach to screen a human liver cDNA library. This screen showed that ATP7B interacts with P62 (Dynactin 4), a subunit of the motor protein dynactin. The interaction with p62 requires copper and depends on the CXXC motifs as well as the region between MBD4 and MBD6. This interaction suggests that P62 is a key component of the copper-regulated trafficking pathway that delivers ATP7B to subapical vesicles of hepatocytes for the removal of excess copper (Lim et al., 2006).

3.2.2. Role of ATP7B Transmembrane Domains

ATP7B is a membrane protein that contains eight transmembrane domains. These domains form the channel required to recognize copper and translocate it across the membrane permeability barrier. The ATPase P1B subfamily shares certain amino acid residues including His, Gly, Asp, Ser, and Met that are required for metal coordination by the various transporters. The arrangement of these metal binding residues and the mechanism by which they synchronize metals is under investigation. The P1B ATPase subfamily has a Tm6 that coordinates the metal during transport. The conserved proline is found in all P- type ATPases. P1-type ATPases have this proline flanked between cysteine and X residues. The CPX motif is a defining element for P1-type ATPases (Bull and Cox, 1994; Solioz and Vulpe, 1996). Studies have shown that mutating cysteine in the CPX motif impairs copper binding of the transmembrane domains (Mandal Arguello 2003).

Tm3 to 8 have equivalents in their structure in all P- type ATPases. Tm1 and Tm2 are specific for P1B ATPases such as ATP7B and ATP7A. Tm2 has been shown to be essential for ATP7B function. The animal model, Jackson toxic milk mouse (tx^J) is reported to have clinical and biochemical features of WND (Theophilos et al., 1996). Coronado et al have shown that the causative mutation of this phenotype is G712D that is located in Tm2 (Coronado et al., 2001). Tm1 and 2 also contain a number of residues that could be involved in metal coordination and translocation within the intramembrane region. The structural analysis of these two domains shows two cysteine residues that face each other in both ATP7A and ATP7B. This positioning suggests the involvement of these cysteines in either coordinating metal translocation or forming a disulfide bridge that might be crucial for the structure of the channel. Tm1 and 2 present another

interesting feature. The luminal ends of Tm1 and 2 show highly conserved methionine residues in all copper ATPases (http://www.patbase.kvl.dk/IB.html). Methionine is an appropriate ligand for copper in its reduced state. Copper binds to the N-terminal MBD in the mono-valent form (Cu+) and is thought to be imported across the membrane in the same form. Therefore, these methionine residues might play a role in the transfer of copper through the membrane (Lutsenko et al., 2007b).

3.2.3. Role of the ATP Loop

The ATP loop is the second largest cytosolic portion of ATP7B. It encompasses two major domains: the phosphorylation domain (P-domain) and the nucleotide -binding domain (N-domain). All P-type ATPases, including ATP7B, are characterized by the presence of these domains as part of the catalytic activity. The P-domain contains motifs that are required for ATP hydrolysis such as the signature motif (DKTG), found in all P-type ATPases. The aspartate residue of this motif is phosphorylated during the transport cycle of ATP7B. The sequence homology existing between the P-domain of Cu ATPases and SERCA Ca^{++}- ATPase was used to produce a structural model of the ATP7B P-domain (Fatemi and Sarkar, 2002; Efremov et al., 2004)

The N-domain of the ATP-loop contains sites that are involved in binding and coordinating the nucleotide molecule (ATP). The primary sequence of the N-domain of Cu ATPase has little sequence homology with equivalent domains of other P type ATPases. However, the high-resolution structure of the ATP7B N-domain indicates that the three-dimensional folding pattern of the N-domain is similar in all P- type ATPases (Dmitriev et al., 2006). Sequence alignment reveals invariant residues in the ATP7B N-

domain including: p.E1064, p.H1069, p.G1099, p.G1101, p.G1149. NMR mapping of the ATP loop showed that the invariant residues are located in the ATP binding sites. p.G1101 and p.G1099 are close to the α- and β- phosphates of ATP. This might contribute to the tight binding of ATP. p.G1149 creates a pocket that coordinates ribose. The adenine moiety is in close proximity to p.H1069 and is surrounded by hydrophobic side chains of p.I1180 and p.I1102 (Lutsenko et al., 2007a). The residue p.E1064 is necessary for ATP binding (Morgan et al., 2004), however the functional role of this residue in nucleotide coordinating is still unclear.

3.2.4. Role of the C-Terminal Region

The C-terminus of ATP7B is made up of 80 to 100 amino acid residues. Structural information on the C-terminal tail of human copper ATPases is still incomplete. The C terminus of ATP7B contains a conserved trileucine motif (1454-1456 LLL) that is necessary for the TGN localization of ATP7B (Petris et al., 1998; Cater et al., 2006). This motif retrieves the trafficked ATP7B molecules from the plasma membrane and the vesicle back to the TGN (Mercer and Llanos, 2003). The LLL>AAA mutation causes ATP7B to localize to vesicles when expressed in chinese hamster ovary cell lines (Cater et al., 2006). These results suggest that residues within the C- terminus might be responsible for mimicking the response to elevated copper.

Mutations resulting in the deletion of the entire C-terminus are deleterious to protein stability (Hsi et al., 2004) and are associated with disease (http://www.medicalgenetics.med.ualberta.ca/wilson/index.php). The C-terminus may interact with other proteins that promote folding and possibly protect ATP7B from

intracellular proteases. Hsi et al. showed that truncated ATP7B, missing 60 amino acids from the C-terminal tail (almost two thirds of the tail), has near wild type activity (Hsi et al., 2004). The C-terminal tail of ATP7B, while not required for the catalytic activity, is important for the stability and proper localization of ATP7B.

A recent study using yeast two-hybrid screening revealed that the C-terminus of ATP7B interacts with the 45-kDa isoform of PLZF (Ko et al., 2006). The promyelotic leukemia zinc finger (PLZF) protein has been described as a transcriptional repressor for the BTB-domain/zinc-finger family (Li et al., 1997). PLZF regulates the expression of Hox genes (a subgroup of the homeobox genes) during embryogenesis (Barna et al., 2002) as well as the expression of cyclin A in the cell cycle progression (Yeyati et al., 1999). The interaction with ATP7B suggests the existence of a mechanism that regulates ERK signaling via the C-terminus of ATP7B and the ATP7B-interacting hepatocytic PLZF isoform. In hepatocytes, the kinase activity of ERK was enhanced as a result of expression of ATP7B and PLZF, however this enhancement was abrogated by the deletion of the C-terminus of ATP7B. Furthermore, the immunostaining of HepG2 cells revealed that ATP7B and PLZF are co-localized into the trans-Golgi network (Ko et al., 2006).

3.3. Transport Mechanism of ATP7B

P-type ATPases transfer copper from the cytosol to the lumen of different cellular compartments. This transport requires the translocation of ions from MBDs in the cytoplasmic regions to those in the intramembrane regions of the protein. The transport of copper is particularly complex. Copper moves within the cell in its mono-

valent form. Cu (I) is not stable in solution and switches into Cu (II) and Cu (0) if not bound to proteins. Therefore, a protein-based pathway is involved in the transport of copper. The six MBDs of ATP7B acquire Cu (I) from its donor, ATOX1, and then transfer it to ceruloplasmin the biosynthetic target of Cu-ATP7B.

Copper is carried by ATOX1 from various cytoplasmic locations to the N-terminal MBDs of ATP7B. Interactions between ATOX1 and MBDs load ATP7B with copper. Although the domains have similar affinity for copper (Wernimont et al., 2004), the protein surfaces adjacent to these motifs differ (Huffman and O'Halloran, 2001). This favors the interaction of ATOX1 with MBD4 as described earlier (Larin et al., 1999). The facile copper transfer between MBDs permits inter-domain interactions that transfers copper from MBD 4 to MBD5 and MBD6 (Achila et al., 2006). Copper free MBD5 and 6 interact with the N domain and prevent ATP binding. Therefore, loading MBD5 and 6 with copper releases the auto-inhibitory effect of ATP7B. Specific residues in the N-domain such as p.H1069, p.G1099, and p.N1150 are involved in coordinating ATP (Dmitriev et al., 2006). ATP hydrolysis phosphorylates the aspartate residue in the signature DKTG motif of the P domain. This phosphorylation is accompanied by the transfer of copper from the cytosolic to transmembrane sites, while its release to the opposite side is associated with dephosphorylation of ATP7B (Voskoboinik et al., 2001; Tsivkovskii et al., 2002). The CPC motif in Tm6 as well as the methionine cluster in Tm1 and 2 are copper binding sites in the transmembrane channel. Other residues such as p.Y1331, p.N1332, p.M1359, and p.S1362 are likely to form binding sites in the transmembrane domain (Lutsenko et al., 2007a).

The catalytic cycle of ATP7B involves significant conformational changes that are reflected in the architecture of the protein (Voskoboinik et al., 2001). The binding of copper from the cytosol occurs as the protein is present in the so-called E1 state, characterized by high affinity of intra-membrane sites for copper. Copper binding to the intra-membrane sites is accompanied by ATP7B phosphorylation and switching into the transient phosphorylated E1P state. This state sequesters copper in the transmembrane sites and subsequently undergoes conformational changes to E2P. E2P is characterized by less affinity for copper. It is thought that the in this state copper is released into the lumen. The copper release is accompanied by dephosphorylation and return to the E2 phase. These changes stimulate conformational transition to the high affinity E1 state. A second cycle starts as E1 binds copper again.

4. ATP7B Functional Assays

The functional characterization of ATP7B variants is critical for full understanding of the protein and its functional domains. Identifying ATP7B residues that are crucial for copper homeostasis also assists in the diagnosis of WND. A useful system for analyzing ATP7B variants should ideally be simple, sensitive, and accurate. There is a wide range of WND mutations thus the system should be high-throughput so that reliable results can be rapidly produced.

ATP7B is a membrane protein that has a low expression level (0.005% of total membrane proteins). Most ATP7B molecules are localized to the intracellular membranes (Tsivkovskii et al., 2002). WND patients are mostly compound heterozygotes. Thus, characterizing a specific mutation using endogenously expressed

ATP7B is not feasible, especially with the large number of ATP7B variants reported in the WND mutation database (Kenney and Cox, 2007). Alternative methods that use exogenous expression of ATP7B are essential for the study of ATP7B variants.

The function of ATP7B requires specific activities of its individual domains. Specific ATP7B domains bind and translocate copper as well as bind and hydrolyze ATP. Moreover, ATP7B function involves its interaction with various proteins such as ATOX1 for copper exchange (Hamza et al., 1999), COMMD1 (MURR1) (de Bie et al., 2007) and dynactin (Lim et al., 2006) for the trafficking of ATP7B from the TGN to cytoplasmic vesicles as a response to elevated copper in the cytoplasm, and PLZF that is associated with ERK signaling (Ko et al., 2006). Therefore, assessing ATP7B function requires a clear observation of these different activities. Up to date there is no way to include all these aspects of ATP7B in one single experiment. Thus, different assays are being used to assess some of the individual aspects of ATP7B.

4.1. Yeast Complementation Assay

The yeast assay is used to assess the transport activity of ATP7B variants. Ccc2p is the yeast orthologue of ATP7B. This assay is based on complementing *ccc2* deficient *Saccharomyces cerevisiae* by human ATP7B variants (Yuan et al., 1995). In yeast, Ftr1p the high affinity iron transporter, is associated with the Cu-dependent ferroxidase, Fet3p. This complex co-localizes on the plasma membrane of the yeast (de Silva et al., 1997; Singh et al., 2006). Fet3p converts Fe^{2+} to Fe^{3+}, which is then transported by Ftr1p across the membrane (De Silva et al., 1995). Active Fet3p requires copper loading from Ccc2p in the TGN. Copper enters the yeast cell through copper transporter (Ctr1) located on the plasma membrane. Copper is then carried by Atx1p throughout the

cytoplasm, to exchange with Ccc2p at the TGN. Active Ccc2p is necessary for yeast growth in iron limited medium. In our laboratory, a *ccc2* yeast deficient stain was created, and then transformed with different ATP7B variants. The yeast growth results were used to analyze the ability of ATP7B variants to transport copper through the membrane and deliver it to Fet3p, the yeast orthologue of human CP (Forbes and Cox, 1998).

The yeast assay also includes measuring the oxidase activity of Fet3p. Fet3p is a ferroxidase located at the cell membrane of the yeast (de Silva et al., 1997). Our laboratory has previously used a gel system to detect Fet3p oxidase activity in yeast (Forbes and Cox, 1998). This assay, although very specific, is not quantitative and is time consuming. De Silva et al used yeast spheroplasts to measure Fet3p activity through correlation with iron-dependent oxygen consumption. This oxidase activity was blocked by using an antibody that targets the ferroxidase domain of Fet3p. These findings indicate that Fet3p is a plasma membrane, in which the ferroxidase containing domain is localized on the external cell surface (De Silva et al., 1995).

4.2. Localization and Other ATP7B Assays

Localization assays determine the distribution of ATP7B in response to copper concentrations in the cytoplasm. The original assay was done using HepG2 cells transfected with wild type *ATP7B* (Hung et al., 1997; Yang et al., 1997; Lutsenko and Cooper, 1998). Other assays were made using human and rat liver as well as other hepatic cell lines (Schaefer et al., 1999a; Schaefer et al., 1999b). The localization assays used immunofluorescence techniques to localize ATP7B variants in the cytoplasm of the

cell (Forbes and Cox, 2000; Huster et al., 2003) . Hamza et al used mammalian cell lines (HEpG2 and HeLa) as well as human tissues to assess the interaction of ATP7B variants with ATOX1 (Hamza et al., 1999).

Other ATP7B assays use *Enterococcus hirae* to explore the ability of various WND mutations to confer copper resistance and ATPase activity in a bacterial model (Okkeri et al., 2002). An insect cell model was created to enable robust expression of ATP7B for studying the enzymatic steps of ATP7B during transport activity (Voskoboinik et al., 2001). A cytotoxicity assay using a chinese hamster ovary cell line to determine the ability of cells transfected with ATP7B variants to resist toxic levels of copper is under development in our laboratory (unpublished data). This assay measures the transport as well as the trafficking activity of ATP7B variants. Characterizing ATP7B variants requires several assays that analyze the different functional aspects of ATP7B. Prediction programs might be helpful in developing a hierarchical plan for selecting variants for the more complex functional testing.

5. Genetic Variation and Prediction Programs

Non-synonymous variants or missense variants are mutations that cause a single amino acid change within a protein sequence. This change may or may not affect protein function. Missense variants that change the function of a protein could affect the cellular phenotype at different levels. An amino acid substitution might directly affect the stability or folding pattern of a protein, thus increasing its sensitivity to degradation and resulting in a decrease of protein concentration (Karchin et al., 2005). Other missense variants, residing in functional motifs, may disturb protein catalytic activity or its

interaction with other proteins, affecting other biochemical activities inside the cell (Sunyaev et al., 2001). Other missense variants could affect transcription, translation, as well as post translational events (Wang and Moult, 2001). Therefore, some variants could directly lead to a disease phenotype and are reported in the literature as disease causing variants. Other missense variants are neutral and reported not to change the phenotype. Such variants are referred to as normal variants or non-disease causing variants. Most of the missense variants that are reported in patients are still not functionally characterized. The disease database includes 518 variants of which 198 are missense only 50 variants have been functionally characterized (Kenney and Cox, 2007).

Classifying missense variants as defective or neutral is critical for several reasons. Defective variants should highlight amino acid residues that are functionally significant. This will enhance our understanding of the protein and its function and will guide further research. The other application would be for diagnostic and therapeutic approaches. Accurately identifying variants that cause disease will provide appropriate risk assessment and therapeutic decisions. This issue becomes even more critical with Wilson disease. Wilson disease is effectively treated once diagnosis is confirmed and appropriate treatment is provided. Therefore, it is very useful to identify disease-causing ATP7B variants.

In vitro assays can be very helpful in identifying functionally significant ATP7B variants, but testing all missense variants will be challenging with 379 probable disease causing variants and 139 probable non disease causing variants as presented in the Wilson disease database (Kenney and Cox, 2007). Furthermore, functional assays that

are used to characterize ATP7B variants usually address only one aspect of the protein. Therefore multiple assays are required to fully characterize each ATP7B variant. The assays which are carried out in model systems may not replicate activity in mammalian organs. The functional assays reported to explore ATP7B are described above. Although these assays are effective, it would be more practical to have reliable computer prediction programs that could select variants that may require functional studies.

Numerous prediction programs have been generated using conservative, biochemical, and computational methods (Grantham, 1974; Henikoff and Henikoff, 1992; Ramensky et al., 2002; Ng and Henikoff, 2003) . Such programs were developed to provide valuable predictive scores for classifying missense variants for CDKN2A, MLH1, MSH2, MECP2, and TYR (Chan et al., 2007) as well as for a large number of protiens (Greenblatt et al., 2003; Abkevich et al., 2004; Bao and Cui, 2005). The effectiveness of these programs appear to vary between proteins (Chan et al., 2007). Prediction programs might identify putative functional variants using various types of properties including: amino acid, protein structure, and evolutionary properties.

5.1. Amino Acid Properties

The basic chemical properties of the 20 amino acids including molecular mass, polarity, isoelectric point, aromaticity, and conformational flexibility play the role in protein folding and stability and account for the major protein structural properties. The direct use of these chemical properties, such as the absolute mass and volume of the side chain, were used to predict the tolerance of an amino acid substitution (Voet D, 1995). Kyte and Doolittle proposed a scale to predict the tolerance of an amino acid

substitution based on the hydrophobic characteristic of the amino acids. This scale measures the hydrophobicity of the two amino acid variants and estimates how well the hydrophobic features are conserved (Kyte and Doolittle, 1982). In 1974, Grantham proposed a matrix that evaluates the compatibility of an amino acid substitution using a quantitative measure of the chemical distance between the different amino acids (Grantham, 1974). This matrix considers composition, polarity, and molecular volume of the amino acid. A recent study has combined the classic Grantham matrix with sequence variation in multiple sequence alignments to create a more evolutionary – based protein specific "Grantham score" (Align-GVGD). Align-GVGD reflects how the chemical characteristics of a variant amino acid fit within the range of variation tolerated at the substitution site. This score uses the biochemical properties of the selected residues, as well as their conservation score throughout the alignment, to determine the effect of the amino acid substitution. This method was first developed for analyzing single nucleotide polymorphisms in BRCA1 (Tavtigian et al., 2006) and P53 genes (Mathe et al., 2006).

5.2. Protein Structural Properties

Structural properties represent an essential tool for studying the effect of missense variants on protein phenotype. Protein structures are usually maintained through defined biochemical properties such as presence of: hydrogen bonds, salt bridges, disulfide bridges, etc. Distorting these structural properties usually disturbs the protein and alters its phenotype. Predictive scores based on these factors have been used to identify missense variants with deleterious effects on the protein (Wang and Moult,

2001). Wang used more factors, such as inserting a proline into an alpha helix or introduction of a buried polar residue, to assess the effect of certain amino acid substitutions on the structural stability of a protein. Similar rules were employed by others (Chasman and Adams, 2001; Sunyaev et al., 2001). For example, the B-factor of the polymorphic model residue was used to identify putative functional missense variants (Matthews, 1995). Unfortunately, little structural information is available for most of the proteins identified, including ATP7B. Therefore, further applications are yet to be tested.

5.3. Evolutionary Properties

Highly conserved residues within a protein family are usually associated with important functions of the protein. Multiple sequence alignment of homologous proteins can be used to recognize residues with high conservation scores. Such scores may be used to predict missense variants that are deleterious to the protein. There are two commonly used programs that utilize these tools for classifying missense variants: PolyPhen and SIFT

5.3.1. PolyPhen

PolyPhen (Polymorphism Phenotyping) combines conservation scores with additional properties of the protein, mainly structural ones (Sunyaev et al., 2001). Incorporating structural data available on ATP7B as well as evolutionary data would provide an important tool to classify ATP7B missense variants. PolyPhen searches Protein Data Bank (PDB) or Protein Quaternary Structure (PQS) for data available on

the query protein and its homologues. The amino acid substitution is mapped to the available 3D structure to assess the effect on structural properties such as: hydrophobicity of the core protein, electrostatic interactions, interaction with ligands and other important features of the query protein. If no 3D structure is available for the protein of interest, PolyPhen will use homologous proteins with known structure. The sequence alignment generated by PolyPhen cannot be selected and depends on the homologous sequences available at the time the mutations were studied.

5.3.2. SIFT

SIFT (Sorting Intolerant From Tolerant) predicts whether an amino acid substitution could be tolerated within an alignment of homologous sequences (Henikoff and Henikoff, 1992; Ng and Henikoff, 2003). SIFT is a multi step process that: searches for homologous sequences in the database; aligns the selected sequences; calculates normalized probabilities for all possible substitutions from the alignment. All amino acid substitutions that have normalized probabilities less than 0.05 are considered defective. SIFT considers the position and the type of the amino acid substitution. If a position in the alignment contains the non-polar amino acids phenylalanine, methionine or tryptophan, then SIFT assumes that this position can only contain a non-polar amino acid. A missense variant that leads to a polar amino acid at this position will be predicted as deleterious. SIFT analysis depends directly on the alignment used for predicting the conserved residues. Therefore, manipulating the alignment through selecting protein sequences that are more related to ATP7B might enhance the accuracy of the analysis.

PolyPhen and SIFT scores depend greatly on the multiple sequence alignment used for their analysis. Both programs generate their multiple sequence alignment from an automated search for homologous sequences throughout the database as indicated in Chapter 3. The assumption is that protein sequences available from the source database are accurate, but extra investigation for appropriate sequences is always better. Furthermore, manually selecting sequences to be used for the alignment, if possible, will remove inappropriate sequences and produce more biologically meaningful alignments.

All predictive scores have strengths and weakness. Their effectiveness may also differ among various proteins. Therefore, it is important that these computational scores to be validated through comparison with the functional data available on ATP7B variants.

6. Aim of the Study:

- This study uses the yeast complementation assay to functionally characterize ATP7B missense variants detected in WND patients. In addition to aiding patient diagnosis, this will identify particular amino acid residues that may be important for the transport activity of ATP7B.
- The functional data available on ATP7B missense variants is used to assess selected prediction scores. This analysis might validate useful tools that could be used to develop a hierarchical plan for selecting future variants for the more complex functional testing.

Chapter 2

FUNCTIONAL ASSESSMENT OF ATP7B VARIANTS

1. Introduction

WND disease is a hepatic disorder caused by mutations in ATP7B. The treatment of WND is effective if adequate treatment is provided in the early stages of the disease. WND is presented with highly variable symptoms. The parameters used to diagnose WND are observed in other hepatic disorders. Thus, the diagnosis of WND is often difficult. In some situations diagnosis is missed and leads to serious disease. Mutation analysis is an important diagnostic tool. More than 500 variants have been found in the ATP7B gene. Most of the variants are missense mutations that are classified as suspected disease causing variants (Kenney and Cox, 2007). Functional data on these variants is still limited.

ATP7B transports copper across the cell membrane. It delivers copper to CP, its biosynthetic target, at the TGN. Deficiency in the transport of copper is usually associated with WND. A yeast complementation assay has been used previously in our lab to study the effect of ATP7B mutations on transport activity. In yeast, Fet3p activity, a ferroxidase required for high affinity iron transport, is first inhibited by the deletion of yeast Cu-ATPase Ccc2p. The yeast strain becomes iron deficient and grows only in media supplemented with iron or copper. The yeast *ccc2p* strain is complemented by heterologous expression of human ATP7B.

The functional characterization of ATP7B variants presents an important tool for WND diagnosis as well as identifying amino acid residues that are crucial for ATP7B

function. In this chapter, I describe the functional studies I have carried out on 21 variants observed in patients with WD.

2. Materials and Methods

2.1. Growth of Bacteria and Yeast

Reagents and chemicals used were obtained from Sigma-Aldrich, unless other sources are specified. Media used to grow bacteria were made up of Lauria-Broth (LB) (Difco, MI). LB plates were made from LB media supplemented with 2% agar (Fisher, NY). Bacterial liquid cultures were grown at 37 °C for 16 hours at 250 rpm.

Yeast cells were grown in Yeast Peptone Dextrose (YPD) media prepared as follows: 10g of yeast extract (BD, MD), 20g of peptone (BD, MD), 20g of glucose added to 1000ml of water. YPD-plates were prepared from YPD media supplemented with 2% bacto agar (BD, MD). For technical reasons, yeast cells were grown in other selective media that will be described later. Yeast liquid cultures were grown at 30 °C for 18 hours at 250 rpm.

Gel electrophoresis was carried out in 0.8% agarose gel (Invitrogen, CA) containing ethiduim bromide. The gel was run in tris-borate-EDTA (TBE) buffer for 80Vhr – 120Vhrs.

Polymerase chain reaction (PCR) was performed using Taq polymerase from New England Biolabs (NEB, MA). Most of the PCR reactions were performed in 10 µL reaction that includes 2.5 mM of deoxynucleotide triphosphates (dNTPs) (NEB, MA), 1µL of 10x Taq buffer (NEB, MA), 25 ng of primer pairs we designed (Sigma), and 50ng of template DNA.

2.2. Construction of *ATP7B* cDNA Variants

A cDNA for *ATP7B* was previously constructed in our laboratory and then cloned into pUC19 vector. *ATP7B* cDNA was generated from reverse transcription of human liver RNA (Forbes and Cox, 1998). *ATP7B* cDNA was used as a template for the polymerase chain reaction (PCR) to amplify five overlapping fragments of DNA that include the entire *ATP7B* cDNA. The five primer pairs used for PCR were designed such that a unique restriction site was present at the ends of each cDNA fragment. This facilitated the construction of the whole ATP7B cDNA, 4395bp. A 5' *Bam*H1 site was added to the PCR primer sequence immediately preceding the initiating ATG codon, for use in cloning into expression vectors. To ensure fidelity of PCR, each DNA fragment was sequenced according to the manufacturer's protocol (Amersham, Sweden). Correct cDNA fragments were gel-purified and then ligated to form the full length of ATP7B cDNA. The final cDNA construct was cloned into pUC19 vector using the 5' BamH1 site and a 3' Sal I site from the polylinker of the Promega T/A vector (Forbes and Cox, 1998).

I used the backbone pUC19*ATP7B* generated by Forbes to generate my subsequent ATP7B variants. Two complementary oligonucleotide primers bearing the desired point mutation were designed for each variant as indicated in Table 2.1. These mutagenic primers were prepared so that approximately 15 nucleotide bases of matched normal sequence flanked the point mutation. Table 2.1 lists the sequence of the mutagenic primers used in this study as well as the location of the mutation. The PCR reaction for the mutagenesis was carried out as follows: 20 ng of *ATP7B* cDNA as a template, 62.5 ng of each mutagenic primer, 2.5 units of *Pfu* polymerase, 2.5 mM of each dATP,

dCTP, dGTP and dTTP supplemented with the manufacturer's buffer; water was added to a final volume of 25 µL. The PCR cycles were programmed as follows: 95°C for 1 min. as an initial denaturation step, followed by 18 cycles of 50 seconds at 95°C for denaturation, 50 seconds at 60°C for primer annealing, 8 min. at 68°C for polymerase extension, then a last step at 68°C for 7 min. The PCR product obtained was digested with 5 units of DpnI (Stratagene, CA) for 2 hour at 37 °C. DpnI is an endonuclease that digests methylated and hemi-methylated DNA of the parental plasmids. 1ul of DpnI-digested DNA was transformed into 30 µL of chemically competent XL10 Gold *E. coli* cells according to the manufacturers protocols (Stratagene, CA). Transformed XL10 Gold cells were plated on Luria Bertani (LB) broth agar plates that were supplemented with 100 µg/mL carbenicillin (Sigma, MO). LB plates were made up from 2.5% LB (Difco, MI) with 2% agar (Fisher, NY). Transformed XL10 Gold cells were selected on the LB plates and then streaked for single colonies. Plasmid DNA from these colonies was prepared using a miniprep kit provided by (Qiagen, ON). To ensure that there was no secondary mutation during the mutagenesis reaction, 800bp surrounding the desired mutation was sequenced using a 3130XL Genetic Analyzer (Applied Biosystems, CA). The full sequence of *ATP7B* cDNA was done at the end of the functional test.

Table 2.1 List of Mutagenic Primers

Site directed mutagenesis primers were used to generate ATP7B variants. The forward strand as well as its complementary reverse strand of each primer was designed so that 15 nucleotide bases of matched normal sequence flanking the point mutation. p.R1415Q has 20 nucleotides of matched normal sequence flanked the point mutation.

Variant	Forward strand of the Mutagenic Primers
p.N41S	GTTTTGCTTTTGACAGTGTTGGCTATGAAGG
p.A604P	GAGGCATAAGTGATGTCATTTGTCCTCGTGA
p.R616Q	AAATTATCGGTCCACAGGATATTATCAAAAT
p.M665I	TGGCATCCCTGTCATTGCCTTAATGATCTAT
p.S657R	GTCTTTCCTGTGCAGACTGGTGTTTGGCATC
p.G710V	TTGTCCAGCTCCTCGTTGGGTGGTACTTCTA
p.G711R	GTCCAGCTCCTCGGTCGGTGGTACTTCTACG
p.S744P	ATTGCTTATGTTTATCCTCTGGTCATCCTGG
p.T766M	TGACATTCTTCGACATGCCCCCCATGCTCTT
p.L795F	GAAGCCCTGGCTAAATTCATGTCTCTCCAAG
p.S921N	TGGCTGACCGGTTTAATGGATATTTTGTCCC
p.G943C	GTATGGATTGTAATCTGTTTTATCGATTTTG
p.T991M	CCCTGGGGCTTGCCATGCTCACGGCTGTCAT
p.G1000R	GTCATGGTGGGCACCAGGGTGGCCGCGCAGA
p.G1176E	ACCACGAGATGAAAGAACAGACAGCCATCCT
p.G1287S	GTGGGCATTGGCACCAGCACTGGATGTGGCCA
p.A1328T	ATCAACCTGGTCCTGACACTGATTTATAACC
p.G1341D	TCCTGGCACTGATTTCTAACCTGGTTGGGAT
p.G1341S	ATACCCATTGCAGCAAGTGTCTTCATGCCCATC
p.C1375S	CCCTGCAGCTCAAGTCCTATAAGAAGCCTGA
p.R1415Q	GACAGGTGGCGGGACTCCCCCCAGGCCACAC CATGGGACCAGGTC

3. Yeast Expression Vectors

PG4 is a yeast expression vector previously modified (Forbes& Cox 1998) from PG3 (Schena et al., 1991). PG4 uses a strong, constitutive glyceraldehyde-3-phosphate dehydrogenase (GAPDH) promoter, a phosphoglycerate kinase (PGK) terminator and polyadenylation sequence, and a tryptophan selectable marker. PG4 vectors as well as pUC19ATP7B variants were digested with both BamHI and SalI according to the manufacturer's protocol (Invitrogen, CA). DNA fragments obtained from the double digestion were isolated by gel electrophoresis then purified according to the manufacturers protocol (Qiagen, ON). Purified ATP7B fragments were then ligated into PG4 fragments using T4 DNA ligase as indicated by the manufacturer (NEB, MA). The product of the ligation reaction was transformed into competent DH5α following the manufacturer's protocol (Invitrogen, CA). Transformed cells were then plated onto LB plates that were supplemented with 100 μg/mL carbenicillin. Successfully transformed *E. coli* cells were selected on the agar plates and then streaked to obtain single colonies. Plasmid DNA was prepared from these colonies using a miniprep kit (Qiagen, ON) to be used later for yeast transformation.

2.4. Yeast Strain and Transformation

The wild type yeast used in all experiments was the S. cerevesiae strain BJ2168 (MATa pep4-3 prc1-407 prb1-1122 ura3-52 trp1 leu2) (Zubenko et al., 1980). This strain is vacuolar protease deficient to minimize potential proteolysis during protein preparations and assay. The yeast strain was originally provided by Dr. Morrie Manolson at the University of Toronto (Toronto, Canada). The ccc2 mutant yeast was made from the BJ2168 strain using the E5-URA3.4 gene disruption plasmid (Forbes and

Cox, 1998). This knockout BJ2168 strain was used for all subsequent yeast transformations.

5 ug of PG4ATP7B prepared by miniprep (Qiagen, ON) were linearized with 20 units of XbaI (Invitrogen, CA) overnight at 37 °C. The digested DNA was transformed into yeast using a modified lithium acetate method (Elble, 1992) (Kaiser C, 1994). Yeast transformants were selected on synthetic dextrose (SD) medium lacking tryptophan and uracil (SD-T-U), containing 0.17% yeast nitrogen base without amino acids or ammonium sulfate (Difco, MI), 0.072% complete supplement mixture lacking tryptophan and uracil (Bio101, ON), 2% glucose, 0.5% ammonium sulfate (Kaiser C, 1994). SD medium with 2% Bacto-agar (BD) was used to make the plates. Successfully transformed yeast cells were able to grow on these selection plates after incubation for 72 hours at 30 °C.

2.5. Southern Blotting

Yeast cells containing *ATP7B* variants in their genome were inoculated into SD-T-U medium prepared as above. 1 ml of culture was used to extract genomic DNA with a Wizard Genomic DNA Purification Kit (Promega). 5ug of genomic DNA were digested with 15 units BamHI (Invitrogen, CA). Digested DNA was electrophoresed on a 0.8% agarose gel running at 80mV for 4hrs. An image was taken to check for the efficiency of the digestion using Image Master (Pharmacia Biotech, Israel). The gel was incubated in 0.25M of HCl with shaking for 30 minutes at room temperature. The gel was then washed with 0.4M NaOH for 30min with shaking at room temperature. DNA on the gel was transferred onto Hybond-N+ membrane as described by the manufacturer (Amersham Pharmacia Biotech, Bukinghamshire, UK). The transfer was continued

overnight. The blot was washed with 2x SSC buffer (150 mM sodium chloride, 15 mM sodium citrate) then stored at room temperature for further applications. Most of the Southern analysis was done using a radioactive ^{32} P isotope. *ATP7B*cDNA was labeled with ^{32}P-dCTP isotope using a random prime labeling kit Rediprime II (Amersham Pharmacia Biotech, Bukinghamshire, UK). This radioactive probe was used to hybridize the blot in the presence of Express Hyb solution as described by the manufacturer's protocol (Clontech, CA). The blot was visualized by auto-radiography (Kodak Bio Max MS film, NY). In some cases a Dig- labeled probe was used instead. *ATP7B* cDNA was labeled using DIG High Prime labeling kit as indicated by the manufacturer's protocol (Roche, IN). The labeled probe was added to the Express Hyb (Clontech, CA) solution to hybridize DNA on the blot. Phosphatase-conjugated anti-DIG antibody was added following a DIG-Luminescent Detection Kit (Roche, IN). The blot was then incubated with 1 ml of Chemiluminescent Alkaline Phosphatase Substrate (CSPD) for 15 min at 37 °C. Visualization was obtained after exposing the blot to X-ray film (FUGI, Japan) for 1 hour at room temperature.

In either assay, a single copy variant yields a single band of 12 kb size. However, a multicopy integration shows a double band: one at 12 kb and another heavier one at the 9 kb position.

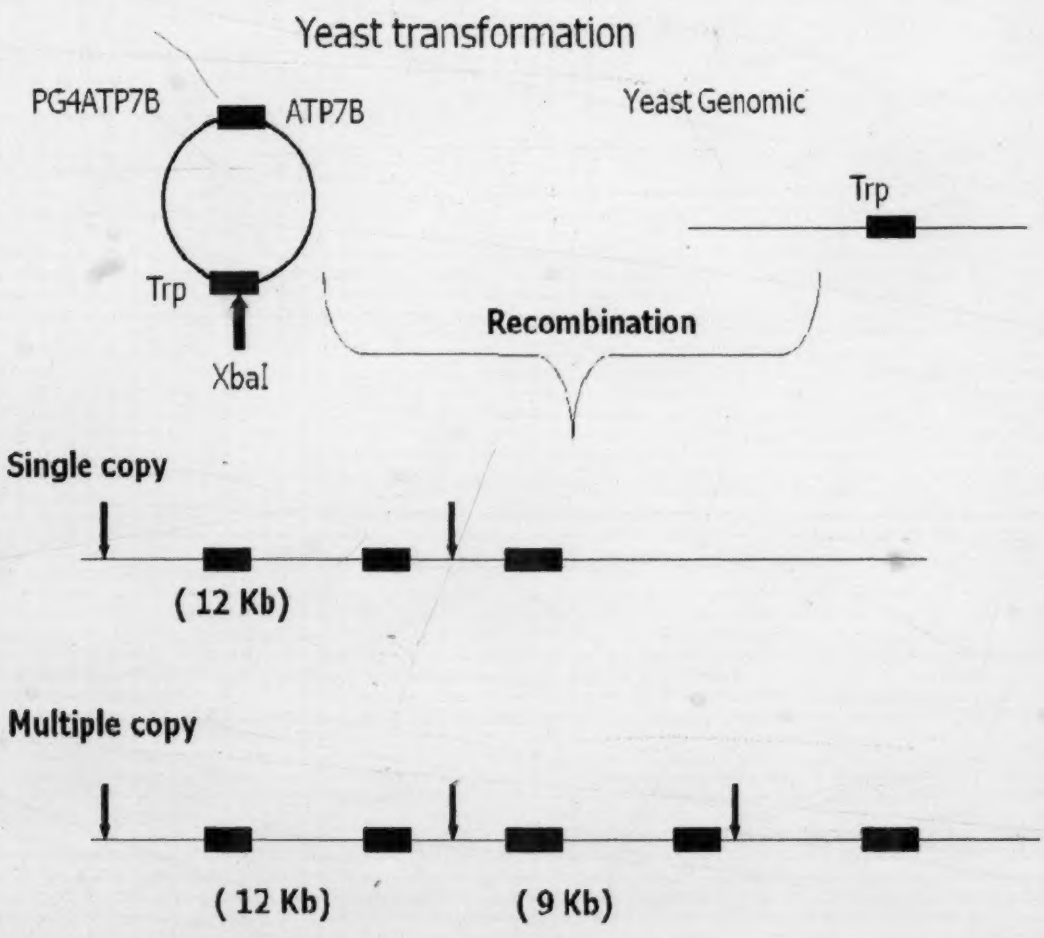

Figure 2.1 *ATP7B* integration into the yeast genome

XbaI (dark blue arrow) was used to cut tryptophan (*Trp*) gene (light blue box). Linearized PG4*ATP7B* could recombine into the yeast genome (purple box) either by a single copy insertion or multiple copy insertion. BamHI (light blue arrow) was used to digest yeast genomic DNA after transformation. A single copy insertion results in a 12kb fragment containing the *ATP7B* variant. However, a multiple copy insertion of *ATP7B* would result in a 12kb fragment as well as 9 kb fragments depending upon the number of insertions.

2.6. Yeast Complementation Assay

Yeast cells were grown in 2 ml of SD-T-U medium overnight at 30 °C. Cells were pelleted, and then double washed with filter sterilized deionized water (Millipore, MA). The pellet was resuspended in 200µl of iron limited medium: 2% glucose, 0.5% ammonium sulfate, 0.072% complete supplementary mixture lacking tryptophan and uracil (Bio101, ON), 0.17% yeast nitrogen base lacking dextrose, amino acids, ammonium sulfate, iron and copper (Bio101, ON), 50mM of MES buffer at pH 6.1, 350 µM ferrous ammonium sulfate, 1µM copper sulfate, 1mM of iron chelator ferrozine. This culture was diluted to an optical density of $A_{600} = 0.1$.

Three various types of agar plates were used to test the complementation of ATP7B variants in *ccc2* yeast. The basal medium used to make these plates contained 2% glucose, 0.5% ammonium sulfate, 0.072% complete supplementary mixture lacking tryptophan and uracil (Bio101, ON), 0.17% yeast nitrogen base lacking dextrose, amino acids, ammonium sulfate, iron and copper (Bio101, ON), 50 mM of MES buffer at pH 6.1, 2% bacto agar (BD, MD). The iron limited plates were supplemented with 50 µM ferrous ammonium sulfate, 1 µM copper sulfate, and 1mM of the iron chelator, ferrozine. The iron sufficient plates were supplemented with 350 µM ferrous ammonium sulfate, 1 µM copper sulfate, and 1 mM of iron chelator ferrozine. The copper sufficient plates were supplemented with 50µM ferrous ammonium sulfate, 500 µM copper sulfate, and 1 mM of iron chelator ferrozine. The final mixture to be added to the autoclaved agar was always filter sterilized using 0.22 µm pore stericups (Millipore, MA). The same volume (10 ul) of the final suspension was used to streak the various test plates. The plates were incubated at 30 °C for 72 hours, and then photographed.

2.7. Fet3p Oxidase Assay

The Fet3p oxidase assay measures the oxidase activity of Fet3p when loaded with copper that is delivered by ATP7B variants inserted in the yeast genome. This assay was modified from the original version described (Yuan et al., 1995). Yeast cells were inoculated into 5 ml of YPD. The culture was grown at 30°C for 20 hrs. Yeast cells were harvested, and then washed twice with filter sterilized deionized water (Millipore, MA). The yeast pellet was resuspended in low iron medium, and culture density was originally read at A_{600}. The culture was diluted in low iron media so that the final A_{600} was 0.5 OD in a total volume of 5 ml. The diluted culture was incubated at 30 °C for 3 hrs at 250 rpm. The culture was centrifuged at 4200 rpm for 15 minutes using a Beckman J6M1 centrifuge (CA, USA). The yeast pellet was then washed twice with filter sterilized deionized water (Millipore, MA).The yeast pellet was resuspended in 5ml of assay buffer containing 100 mM sodium acetate at pH 5.7, 1 mg/ml p-phenylenediamine dihydrochloride (pPD), 1 mM bathocuproine disulfonate (BCS). The starting cell density was determined by taking 100 ul of yeast suspension from each tube and reading at A_{600} using 96 well plate reader. The oxidase activity was determined by taking a small aliquot (about 600 ul) from each tube. Each aliquot was centrifuged to pellet down yeast cells and other debris. 250 ul of the supernatant was read at A_{520}. The ratio of A_{520}/A_{600} was calculated to determine the oxidase activity relative to cell density. The relative oxidase activity was then normalized to the wild type activity. This new version of the oxidase assay was validated using control variants that have been previously studied in our lab. D765N was selected as a control variant that showed normal oxidase

activity in the gel-format fet3p oxidase assay. CPC and T997M were used as two variants that showed no oxidase activity in the gel-format oxidase assay.

2.8. Western Blotting

Yeast cells were inoculated into 5 ml of YPD. The culture was grown at 30 °C until a cell density of 1.0 OD_{600} was obtained. Yeast membrane fractions were prepared using a membrane protein extraction kit (MemPrep, Pierce, IL). The different membrane fractions were cleaned up using an SDS-PAGE Sample Prep kit (Pierce, IL). Alternatively, protein samples were prepared from total yeast cell lysate. Yeast total cell protein extracts were prepared using homogenization buffer consisted of 25 mM HEPES-NaOH pH 7.4, 150 mM NaCl, 1 mM DTT, and a protease inhibitor cocktail containing 30 μM leupeptin, 10 μM pepstatin A, 5 μM aprotinin and 1 mM EDTA. Cells from 10 ml of stationary culture were washed twice with ice-cold distilled water, followed by a wash with homogenization buffer. The cell pellets were resuspended in 200 μl of homogenization buffer. Cells were broken by vortexing in the presence of acid washed glass beads (425-600 micron diameter, Sigma) for a total of 5 min (10 cycles of 30 s of vortexing and 1 min on ice). The homogenate was centrifuged for 30 s at 1,000 or 10,000x g , to remove unbroken cells and heavy organelles. Protein samples were then quantified using Coomassie Plus Protein assay (Pierce, IL). Sodium dodecyl sulfate polyacrylamide gel electrophoresis (SDS-PAGE) was performed using a 4.5% stacking gel on top of a 7.5% running gel. 10 μg of protein sample were prepared in 3xSDS loading buffer containing 50 mM DTT and heated at 85°C for 10 minutes. Gels were run for 45 minutes at 200 mV in a Mini-Protean 3 Cell (BioRad, CA). Alternatively, the gels

were run for 3hrs at 4°C. The gels were then transferred onto nitrocellulose membranes using Mini Trans-Blot Electrophoretic Transfer Cell (BioRad, CA). The transfer was done at 30 mV for 16 hrs at 4°C in Towbin buffer containing 15% methanol, and 0.01% SDS. The membranes were then blocked for 3 hrs with 5% milk powder in Tri-buffered saline (TBS, 100mM Tris HCL PH7.5, 150mM NaCl, and 0.1% Tween-20), rinsed and washed in TBST (TBS containing 0.05% Tween-20) for 30 minutes. Membranes were then incubated with ATP7B primary antibody in TBST for 16 hrs at 4°C (Forbes and Cox, 1998), rinsed twice, and then washed with TBST for 30 minutes. Secondary antibody solution was prepared fresh in TBST buffer containing 4% milk powder. The concentrations of primary and secondary antibodies are indicated later with each figure. The membranes were incubated with the secondary antibody solution for 1 hour at room temperature, rinsed, and washed for 40 minutes in TBST at room temperature. Bound antibody was detected by enhanced chemiluminescence (ECL) using super signal substrate (Pierce, IL). The ECL was visualized by exposure to autoradiography films (Fuji, Tokyo) and Image Station 4000M supplemented with Molecular Imaging Software (Kodak, NY).

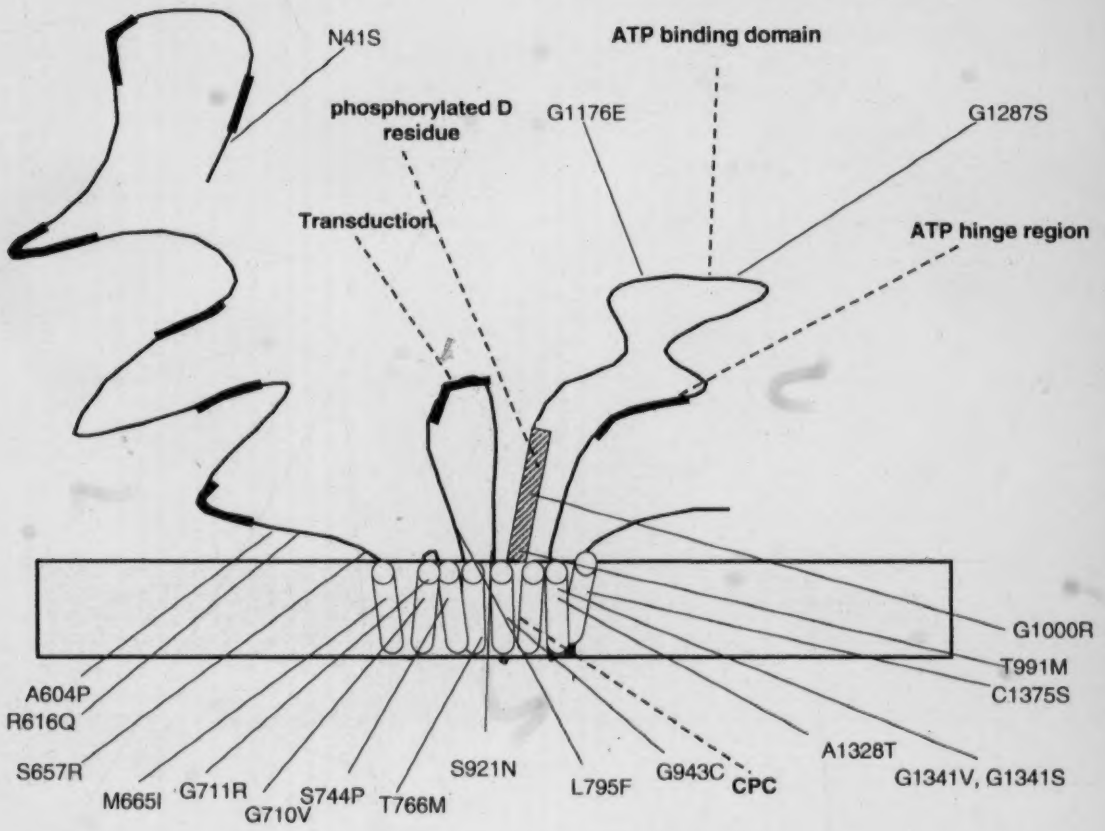

Model from Bull, P.C. and Cox, D.W. Trends in Genetics 10:246

Figure 2.2 ATP7B model showing variants analyzed in this thesis.

2.9. ATP7B Modeling Analysis

Selected ATP7B mutations were analyzed using a 3D model of ATP7B using the liquid structure of the N-terminal hinge region (Cu5, Cu6, Cu6/Tm1) (Achila et al., 2006; Dmitriev et al., 2006). The analysis was performed using Chimera software (http://www.cgl.ucsf.edu/chimera/).

3. Results

3.1. Construction of ATP7B Variants

21 ATP7B variants were selected from the Wilson disease mutation database (http://www.medicalgenetics.med.ualberta.ca/wilson/index.php). These variants were constructed in the bacterial system as described earlier. The sequencing results confirmed the desired mutations in all the variants. Yeast PCR results showed that 21 ATP7B variants were successfully integrated into the yeast genome (Tables 2.2 and 2.3). The Southern blot results showed that most of the constructs contained a single copy, except that M665I and G711R contained multiple copies. N41S, S744P, S921N, G943C, A1328T, G1341S, R1415Q are variants for which the Southern analysis did not provide enough data to decide on the copy number. The copy number analysis was performed using both chemiluminescence and radioactive probes. The data showed that using a radioactive probe is more sensitive to detect human *ATP7B* cDNA in the yeast genome as compared with the DIG-labelled probe (Fig 2.2).

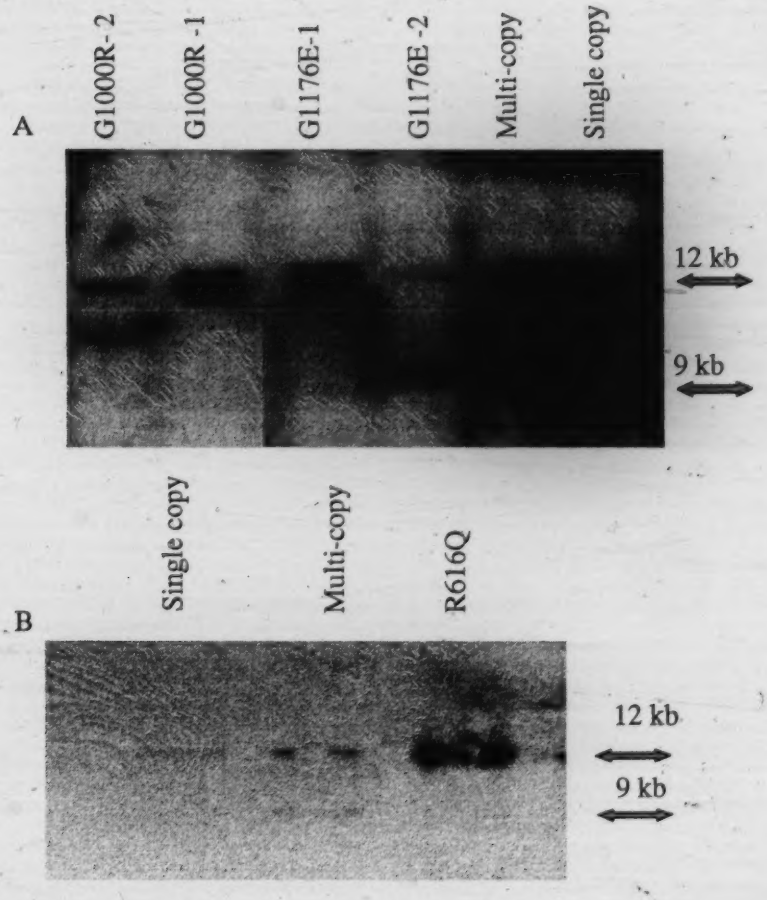

Figure 2.2: Southern blot analysis of selected ATP7B variants for information using radioactive and DIG-labeled probe.

ATP7B variants were integrated into the genome of *ccc2* mutant yeast. Southern blot, using ^{32}P-dCTP labeled probe (A) and DIG-labeled probe (B), was used to analyze copy number insertion. The yeast genomic DNA with single copy insertion shows a single 12 kb band. Multi-copy integration shows a 12 kb band as well as a 9 kb band of variable intensity.

3.2. Yeast Growth Assay

The yeast growth assay on low iron plates showed that 18 ATP7B variants were defective and three were normal. Figure 2.3 shows yeast growth in high copper, high iron and low iron agar plates for all ATP7B variants studied. Table 2.2 summarizes the results of the yeast growth assay for single copy variants. There are three apparently normal ATP7B variants: R616Q, L795F, and T991M. These three normal variants have single copy insertions. Table 2.3 shows that the two multi-copy variants, M665I and G711R, were defective in the yeast transport assay.

3.3. Western Blot Analysis

Western blot analysis was performed using a Mem-PER kit (Pierce) and total cell lysate from yeast cells. The Mem-PER kit was not effective in extracting ATP7B in the hydrophobic fraction (Figure 2.9). Thus, results obtained using the Mem-PER kit were only used for the analysis of expression, and not localization, of ATP7B in yeast variants. The method described for total cell lysate preparation was more effective in extracting ATP7B from yeast cells. Figure 2.10 and Figure 2.11 showed that all yeast variants express ATP7B. G1287S was the only variant not showing ATP7B expression using both (1,000g and 10,000g) centrifugation speeds. Table 2.4 summarizes the western blot results for the variants studied.

3.4. Yeast Oxidase Assay

The oxidase assay was performed directly on yeast cells and was presented as a percentage of wild type activity. The control variants (CPC and T977M) used to validate

this new version of the oxidase assay showed consistent results as compared to previous studies conducted in our laboratory using the gel-format oxidase assay. p.D765N that appeared normal in the gel-format showed 65% of wild type oxidase activity ($P<0.05$, t-test). Tables 2.2 and 2.3 show that 18 ATP7B variants had their oxidase activity reduced to less than 16% of wild type oxidase activity. p.G1341V showed 26.4% of wild type activity. p.R616Q and T991M have about 44% of wild type oxidase activity.

3.4. Modeling analysis

ATP7B missense mutations were analyzed using Chimera. This analysis showed that p.R616Q and p.A604 P are located in the hinge region of the N-terminal ATP7B. The side chain of R616 is extending outside the protein; however, p. A604 is totally embedded inside the hinge domain. This suggests that p.R616 is more exposed and the side chain is pointing outwards. Further analysis shows that p.A604 is localized on the backbone of β sheet. Proline mutation suggests that p. A604 P has more distorting effects on the intra-domain interaction and could lead to subsequent conformational changes that affect the transport activity of ATP7B (Figure 2.6).

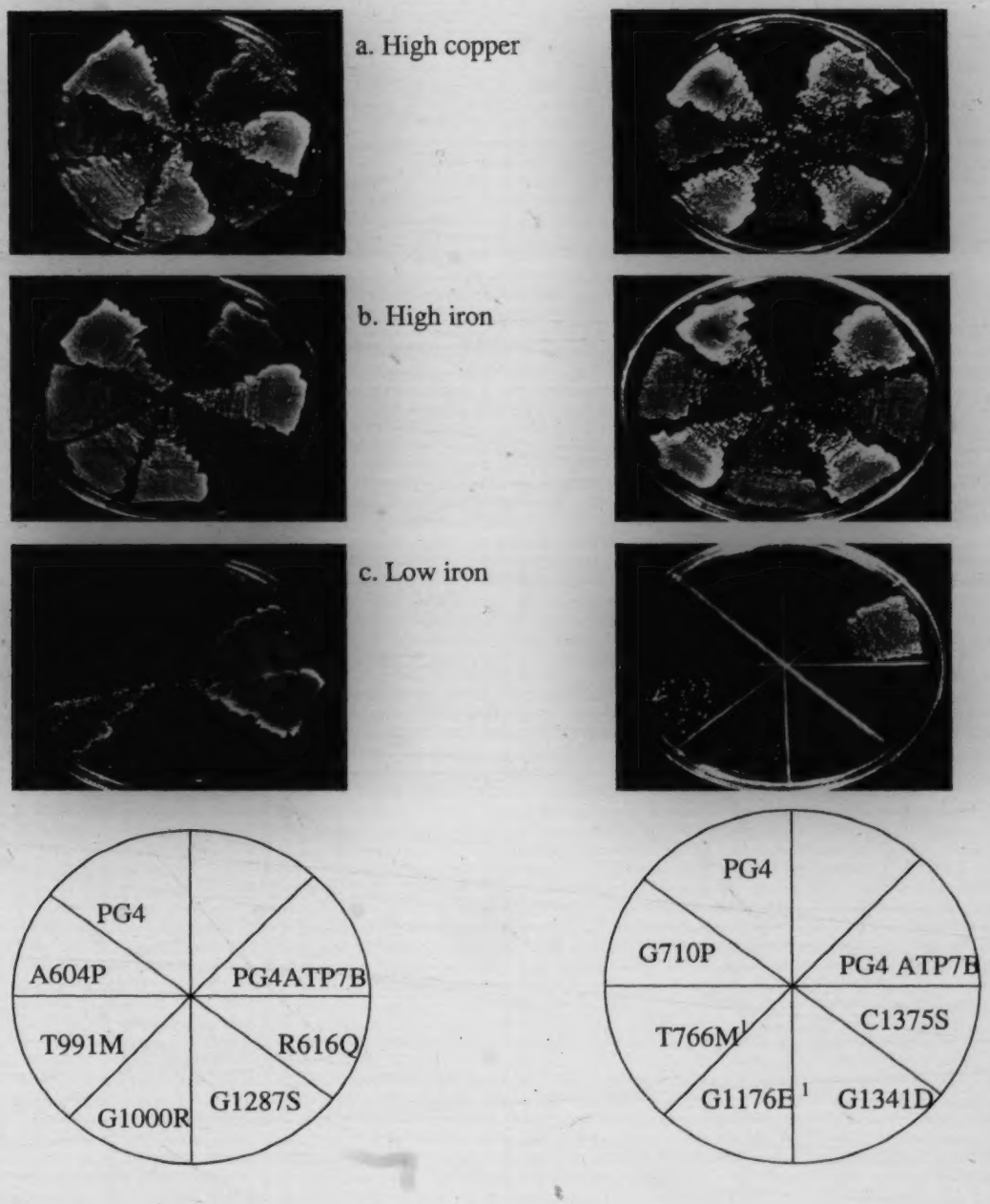

Figure 2.3.a yeast growth assay

ccc2 mutant yeast was transformed with empty vector (PG4), wild type ATP7B (PG4ATP7B) and ATP7B variants. Yeast cells were streaked on high copper plates (a), high iron plates (b) and low iron plates (c). Defective ATP7B variants have limited growth on low iron plates because of inadequate copper transport.[1] No true colonies were observed in the first 5 days

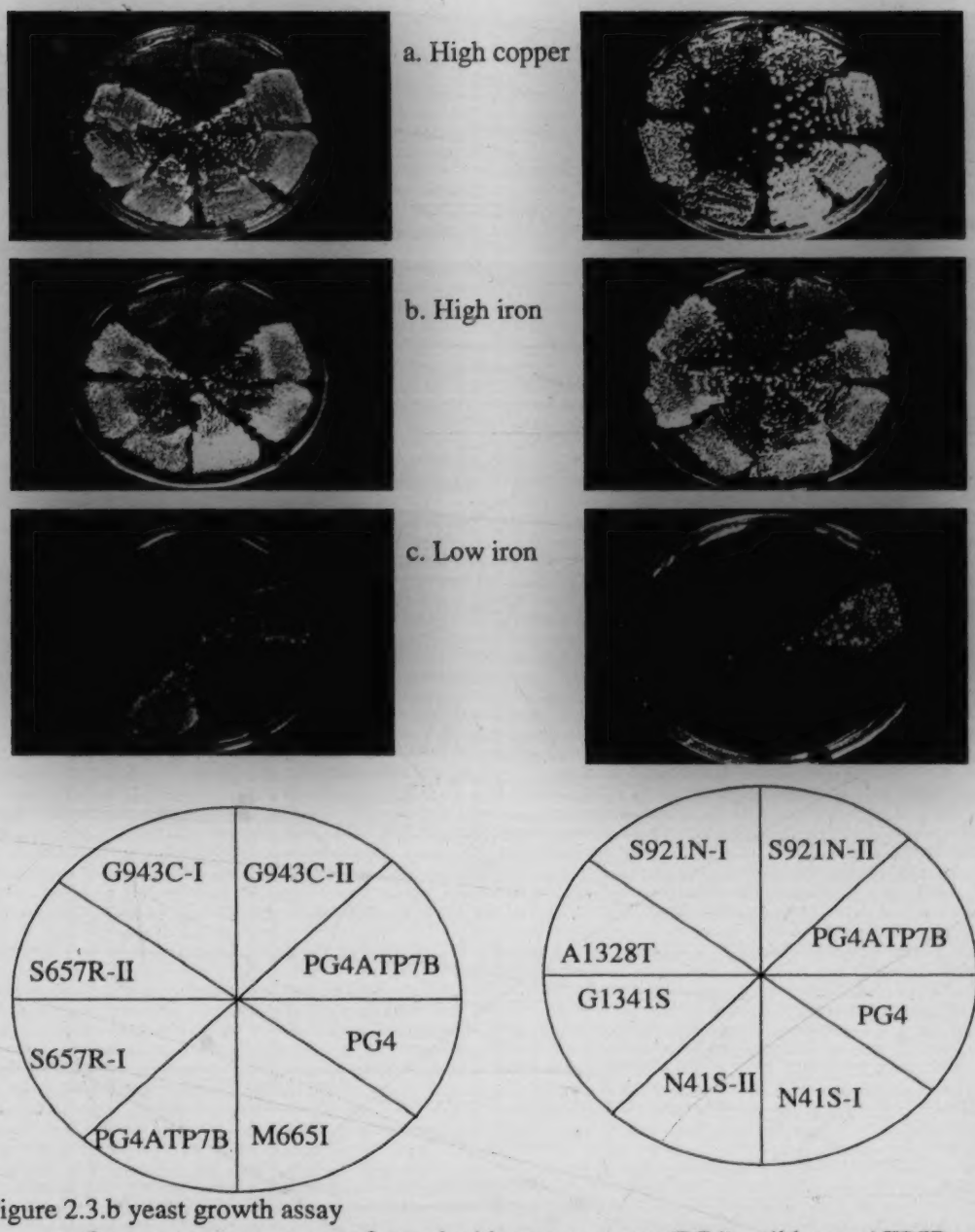

Figure 2.3.b yeast growth assay

ccc2 mutant yeast was transformed with empty vector (PG4), wild type ATP7B (PG4ATP7B) and ATP7B variants. Yeast cells were streaked on high copper plates (a), high iron plates (b) and low iron plates (c). (I) and (II) represent two independent colonies studied in the transport assay. Defective ATP7B variants have limited growth on low iron plates because of inadequate copper transport.

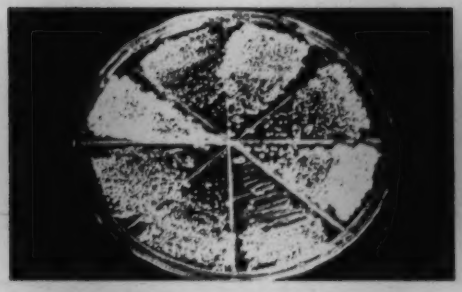

a. High Copper

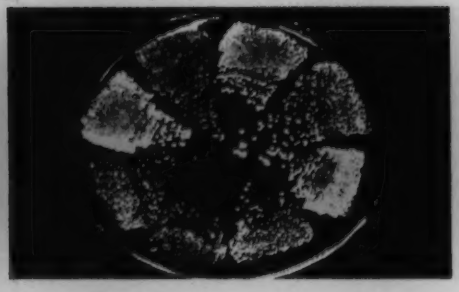

b. High iron

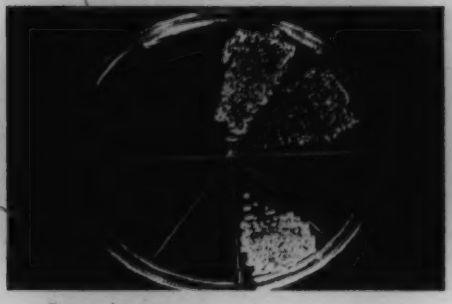

c. Low iron

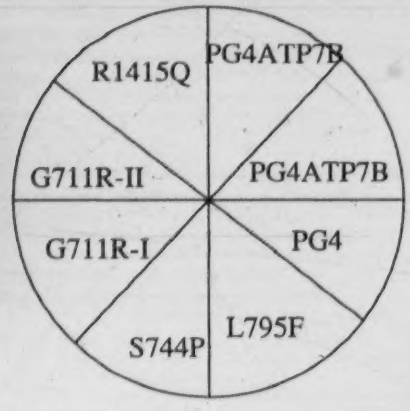

Figure 2.3.c yeast growth assay

ccc2 mutant yeast was transformed with empty vector (PG4), wild type ATP7B (PG4ATP7B) and ATP7B variants. Yeast cells were streaked on high copper plates (a), high iron plates (b) and low iron plates (c). (I) and (II) represent two independent colonies studied in the transport assay. Defective ATP7B variants have limited growth on low iron plates because of inadequate copper transport.

A

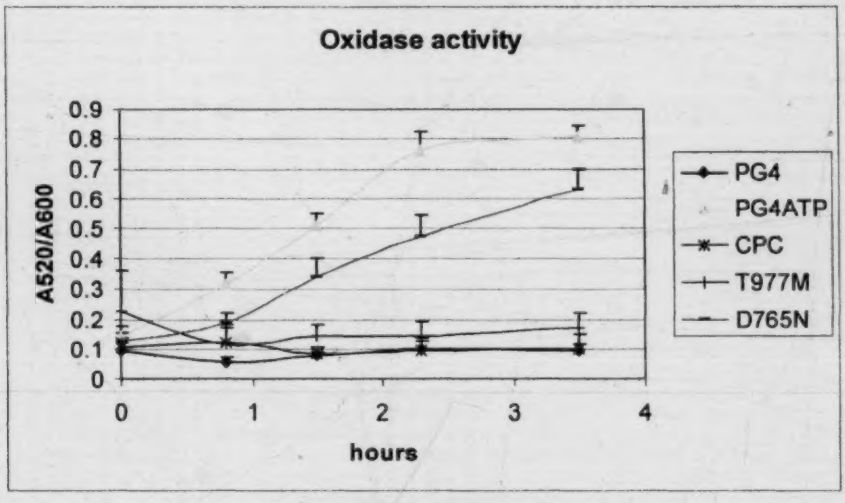

B

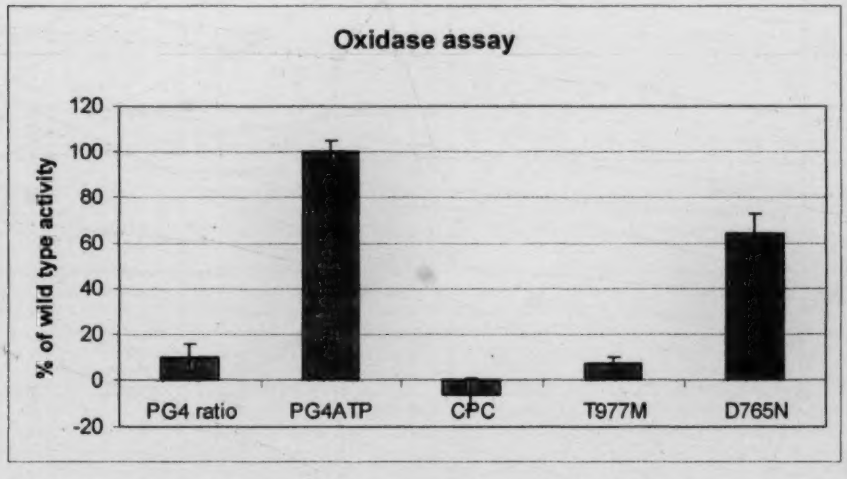

Figure 2.4 Oxidase activity of ATP7B control variants

Selected ATP7B variants were used to validate the 96-well plate oxidase assay. CPC and T977M are used as negative control. D765N is a normal variant and is used as a positive control. Oxidase activity curves (A) were used to calculate the rate of oxidase activity of each variant. Figure B shows the rate as a percentage of wild type activity. The t-test analysis indicated the following significant levels when compared with normal: CPC and T977M have $P < 0.0001$ and D765N has $P < 0.05$.

A.

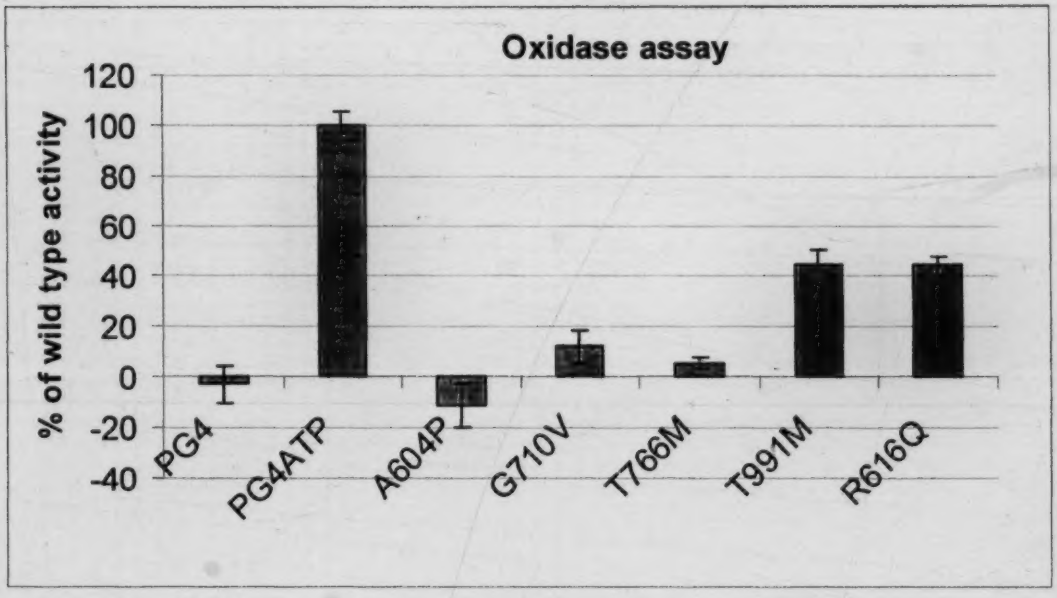

B.

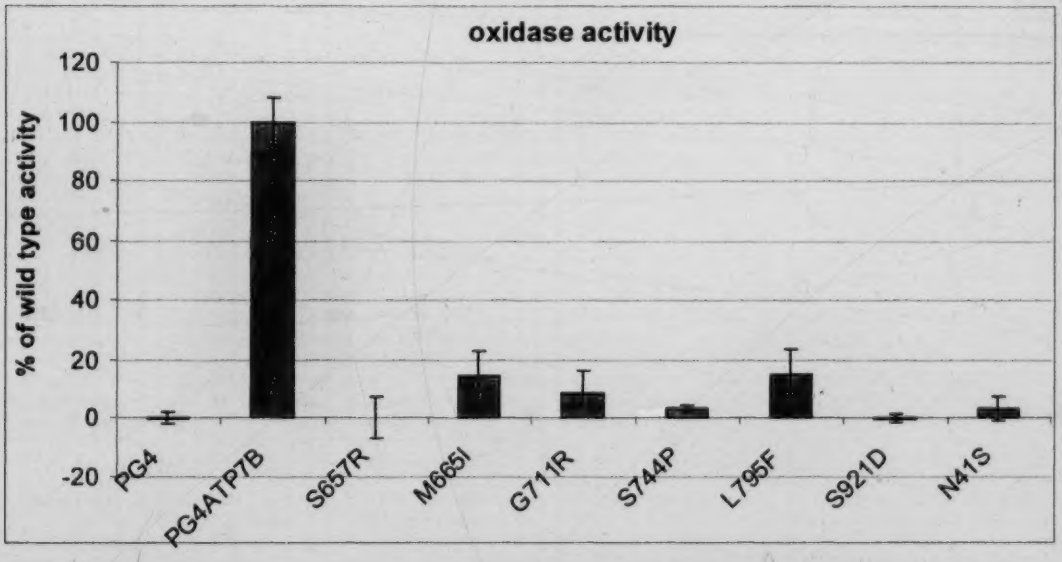

Figure 2.5 Oxidase assay of ATP7B variants compared with control (PG4ATP7B). The data represents the %of wild type activity ±standard deviation. The t-test analysis indicated the following significant levels when compared with wild type: all variants showed $P < 0.0001$ except for R616Q and T991M showed $P < 0.001$.

C.

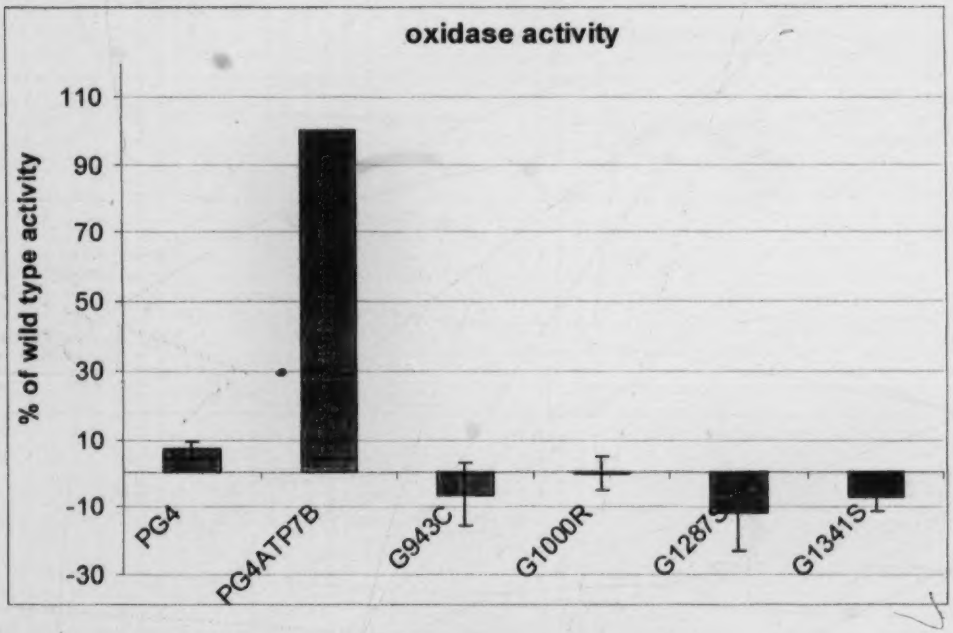

D.

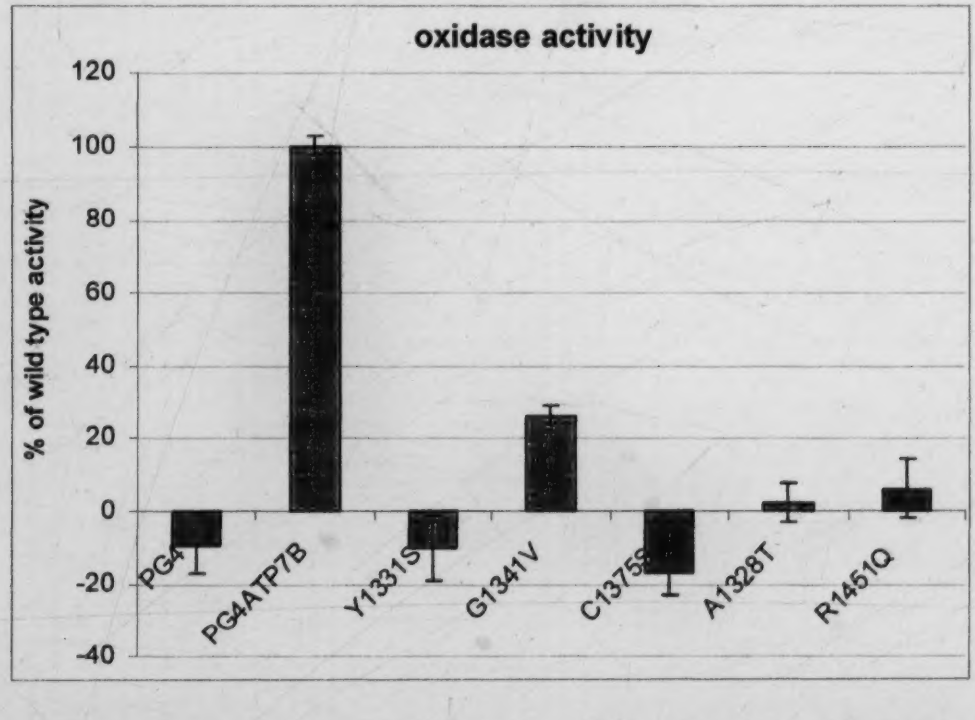

Figure 2.5 Oxidase assay of ATP7B variants (continued). The data represents the %of wild type activity ±standard deviation. The t-test analysis indicated the following significant levels when compared with wild type: all variants showed $P < 0.0001$ except for R616Q and T991M showed $P < 0.001$.

Table 2.2 Functional characterization for ATP7B single copy variants: Yeast growth assay and Fet3p oxidase assay.

Variant	Domain	Copy number[1]	Yeast assay[2]	Oxidase assay[3]
p.A604P	Cu6/ Tm1	Single	D	-11± 5
p.R616Q	Cu6/ Tm1	Single	N	44 ± 2
p.S657R	Cu6/ Tm1	Single	D	0 ± 4
p.G710V	Tm2	Single	D	12± 3
p.T766M	Tm4	Single	D	6 ± 1
p.L795F	Td	Single	N	15± 4
p.T991M	Ph	Single	N	45 ± 3
p.G1000R	Ph	Single	M	0 ± 3
p.G1287S	ATP loop	Single	D	-11 ± 6
p.G1176E	ATP loop	Single	D	-9± 5
p.G1341V	Tm7	Single	D	26± 2
p.C1375S	Tm8	Single	D	-16± 3

1: Copy number was analyzed by Southern blot analysis. These variants were all single copy variants.
2: (D), (N), and (M) indicate defective, normal and moderate phenotype in yeast growth assay respectively.
3: The oxidase activity is presented as a percentage of wild type activity ±SEM ($P<0.05$, t-test).

Table 2.3 Functional characterization of ATP7B multiple or unknown copy number variants:

ATP7B variants studied in yeast growth assay and Fet3p oxidase assay.

Variant	location	Copy number[1]	Yeast assay[2]	Oxidase assay[3]
p.N41S	N-ter	N/A	D	3 ± 2
p.M665I	Tm1	Multiple	D	15 ± 4
p.G711R	Tm2	Multiple	D	8 ± 4
p.S744P	Tm3	N/A	D	3 ± 1
p.S921N	Td	N/A	D	0 ± 1
p.G943C	Tm5	N/A	D	-3 ± 13
p.A1328T	Tm7	N/A	D	3 ± 6
p.G1341S	Tm7	N/A	D	-7 ± 2
p.R1415Q	3'COOH	N/A	D	6± 4

1: Copy number was analyzed using Southern blot. (N/A) indicates variants where Southern blot analysis did not provide enough information to determine the copy number. These variants had ATP7B inserted in their genome as shown by yeast PCR. (Multiple) indicates yeast variants that showed multiple copy insertions of human ATP7B cDNA in their genome.

2: (D), (N), and (M) indicate defective, normal and moderate phenotype in yeast growth assay respectively.

3: The oxidase activity is presented as a percentage of wild type activity ±SEM. ($P<0.05$, t-test).

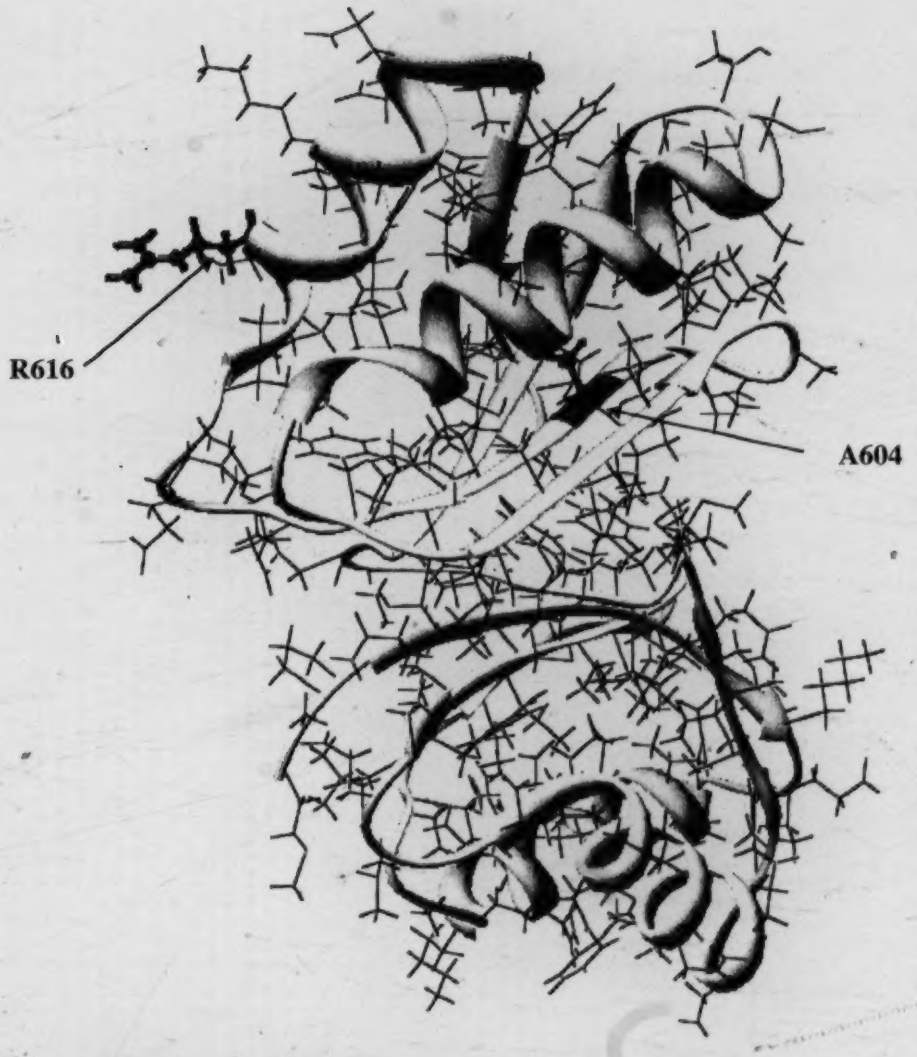

Figure 2.6 Analysis of R616Q and A604P using Chimera software

The Figure above shows a 3D structure of Cu5, Cu6, and the N-terminal hinge (Cu6/Tm1) of ATP7B (Achila et al., 2006; Dmitriev et al., 2006). A604P is embedded in the N-terminal hinge suggesting that it might be involved in the regulation of the transport mechanism of ATP7B. R616Q is a more superficial residue could be involved in interaction of ATP7B with other proteins.

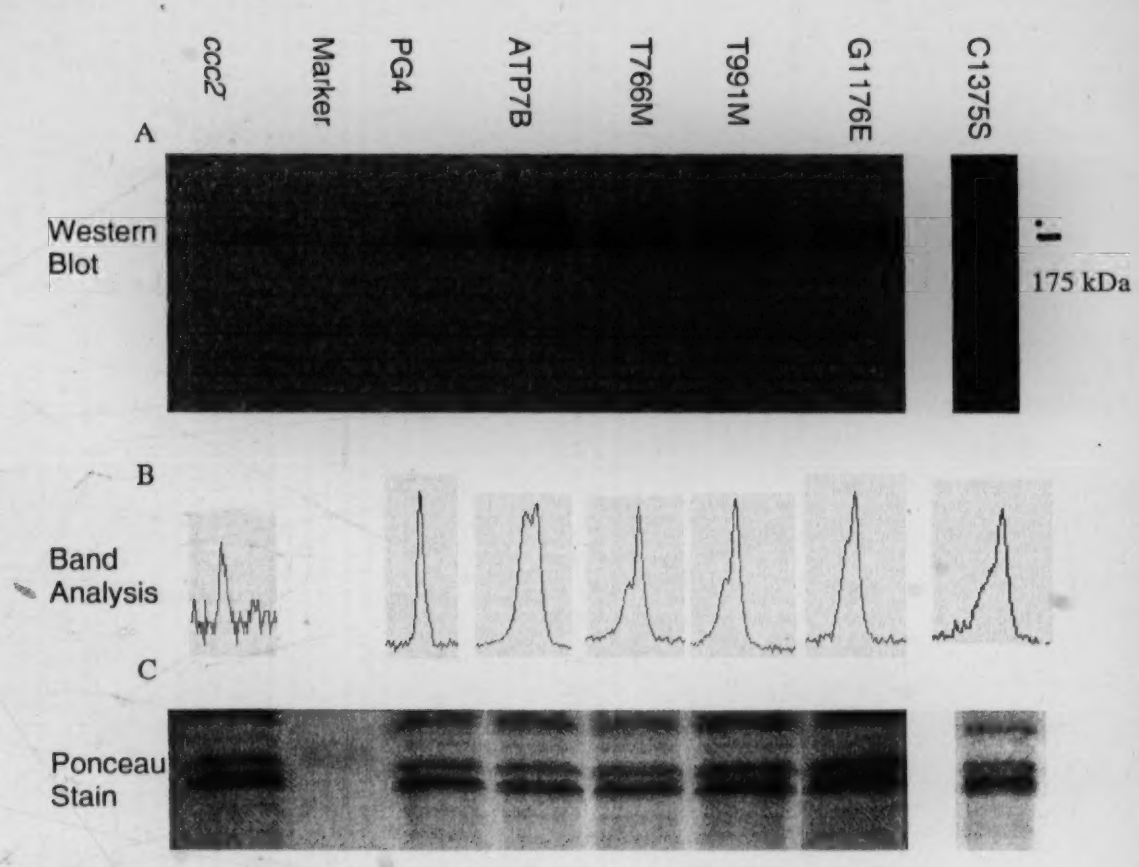

Figure 2.7 Western blot analysis and band analysis of ATP7B variants using MemPrep kit.

ATP7B variants were expressed in *ccc2* mutant yeast cells. Protein samples were prepared using MemPrep kit. 25 μg of the hydrophobic fractions were separated using PAGE run at 200mv for 45 minutes. A, Western blot using N-terminal ATP7B antibody. ATP7B band was obtained at a size of 175 kDa (dot). A cross reactive band was also obtained at a similar size (dash). The intensity of each band was analyzed using molecular imaging software (Kodak). Each peak represents an individual band (B). Ponceau stain was used to show equal loading (C).

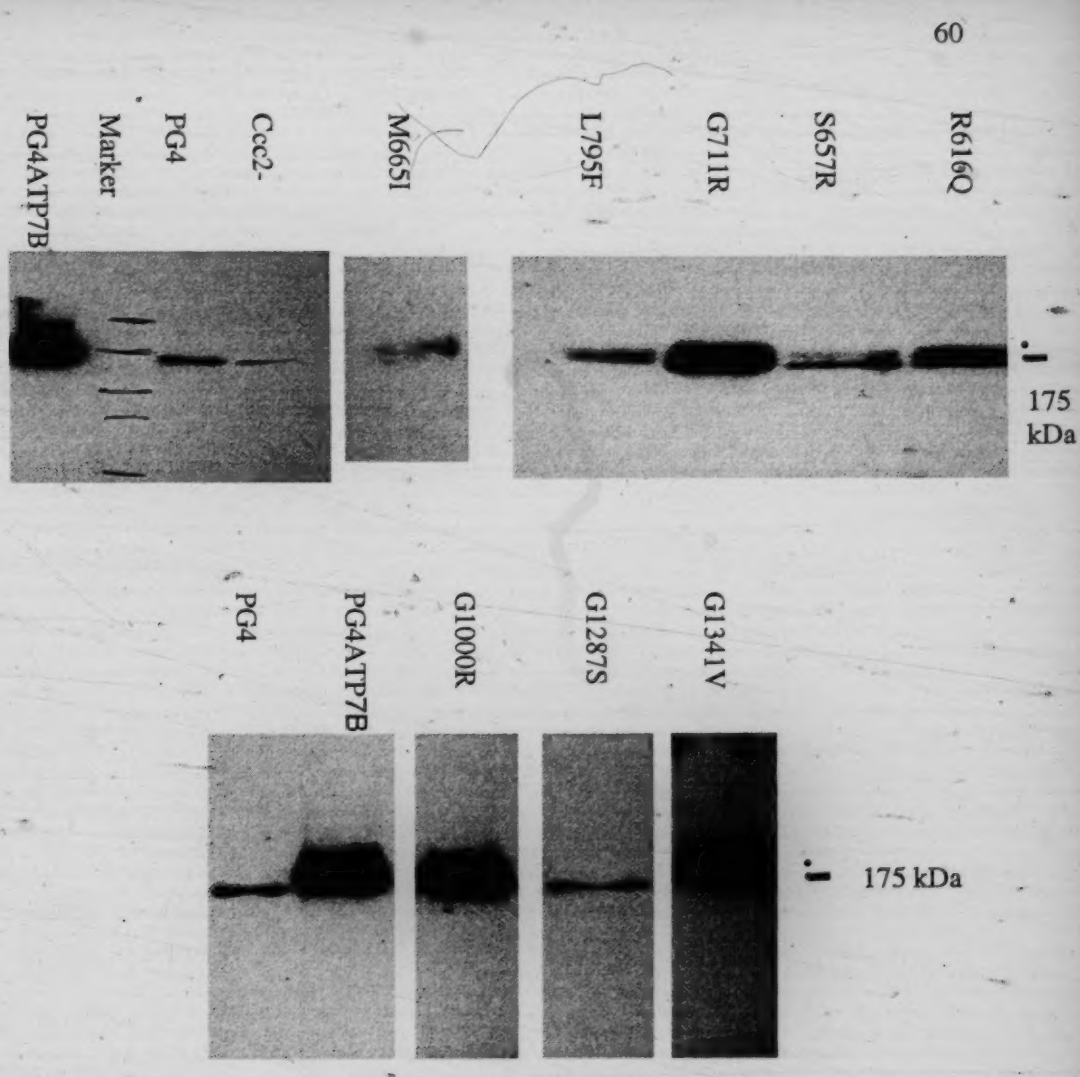

Figure 2.8 Western blot analysis of ATP7B variants using Mem-PER kit

ATP7B variants were expressed in *ccc2* mutant yeast. 25 µg of the hydrophobic fractions were separated using SDS- PAGE run at 200 mv for 45 min as extracted in Fig 2.8. N-terminal ATP7B antibodies was applied to the blots. Dot: indicates ATP7B band. Dash: indicates a crossreactive band as shown in Fig 2.8.

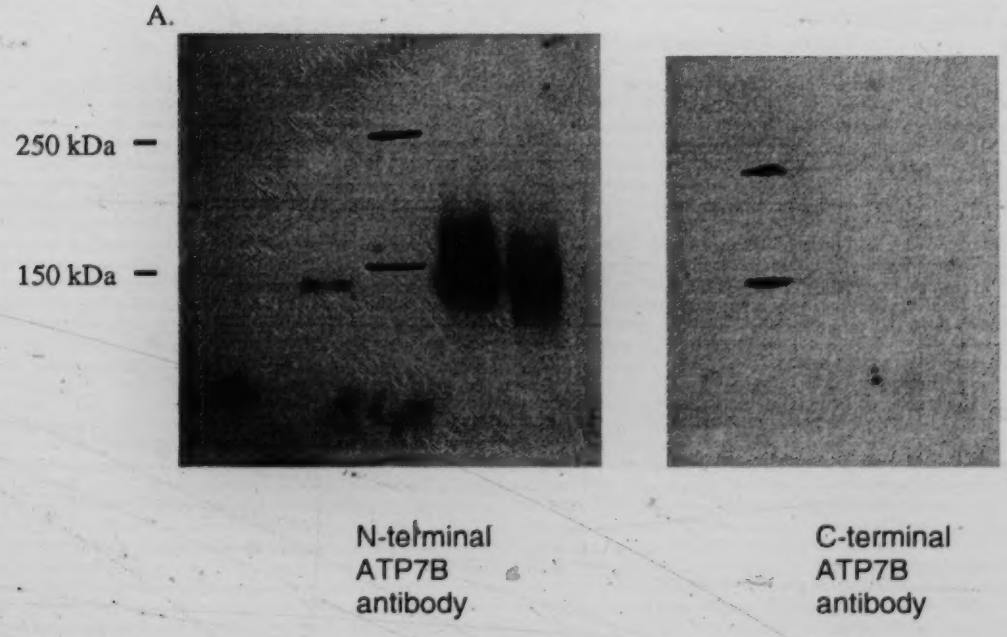

Figure 2.9 Western blot analysis of the hydrophilic and hydrophobic membrane fractions using Mem-PER for information on cross reactive component.

10μg of hydrophilic protein fractions (H) and membrane protein fractions (M) were separated using PAGE running for 3hrs at 4 °C. N-terminal (A) and C-terminal (B) ATP7B antibodies were applied on blots as in Fig 2.8 and 2.9.

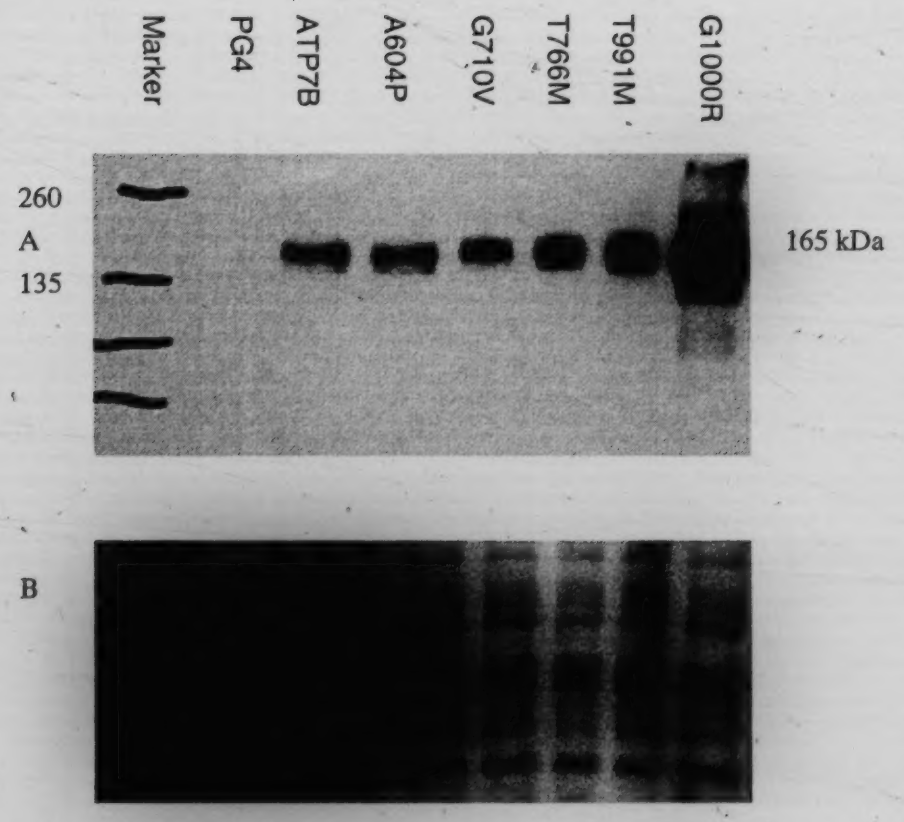

Figure 2.10 Western blot analysis of selected ATP7B variants using a modified protocol for protein extraction.

ATP7B variants were expressed in *ccc2* mutant yeast cells. A, Western blot using N-terminal ATP7B antibody applied on the blots of the total cell lysate as described in materials and methods. B, Ponceau stain was used to show loading concentrations. Note that contaminant is not observed.

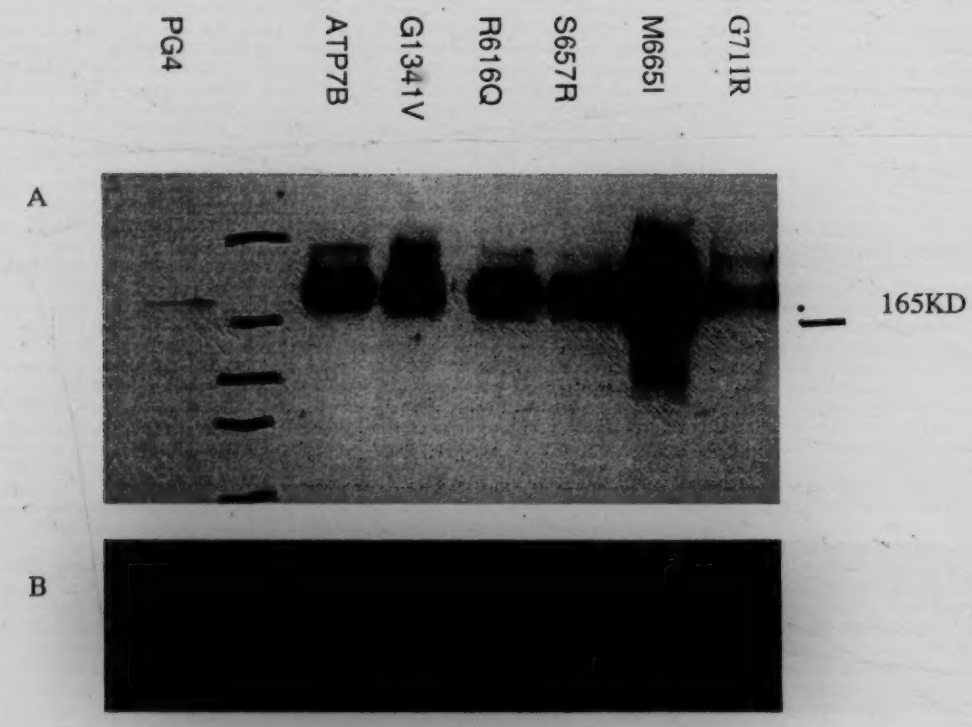

Figure 2.11 Western blot analysis of selected ATP7B variants using a modified protocol for protein extraction.

ATP7B variants were expressed in *ccc2* mutant yeast cells. A, Western blot using N-terminal ATP7B antibody applied on the blots of the total cell lysate as described in materials and methods. B, Ponceau stain was used to show loading concentrations. Note that contaminant is not observed.

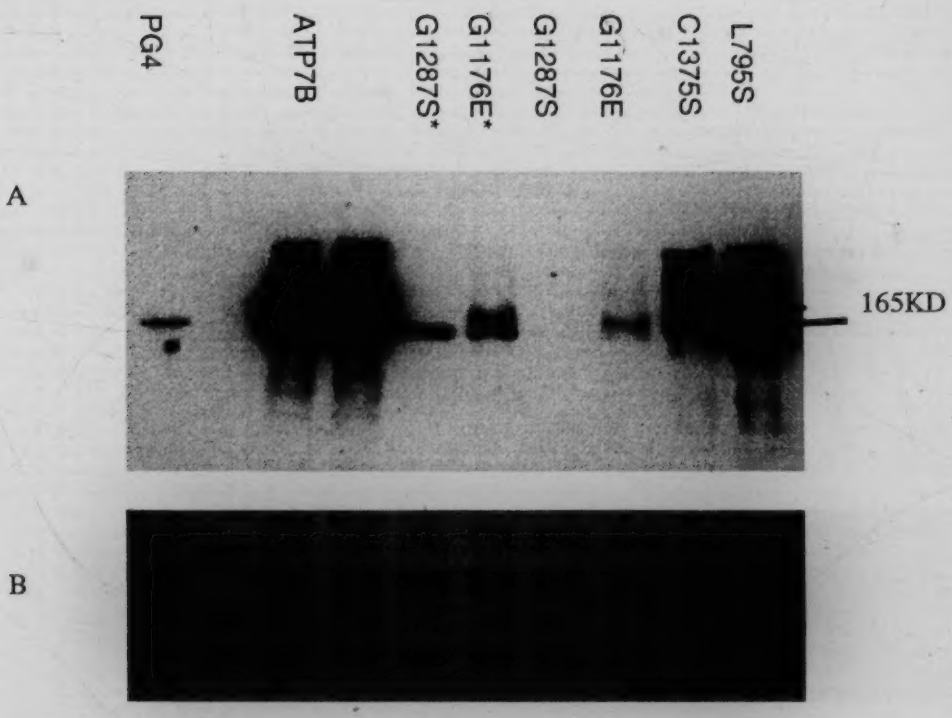

Figure 2.12 Western blot analysis of selected ATP7B variants using a modified protocol for protein extraction.

ATP7B variants were expressed in *ccc2* mutant yeast cells. A, Western blot using N-terminal ATP7B antibody applied on the blots of the total cell lysate prepared at 10,000xg as described in materials and methods using a . Asterisk: indicates total cell lysate prepared at 1,000xg. B, Ponceau stain was used to show loading concentrations. Note that contaminant is not observed.

Table 2.4 Summary of functional characterization of ATP7B variants

Variant	location	Copy number[1]	Western Blot[2]	Yeast assay[3]	Oxidase Activity[4]	Conclusion[5]
p.R616Q	Cu6/ Tm1	Single	+	N	44%	Not defective
p.S657R	Cu6/ Tm1	Single	+	D	-0.03%	Defective
p.T766M	Tm4	Single	+	D	5.6%	Defective
p.L795F	Td	Single	+	N	15.37%	Defective
p.T991M	Ph	Single	+	N	44.56%	Not defective
p.G1000R	Ph	Single	+	D	-0.07%	Defective
p.G1176E	ATP loop	Single	+	D	-9.6%	Defective
p.G1287S	ATP loop	Single	-	D	-11.77%	Probable defective
p.G1341V	Tm7	Single	+	D	26.4%	Defective
p.C1375S	Tm8	Single	+	D	-16.8%	Defective
p.M665I	Tm1	Multiple	+	D	14.61%	Defective
p.G711R	Tm2	Multiple	+	D	8.42%	Defective

1: Copy number analysis using Southern blot.
2: (+) indicates that ATP7B band was detected in the western analysis.
3: (N) and (D) indicate normal and defective phenotype in the yeast assay, respectively.
4: The oxidase activity is presented as a percentage of wild type activity
5: Indicated the overall assessment of the effect of each missense variants on the transport activity of ATP7B.

Table 2.5 Analysis of the biochemical changes of ATP7B missense variants studied in yeast transport assay

Variant	Domain	Mass shift	Expected amino acid	Altered amino acid	SIFT -cor[1]	Transport function
p.A604P	Cu6/ Tm1	26	Non-polar, weakly hydrophobic	hydrophobic, non-polar, cyclic	D	Defective
p.R616Q	Cu6/ Tm1	-28	basic, polar, hydrophilic, (+) charged	Polar, hydrophilic, non charged	D	Not defective
p.S657R	Cu6/ Tm1	69	polar, uncharged, OH group	Basic, polar, hydrophilic, (+) charged	D	Defective
p.M665I	Tm1	-18	hydrophobic, non-polar	Hydrophobic, non polar, non charged	D	Defective
p.G710V	Tm2	42	Non-polar, weakly hydrophobic	hydrophobic, non-polar	N	Defective
p.G711R	Tm2	99	Non-polar, weakly hydrophobic	Basic, polar, hydrophilic, (+) charged	D	Defective
p.T766M	Tm4	30	hydrophilic, polar, uncharged, OH group	hydrophobic, non-polar	D	Defective
p.L795F	Td	34	hydrophobic, polar, (+) charged	hydrophobic, non polar, non charged	D	Defective
p.T991M	Ph	30	hydrophilic, polar, uncharged, OH group	hydrophobic, non-polar	D	Not defective
p.G1000R	Ph	99	non-polar, weakly hydrophobic	hydrophilic, basic	D	Defective
p.G1176E	ATP loop	72	non-polar, weakly hydrophobic	hydrophilic, acidic	D	Defective
p.G1287S	ATP loop	30	non-polar, weakly hydrophobic	polar, uncharged, OH group	D	Probable defective
p.G1341V	Tm7	42	non-polar, weakly hydrophobic	hydrophilic, non-polar	D	Defective
p.C1375S	Tm8	-16	hydrophilpc,polar, uncharged, sulfhydryl	polar, uncharged, OH group	D	Defective

1: (D) is predicted to be deleterious (< 0.05) and (N) is predicted to be a normal variant.

Discussion

ATP7B is required to provide copper to Fet3p in the yeast *ccc2* knock out BJ2168 strain. Fet3p loaded with copper (holo-Fet3p) is involved in high affinity iron transport. Therefore, functional ATP7B is essential for yeast growth in low iron medium. Fet3p is involved in iron transport through oxidizing Fe (II) to Fe (III). The oxidase activity of Fet3p depends on copper loading by ATP7B.

A yeast agar plate assay was used to identify ATP7B variants that are altered in their transport activity. Defective ATP7B variants cannot complement for *ccc2* deficiency, therefore yeast colonies will not grow on low iron plates. Fet3p oxidase assay is another tool used to determine the transport activity of ATP7B variants in yeast. The Cox lab has used membrane proteins extracted from yeast cells to determine the oxidase activity of Fet3p (Forbes and Cox, 1998). Fet3p is a membrane protein that requires meticulous preparations for Fet3p to be isolated in its active form. Furthermore, this assay includes separating protein samples in polyacrylamide gel without disrupting the functional activity of Fet3p. The sensitivity of this assay is also limited, as noted with D765N that showed normal oxidase activity in the gel format (Forbes and Cox, 1998).

I have developed a new version of the oxidase assay that uses a 96-well plate format. The ferroxidase domain of Fet3p is localized to the external cell surface (De Silva et al., 1995). This domain oxidizes p-phenylenediamine dihydrochloride substrate (pPD) and changes the initially clear oxidase assay solution to dark brown. The assay quantifies the oxidase activities of each variant that can be presented as a percentage of the wild type oxidase activity. This study showed that the oxidase assay can be carried

out using intact yeast cells and the oxidase activity of Fet3p measured in a 96-well plate format. The 96-well plate oxidase assay was validated using control mutants that were studied previously in the gel format oxidase assay and yeast growth assay. p.T977M and CPC (Cysteine- Proline-Cysteine) were selected as control variants with limited oxidase activity and p.D765N with normal oxidase activity as compared with the wild type (Forbes and Cox, 1998). p.T977M and CPC were found to have less than 10% wild type oxidase activity. Although my results correlate well with Forbes et al., (1998) where he used the gel format to determine the oxidase activity of these variants, p.D765N showed 65% of wild type oxidase activity. Therefore, the 96-well plate assay is more sensitive than the and can be used as a quantitative tool to determine the oxidase activity of ATP7B variants.

I studied 21 ATP7B variants in the yeast growth assay. Eighteen variants were concluded to be defective. These variants are located in various domains of ATP7B, mostly in the transmembrane regions. Transmembrane domains are more sensitive than other ATP7B domains to missense mutations as they are embedded in the plasma membrane and depend upon strict interactions to maintain the appropriate conformation that is required for the transport mechanism of ATP7B.I hypothesize that missense mutations that weaken the hydrophobicity of these domains would be more deleterious to the transport activity of ATP7B and might be associated with disease. The 21 variants were also studied in the oxidase assay and 19 were shown to limit the oxidase activity of Fet3p. The defective variants are localized as follows: p.N41S in the N-terminus end; p.A604P, and p.S657R in the hinge region (Cu6/Tm1); p.M665I, p.G710V, p.G711R, p.S744P, p.T766M, p.G943C, p.C1375S, p.A1328T, p.G1341V and p.G1341S in

transmembrane regions; p.S921N and p.G1000R in the transduction domain; p.G1176E and p.G1287S in the ATP loop; p.R1415Q in the C-terminus (Tables 2.2 and 2.3).

Yeast proteins were prepared using a MemPrep kit as discussed earlier. This kit extracts membrane proteins in a hydrophobic fraction and cytosolic proteins in a hydrophilic fraction. ATP7B was contained mostly in the hydrophilic fraction. This contradicts with the fact that ATP7B is a membrane protein and should be localized to the hydrophobic fraction. In a previous study, this kit was shown to drop its sensitivity from 90% for Cox 4 (cytochrome oxidase subunit 4) which has 1 transmembrane domain to 45% for flotillin that has two transmembrane domains (http://www.piercenet.com/products/). ATP7B is a membrane protein with eight transmembrane domains. Thus, this kit is not appropriate for ATP7B extraction. Alternatively, western blotting was performed on protein samples obtained from total cell lysate. This preparation shows less cross reactivity with other proteins when using an N-terminal antibody. Therefore, the data obtained from Mem-PER will be used only for expression analysis and not to determine any improper localization of ATP7B in yeast cells induced by the missense mutations. ATP7B expression was also determined based on results obtained from total cell lysate using a modified protein preparation protocol.

p.S657R, p.T766M, p.G1000R, p.G1176E, p.G1341V, p.C1375S are single copy variants that showed a defective phenotype in the growth and oxidase assays. The western analysis shows that ATP7B is being expressed at its appropriate size. Therefore, these six missense mutations hinder the transport activity of ATP7B. p.G1287S is a single copy variant that is defective in yeast growth assay and the oxidase assay.

p.G1287S shows no ATP7B band in the western blot analysis. This could be explained in two different ways. The first explanation suggests that p.G1287S expresses ATP7B that is mislocalized and thus not extracted in the regular preparation of membrane proteins using total cell lysate. Thus, ATP7B might be contained in the pellet. I tried to extract ATP7B from the pellet using a reduced centrifugation speed (1,000xg). Results showed that there was no ATP7B detected for p.G1287S using both (10,000xg and 1,000xg) centrifugation speeds. Therefore, p.G1287S might be expressing a form of ATP7B that is degraded at the level of the mRNA or the protein. p.M665I and p.G711R were both multiple copy variants that were defective in the yeast assay and in the oxidase assay. The PCR and southern results showed that *ATP7B* is successfully inserted into the genome. The western blot results show that these two variants express ATP7B at the appropriate size. The defective phenotype of these variants suggests that these missense mutations are deleterious to the transport activity of ATP7B.

p.R616Q and p.T991M are two ATP7B variants that showed a normal phenotype in the yeast growth assay. p.R616Q and p.T991M both have 44% of wild type oxidase activity. It is critical to decide on the percentage of oxidase activity that represents the normal phenotype. According to Forbes et al, p.D765N, reported as a disease causing variant, was characterized as a normal variant based on the growth and oxidase assay (Forbes and Cox, 1998). In my assay, this variant has 65% of wild type oxidase activity. Thus, p.R616Q and p.T991M would be considered as normal variants according to oxidase assay. Wilson disease patients are affected by these missense mutations in a more complicated pathway that involves all aspects of ATP7B function. The yeast assays measure the transport aspect only, and in a yeast system. Therefore, although

these two variants show an oxidase activity close to the wild type, they might have a deleterious effect on the human liver when considering the overall function of ATP7B over the life of the patient.

p.N41S, p.S744P, p.S921N, p.G943C, p.A1328, p.G1341S, and p.R1415Q were defective in both growth and oxidase assays. Although, yeast PCR confirms that these variants contain ATP7B in their genome, there was not reliable information from the Southern analysis of these variants to determine the copy number. The defective phenotype of these variants in the yeast assay suggests that these amino acid residues are involved in the transport activity of ATP7B.

ATP7B modeling techniques represent a useful tool to characterize certain ATP7B variants. R616Q and A604P are two ATP7B variants that are located in the same domain and are only 12 amino acids apart. The PDB (Protein Data Bank) file for the N-terminal hinge region (Cu6/Tm1) was analyzed using the Chimera program. The amino acid p.R616 is more exposed and the side chain is pointing outwards suggesting a possible role in interaction of ATP7B with other proteins. This region of the protein is thought to be involved in interaction with dynactin subunit p62 (Lim et al., 2006) and possibly ATOX1 (van Dongen et al., 2004). The side chain of p.R616 is less likely to be involved in interactions with amino acid residues within the same domain (N-terminal hinge region). I hypothesize that R616 might be involved in the interaction of ATP7B with other proteins, mainly dynactin subunit p26. In the yeast assay p.R616Q was not involved in the transport activity of ATP7B. I suggest that further work on p.R616Q is needed to determine its effect on other aspects of ATP7B functions mainly, trafficking. The amino acid p.A604 is embedded in the hinge domain. This suggests a lesser role of

this residue in the interaction of ATP7B with other proteins. The analysis of the secondary structures associated with ATP7B shows that p.A604 is located in a β-sheet. The amino acid proline disrupts protein folding. Missense mutations that lead to a proline in active domains of a protein are usually associated with disease (Garcia-Rio et al., 2005). The yeast assay shows that p.A604P is defective in transport. p.A604 might be crucial for the transport mechanism and thus, when mutated into proline, the transport activity of ATP7B is distorted.

CHAPTER 3

COMPUTATIONAL ANALYSIS OF ATP7B MISSENSE VARIANTS

1. Introduction

ATP7B is a P–type ATPase that transports copper across membranes (Bull et al., 1993). Members of this protein family include well characterized proteins such as the calcium transporter Sarco/Endoplasmic Reticulum Ca^{2+}-ATPase (SERCA1) (Arguello et al., 2007). The structural information available on SERCA1 as well as other members of the ATPase family was used to highlight structural properties of ATP7B. Homology modeling was used to generate a 3D structure of ATP7B. Furthermore, the structure of separate domains of ATP7B was also generated (Achila et al., 2006; Dmitriev et al., 2006). The structural information that could be inferred for ATP7B represents significant data to integrate structural properties into the analysis of missense variants of ATP7B.

Copper transporters are identified throughout species from bacteria to humans. Non-bacterial species such as *C. elegans* have two copper transporters ATP7A and ATP7B. Aligning ATP7B homologous sequences generates a significant database of evolutionary variation that can be used to determine amino acid residues that are conserved. In this study, I used two sets of multiple sequence alignments. The default alignment is generated by the program as discussed later. The corrected alignment is the one selected manually and containing true ATP7B orthologues and paralogues as indicated in Table 3.1.

PolyPhen, SIFT, and Align-GVGD are three prediction programs that combine different evolutionary and biochemical properties. Prediction scores become much more

accurate when they include biochemical properties of the query protein as well as information on conservation across species (Nakken et al., 2007). The availability of adequate sequence, biochemical and structural data for ATP7B allows the analysis of the missense variants using these three different scores.

More than 50 ATP7B missense variants have been characterized by functional assays. Those that were shown to be defective could present an interesting tool to compare the three prediction scores. In this study, I compare the three predictive scores in both default and corrected settings in predicting defective and normal ATP7B variants. Then, I use the most accurate scores to analyze suspected non-disease causing ATP7B variants.

2. Materials and Methods

2.1. Prediction Programs used

2.1.1. PolyPhen

The PolyPhen (Polymorphism Phenotyping) (Ramensky et al., 2002) methodology was described in the general introduction in chapter 1. PolyPhen analysis was performed using a program available on the internet (http://genetics.bwh.harvard.edu/pph/). The amino acid sequence of ATP7B was entered and the Protein Data Bank (PDB) searched for homologous sequences with default settings as follows: structural database, PDB; sort hits by, identity; map to mismatch, no; calculate structural parameters, for first hit only; calculate contacts, for all hits; minimal alignment length, 100; minimal identity in alignment, 0.5; maximal gap length in alignment, 20; threshold for contacts, 6. The outcome of PolyPhen analysis for each

ATP7B variant entered could be "benign", "possible damaging", "probably damaging", and "unknown". In this study "possible damaging" and "probably damaging" were both classified as defective variants as recommended by the software.

2.1.2. SIFT

SIFT (Sorting Intolerant From Tolerant) considers the position at which the change occurred and the type of amino acid change (Ng and Henikoff, 2003). Normal ATP7B sequence and ATP7B missense variant sequences were entered into an automated program available online (http://blocks.fhcrc.org/sift/SIFT.html). The selected variants were analyzed in two different ways. The default SIFT scores were obtained using default settings (Select database to search: SWISS-PORT 51.3 and TREMBL 34.3, Median conservation of sequences: 3.00, Remove sequence more than 90% identical to query). SIFT generates its own multiple sequence alignment from the homologous sequences available in the database at the time the analysis was done. A second SIFT analysis (corrected SIFT) was performed using selected sequence alignment as indicated in Table 3.1

2.1.3. Align GVGD

Align GVGD (Align Grantham Variation Grantham Deviation) methodology was described in the introduction and elsewhere (Tavtigian et al., 2006). Align GVGD analysis for selected ATP7B variants was obtained through a program available on the internet (http://agvgd.iarc.fr/agvgd_input.php). The multiple sequence alignment used for this analysis was generated in two different ways. The default scores used multiple sequence alignment generated through the SIFT program using default settings as

indicated above. The second set of data was obtained using the corrected alignment as indicated in Table 3.1.

Table 3.1 shows various proteins used for the multiple sequence alignment for ATP7B. The sequences were obtained from several sources including: NCBI (National Center for Biotechnology Information), Swiss Port and TrEMBLE (Translated European Molecular Biology Laboratory). PolyPhen uses a default alignment that contains few duplicates. Alignment used in SIFT and Align-GVGD analysis could be manipulated. 'Yes' means that sequence was included in the analysis. 'No' means that the sequence was not included in the analysis.

2.2. Functional Results Used for Analysis

The functional data on ATP7B variant used in this analysis was collected from various laboratories including the Cox laboratory as mentioned in Tables 3.2, 3.4, and 3.5. 20 ATP7B variants that were studied in this thesis were also included in the prediction analysis.

Table 3.1 List of proteins used for the multiple sequence alignment in the selected prediction programs.

ID	Species	common name	Protein	Poly Phen	SIFT-cor[1]	Align GVGD-cor[1]
P_001020438	*Canis lupus familiaris*	dog	ATP7B	yes	yes	Yes
Q64446	*Mus musculus*	mouse	ATP7B	yes	yes	Yes
BAA84775.1	*Rattus norvegicus*	rat	ATP7B	yes	yes	Yes
NP_001009732	*Ovis aries*	sheep	ATP7B	yes	yes	Yes
XP_001378265	*Monodelphis domestica*	opossum	ATP7B	yes	yes	Yes
Q5T7X7	*Homo sapiens*	human	ATP7B	yes	no	No
XP_001103242	*Macaca mulatta*	rhesus monkey	ATP7B	yes	yes	Yes
XP_417073	*Gallus gallus*	red jungle fowl	ATP7B	yes	yes	Yes
A2A4E0	*Mus musculus*	mouse	ATP7B	yes	no	No
XP_001363336	*Monodelphis domestica*	opossum	ATP7A	yes	yes	Yes
NP_434690	*Rattus norvegicus*	rat	ATP7A	yes	yes	Yes
XP_860306	*Canis lupus familiaris*	dog	ATP7A	yes	yes	Yes
XP_615430	*Bos Taurus*	cattle	ATP7A	yes	yes	Yes
EAW98606.1	*Homo sapiens*	human	ATP7A	yes	yes	Yes
XP_420307	*Gallus gallus*	red jungle fowl	ATP7A	yes	yes	Yes
NP_001036185	*Danio rerio*	zebra fish	ATP7A	yes	yes	Yes
P49015	*Cricetulus griseus*	Chinese hamster	ATP7A	yes	yes	Yes
XP_684415	*Danio rerio*	zebra fish	ATP7B	yes	yes	Yes
Q4SJX4	*Tetraodon nigroviridis*	green puffer	ATP7B	yes	No	No
NP_001005918	*Homo sapiens*	human	ATP7B	yes	No	No
NP_001005918	*Homo sapiens*	human	ATP7B	yes	No	No
Q4SDE7	*Tetraodon nigroviridis*	green puffer	[2]	yes	No	No
Q17RT3	*Homo sapiens*	human	ATP7B	yes	No	No

[1] Corrected as described in the text

[2] V-cation-transporting ATPase

3. Results

3.1. Comparing Predictive Programs Using Defective ATP7B Variants

Functionally defective ATP7B variants were analyzed in the three prediction programs as shown in Table 3.2. Each variant was reported to be defective in at least one of the following assays: copper transport (T), localization (L), phosphorylation (P), interaction with Atox1 (I), or aggregation (A). The prediction scores were obtained either via default settings (def) or corrected (cor) settings using selected alignment as described in the Materials and Methods. The prediction for each variant analyzed could be: defective variant (D), normal variant (N), or unclassified (U) if analyses were inconclusive. An additional column was used to show the location of each variant within the protein. Table 3.2 includes 40 ATP7B missense variants that are reported as defective. Twenty nine variants have been analyzed in the Cox laboratory. The remaining 11 ATP7B variants were reported by other authors as indicated in Table 3.2. Table 3.3 summarizes the analysis of the 40 functionally defective ATP7B variants in the selected prediction programs: PolyPhen, SIFT-cor (SIFT corrected), SIFT–def (SIFT default), Align GVGD-cor (Align GVGD corrected), and Align GVGD-def (Align GVGD-default). PolyPhen predicts 35 variants as defective. SIFT-cor and SIFT-def predicts 37 and 35 variants as defective, respectively. Align GVGD corrected and default predicts 26 and 22 variants, respectively as defective. The highest prediction score was obtained through SIFT-cor. However, PolyPhen and SIFT-def generate the same predictions for 38 variants (defective and normal). The two variants that were not in agreement were p.A604P and p.G591D. The only variant that was predicted as normal in the five scores was p.Q447L. The functional data reported on Q447L show

that it is defective in localization as it associated with a frame shift mutation (Huster et al., 2003). This suggests that the frame shift mutation is responsible for such a defective phenotype rather than the missense mutation alone.

3.2. Analysis of Prediction Scores of Functionally Normal ATP7B Variants

Some ATP7B variants were not defective in one functional assay. These variants were not tested in other ATP7B functional assays. ATP7B variants that were characterized as a normal variant in one of the ATP7B functional assays were analyzed in the prediction programs. The functional data were reported by various authors as indicated in Table 3.4. Table 3.4 shows 17 ATP7B missense variants that were analyzed using selected prediction programs. PolyPhen predicted 15 of 17 to be disease causing variants. SIFT-cor and SIFT-def predict 13 and 14 variants of 17 to be disease causing, respectively. Align GVGD-cor identifies 8, 7, and 2 variants as defective, normal, and unclassified, respectively. Align GVGD-def identifies 4, 10, and 3 variants as defective, normal, and unclassified respectively. Three ATP7B missense variants (p.V995A, p.T991M, and p.P1379S) were predicted to be defective by the three different programs in all alignments. Only one variant, p.A1183T, is predicted to be normal in all three programs.

Table 3.2 Comparison of prediction programs using functionally defective ATP7B variants.

Variant	Site[1]	Function[2]					Poly Phen[3]	SIFT[3]		Align-GVGD[3]		Ref[4]
		T	L	P	I	A		cor	def	cor	def	
Present thesis												
p.N41S	N-ter	D					N	N	N	U	D	1
p.A604P	Cu6/ Tm1	D					D	D	N	U	N	1
p.M665I	Tm1	D					D	D	D	N	N	1
p.S657R	Cu6/ Tm1	D					D	D	D	U	U	1
p.G710V	Tm2	D	N				D	N	D	D	N	1,7
p.G711R	Tm2	D					D	D	D	D	U	1
p.S744P	Tm3	D					D	D	D	D	U	1
p.T766M	Tm4	D					D	D	D	N	N	1
p.S921N	Td	D					D	D	D	N	N	1
p.G943C	Tm5	D					D	D	D	U	N	1
p.G1000R	Ph	D					D	D	D	D	D	1
p.G1287S	ATP loop	D					D	D	D	D	D	1
p.G1176E	ATP loop	D					D	D	D	D	D	1
p.G1341V	Tm7	D					D	D	D	D	N	1
p.C1375S	Tm8	D					D	D	D	N	N	1
p.A1328T	Tm7	D					D	D	D	D	D	1
p.G1341S	Tm7	D					D	D	D	D	N	1
p.R1415Q	3'COOH	D					N	D	N	N	D	1
Cox laboratory												
p.D765N	Tm4	N	D				D	D	D	D	N	2,3
p.L776V	Tm4	N	D				D	D	D	D	D	2,3

p.R778L	Tm4	D	D				D	D	D	D	D	2,3
p.M769V	Tm4	D	N				D	D	D	D	N	2,3,6
p.G943S	Tm5	D	N				D	D	D	N	N	2,3
p.T977M	Tm6	D					D	D	D	U	D	2,3
p.P992L	ATP loop	D	N	D			D	D	D	D	D	2,7,11
p.E1064K	ATP loop	D					D	D	D	D	D	4
p.L1083F	ATP loop	D					D	D	D	D	D	4
p.V1106D	ATP loop	D					D	D	D	D	D	4
p.M1169V	ATP loop	D					D	D	D	D	D	4
Other laboratories												
p.G85V	Cu1		N		D		D	D	D	N	N	6
p.Q447L[5]	Cu4/5		D				N	N	N	N	N	7
p.L492S	Cu5		N		D		D	D	D	D	D	6
p.G591D	Cu6		N		D		N	D	D	D	D	6
p.E1064A	ATP loop			D			D	D	D	D	D	8
p.H1069Q	ATP loop	D	D	D		D	D	D	D	D	D	9,10,11,7
p.A1135R	ATP loop		D			D	N	D	N	N	N	7
p.D1267A	ATP hinge			D			D	D	D	D	D	11
p.N1270S	ATP hinge		D			D	D	D	D	D	D	7
p.P1273L	ATP hinge			D			D	D	D	D	D	11
p.S1362F	Tm8		D			D	D	D	D	D	D	7

[1] N-ter: N-terminal tail; Cu1-6: copper binding domains of the N-terminal region (1 through 6); Tm1-8: transmembrane domains (1 through 8); Td: transduction domain; Ph: phosphorylation domain of ATP loop. 3'COOH: C-terminal tail.
[2] Each variant was reported to be defective in at least one of the following assays: copper transport (T); localization (L); phosphorylation (P); or interaction with Atox1 (I).
[3] defective variant (D); normal variant (N); or unclassified (U)

[4]References 1: Chapter two thesis, 2: (Forbes and Cox, 1998), 3: (Forbes and Cox, 2000), 4: Cullen, 6:(Hamza et al., 1999), 7:(Huster et al., 2003) , 8: (Morgan et al., 2004), 9: (Iida et al., 1998), 10:(Payne and Gitlin, 1998), 11:(Okkeri et al., 2002)
[5] This variant was associated with a frame shift mutation.

Table 3.3 Summary of functionally defective ATP7B variants analyzed in the selected prediction programs.

Prediction program	Defective in functional assay	Predicted defective	Predicted normal	Unclassified
PolyPhen	40	35 (87.5%)	5	None
SIFT- cor	40	37 (92.5%)	3	None
SIFT- def	40	35 (87.5%)	5	None
Align GVGD- cor	40	26 (65%)	9	5
Align GVGD- def	40	22 (55%)	15	3

Table 3.4 Prediction scores of ATP7B variants that are indicated as normal variants in functional assays

Variant	Site[1]	Function[2]					Poly Phen[3]	SIFT[3]		Align-GVGD[3]		Reference
		T	L	P	I	A		cor	def	cor	def	
p.Y532H	Cu5	N					D	D	D	D	U	1
p.R616Q	Cu6/Tm1	N					N	D	D	D	N	2
p.R616T	Cu6/Tm1		N				D	D	D	D	U	3
p.G626A	Cu6	N					D	D	D	N	D	1
p.D642H	Cu6/Tm1	N					D	D	D	U	N	1
p.L655I	Tm1	N					D	N	D	N	N	2
p.P760L	Tm3/ Tm4		N				D	D	D	D	U	3
p.M769V	Tm4	N	N				D	D	D	D	N	4,5
p.T991M	Td	N					D	D	D	D	D	2
p.R969N	Td/Cu6		N				D	D	D	N	N	3
p.V995A	ATP loop	N					D	D	D	D	D	5
p.C1104F	ATP loop			N			D	D	D	N	N	7
p.R1151H	ATP loop			N			D	D	D	U	N	7
p.A1183T	ATP loop	N					N	N	N	N	N	1
p.G1186S	ATP loop	N					D	N	N	N	N	1
p.P1379S	C-ter	N					D	D	D	D	D	6
p.T1434M	C-ter	N					D	N	N	N	N	6

References 1: Cullen, 2: TAHA, 3: (Huster et al., 2003), 4:(Forbes and Cox, 2000), 5:(Forbes and Cox, 1998), 6:(Hsi et al., 2004), 7:(Morgan et al., 2004)

[1, 2, 3] See Table 3.3.

3.3. Analysis of Suspected Non Disease Causing Variants in PolyPhen, SIFT, and Align GVGD.

ATP7B missense variants that are reported in the literature as suspected non-disease causing variants were analyzed using the three prediction programs (PolyPhen, SIFT-cor, and Align GVGD-cor). These variants were described by various authors as suspected non-disease causing variants for several reasons, as indicated in Table 3.5. PolyPhen and SIFT predicted 13 and 14 variants, respectively, to be defective out of 29 reported as normal. Align GVGD predicted only 8 out of 29 variants as defective. There are 17 out of 19 variants detected by both PolyPhen and SIFT- cor as disease causing variants. There are seven variants predicted to be defective in each of the three programs (PolyPhen, SIFT-cor, and Align GVGD-cor). These seven variants were indicated as suspected non disease causing variants for various reasons: p.N728D, p.T935M, p.V995A, p.D1271E were considered as substitutions of highly conserved amino acid change; p.R723G was detected in homozygous normal individuals; M1169V was reported as a possible mutation as no other mutations were found on the chromosomes of the patient; p.P1245S was not detected on normal chromosomes. This reason by itself is a good indication that p.P1245S might be a disease causing variant.

The 19 variants presented in Table 3.5 are located in various regions of the protein. Seven variants are in the N-terminal copper binding domains. The prediction scores of the three programs classify the seven variants as normal. There are eight variants in transmembrane domains Tm3, Tm4, and Tm5; five of these were classified as defective variants using the three programs

Table 3.5 Analysis of suspected non disease causing variants in PolyPhen, SIFT and Align GVGD.

Variant	Site[1]	Reason[2]	Poly Phen[3]	SIFT Cor[3]	Align GVGD cor[3]	Reference
p.A14D	N-ter	c	N	N	N	(Gu et al., 2003)
p.I390V	Cu4	b	N	N	N	(Tsai et al., 1998)
p.A406S	Cu4	b	N	N	N	(Thomas et al., 1995)
p.L436V	Cu4/5	u	N	N	N	(Cox et al., 2005)
p.V446L	Cu4/5	u	N	N	N	(Shah et al., 1997b)
p.L466V	Cu4/5	b	N	N	N	(Thomas et al., 1995)
p.N565S	Cu5	b, d	N	N	N	(Kalinsky et al., 1998)
p.R723G	Tm3	g	D	D	D	(Kalinsky et al., 1998)
p.N728D	Tm3	b	D	D	D	(Fan et al., 1997)
p.D730E	Tm3	b	N	N	D	(Chuang et al., 1996)
p.K832R	Tm4/ Td	c, d, e	N	N	N	(Figus et al., 1996)
p.V864I	Td	c, b	N	N	N	(Kim et al., 1998)
p.T935M	Tm5	b	D	D	D	(Tsai et al., 1998)
p.V949G	Tm5	a, b	D	D	N	(Ha-Hao et al., 1998)
p.R952K	Tm5	b	N	N	N	(Thomas et al., 1995)
p.V995A	Ch/ Tm6	b	D	D	D	(Thomas et al., 1995)
p.A1063V	ATP loop	c	D	D	U	(Nanji et al., 1997)
p.V1106I	ATP loop	b, d	N	N	N	(Wu et al., 2001)
p.V1109M	ATP loop	c, b	N	D	N	(Kim et al., 1998)
p.A1140V	ATP loop	a, c, d, e	N	N	N	(Figus et al., 1995)
p.T1143N	ATP loop	c	N	N	N	(Gu et al., 2003)

p.M1169V	ATP loop	f	D	D	D	(Thomas et al., 1995)
p.A1183G	ATP loop	u	D	D	U	(Shah and Kumar, 1997)
p.H1207R	ATP loop	c	D	D	N	(Loudianos et al., 1999b)
p.P1245S	ATP hinge	c	D	D	D	(Gu et al., 2003)
p.D1271E	ATP hinge	b	D	D	D	(Okada et al., 2000)
p.A1278V	ATP hinge	e, d, h	D	D	U	(Orru et al., 1997)
p.V1297I	ATP hinge	d	N	N	N	(Loudianos et al., 1999a)
p.D1407E	C-ter	d	D	D	N	(Kusuda et al., 2000)

[1, 3] See Table 3.2

[2] a: No change of amino acid, b: conservative change, c: detection on normal chromosomes, d: detection on chromosomes with disease causing mutation already present, e: non conservative change in non essential amino acid, f: possible mutation-no other mutation found on chromosomes, g: homozygous on normal individual, h: not found in normal chromosomes, u: unknown

Table 3.6 Summary of the prediction scores of 29 suspected non-disease causing ATP7B variants.

Prediction program	Predicted normal	Predicted defective	Unclassified	Total
PolyPhen	16	13	none	29
SIFT- cor	15	14	none	29
Align GVGD-cor	18	8	3	29

4. Discussion

The Wilson disease database includes 548 variants of which 198 are missense. Only 50 variants have been functionally characterized (Kenney and Cox, 2007). Classifying missense variants as defective or neutral has important diagnostic and research implications. New computer based algorithms aid in the classification of missense variants using conservative and biochemical features of the amino acid substitutions.

In this study, functional data on ATP7B missense variants was used to compare the prediction accuracy of three computational algorithms: PolyPhen, SIFT and Align GVGD. These algorithms use conservation scores and the nature of amino acid substitutions to predict defective ATP7B missense variants as indicated in the Materials and Methods. PolyPhen, SIFT, and Align-GVGD have been previously used to classify other missense variants occurring in the genome. PolyPhen was first developed to assess the damaging effect of SNPs in protein-coding regions. It has been estimated that ~20% of common human non-synonymous SNPs are damaging to the protein (Sunyaev et al., 2001). SIFT score has been used to predict defective variants in several genes including DNA repair genes (Xi et al., 2004) as well as other cancer related genes (Kaminker et al., 2007). Tavitigian et al used Align-GVGD to analyze the functional effects of missense variants in P53 (Mathe et al., 2006) and BRCA1 (Tavtigian et al., 2006) genes. The accuracy of PolyPhen, SIFT, and Align GVGD has been assessed using several human disease genes such as *CDKN2A, MLH1, MSH2, MECP2, and TYR* (Chan et al., 2007). The sensitivity of PolyPhen, SIFT, and Align-GVGD in identifying defective CDKN2A missense variants was 81.3, 83.3, and 72.9% respectively. These data are in

agreement with our findings in Table 3.3. Analysis of ATP7B missense variants showed that SIFT has the higher sensitivity followed likely by PolyPhen. Align GVGD was the least sensitive among the studied algorithms.

Defective phenotype in at least one of the functional assays is expected to provide evidence that the variant tested is disease-causing. A useful conclusion becomes more difficult when a normal functional phenotype is obtained. A functional assay is limited to one aspect of ATP7B function in a model organism: yeast or cultured cells. Full characterization of each variant may require data from several ATP7B functional assays. Although functional assays are reliable, they have limitations. The transport assay using the yeast model is a useful tool to identify transport defective ATP7B variants (Forbes and Cox, 1998). This assay, as well as other ATP7B assays, does not represent the true activity in human liver. For example a variant that has 80% wild type activity might behave normally in the transport assay. However, in a human liver this variant might be associated with WND, especially after an average human life of 60 years. Therefore, validating neutral and defective variants becomes more challenging with genes such as *ATP7B* that are involved in different functions that cannot be assessed in one assay. Some studies have specified a neutral variant as having more than 85% of wild type activity. This might be applicable for certain genes that are well characterized and can be assessed in a single assay. Chan et al used a cell cycle arrest assay to classify *CDKN2A* variants. *CDKN2A* is a tumor suppressor gene that is relatively simple to study in the laboratory. All *CDKN2A* variants that showed a 15% decrease in cell cycle arrest were classified as defective. This classification was further supported by clinical findings (Chan et al., 2007).

There are several parameters to measure the validity of a prediction program. The most common parameters are: sensitivity, specificity, positive predictive value (PPV), and negative predictive value (NPV). Sensitivity is the proportion of variants predicted to be defective in a population of defective variants. Specificity is the proportion of variants predicted to be normal in a population of normal variants. PPV is the proportion of defective variants in a population of variants predicted to be defective. NPV is the proportion of normal variants within a population of variants predicted to be normal (Mathe et al., 2006; Chan et al., 2007). For ATP7B these parameters could be calculated only after full characterization of a significant number of ATP7B missense variants. Defective variants can be easily identified using functional assays. However a gold standard that identifies normal ATP7B variants is still missing. The functional data available on ATP7B variants are very limited. H1069Q is the only variant that has been tested in all reported ATP7B functional assays. Therefore, the accuracy of these programs will be limited until adequate functional and clinical information are available.

The presence of true positive predictions (functionally defective, predicted defective) and false negative predictions (functionally defective, predicted normal) allows us to assess the sensitivity of each of the prediction programs used. SIFT-cor with a sensitivity factor of 92.5% was the most sensitive score in predicting defective ATP7B variants. Align GVGD-def had the least sensitivity of 55%. The prediction sensitivity obtained by SIFT-cor and SIFT-def were 92.5% and 87.5% respectively. Therefore, changing the multiple sequence alignment from default to corrected did not result in a significant change in SIFT analysis. The slight decrease in sensitivity might be contributed to the multiple sequence alignment used for every analysis. Both

alignments included sequences of ATP7B orthologues and paralogues. However, the multiple sequence alignment for default analysis included more sequences for Cu ATPases that are less related to ATP7B making the algorithm more tolerant and thus less sensitive in picking up the defective variants.

Suspected non disease causing ATP7B variants are classified based on reasons suggested by authors, as described in Table 3.5. Sometimes the same variant is predicted in the three programs as normal. Table 3.5 showed 14 variants that are normal in the three scores. Half of these (seven out of 14 variants) are reported by various authors as having a conserved amino acid substitution. Most of these variants are located in the N-terminal region. In contrast, p.N728D, p.T935M, p.V995A, and p.D1271E are predicted by the three programs as defective although they were classified as having a conserved amino acid substitution. None of these four variants is located in the N-terminus. The variants p.N728D, p.T935M, and p.V995A are located in transmembrane domains, whereas p.D1271E is found in the ATP loop. Some amino acid residues are located in critical positions of the protein. Such domains are more sensitive to missense mutations as they depend on strict interactions to maintain the appropriate conformation. Transmembrane domains tend to be more sensitive to missense mutations. For example, a change that weakens the hydrophobicity is more deleterious to a transmembrane domain as compared with a more flexible region such as the N-terminus. Therefore, a slight change in the biochemistry of this position will be identified as a defective variant by the prediction program.

Prediction programs have varied sensitivity for different proteins. Proteins that are more conserved and have a significant amount of structural data associated with

their domains will be analyzed more accurately in the prediction programs. Furthermore, prediction programs might have varied accuracy in the same protein among various domains. A prediction program will analyze a variant that is located in a highly characterized domain with a higher accuracy. Prediction scores, such as PolyPhen, that depend directly on structural data will be more accurate if the variant studied is located in regions that have sufficient structural data. Active motifs are usually more conserved in the multiple sequence alignment and might not tolerate an amino acid substitution although it is chemically very similar.

In this chapter, we have reported significant progress in the classification of normal versus disease-causing variants of ATP7B. The reliability of prediction programs used may be dependent upon the specific protein tested. Our data suggests that PolyPhen and SIFT are useful for predicting ATP7B defective mutations. Align-GVGD is not as useful for ATP7B analysis, particularly for diagnostic applications.

CHAPTER 4

CONCLUSIONS AND FUTURE DIRECTIONS

Wilson disease (WND) is a potentially lethal hereditary disease that affects vital organs including, liver and brain, and is clinically variable. Early diagnosis, followed by appropriate treatment, can effectively avoid tissue damage. In addition to clinical and biochemical features, mutation analysis of the relevant gene, *ATP7B,* provides an accurate tool for diagnosis. ATP7B is involved in various functions that control copper homeostasis in the body. Distinguishing between disease and normal variants is critical for reliable molecular diagnosis of WND. However, functional data on ATP7B variants are still limited.

In order to functionally characterize ATP7B missense variants, I developed a 96-well plate oxidase assay that uses intact yeast cells to determine the oxidase activity of ATP7B variants. The assay presents a quantitative tool that measures the oxidase activity of each ATP7B variant as a percentage of the wild type oxidase activity. This new assay is less laborious and quicker than the previous gel-format assay. The WND mutation database includes 518 variants. This assay will allow us to investigate these variants in a high throughput assay that saves time and reagents. In WND patients there is usually not a high phenotype genotype correlation. Functional assays that identify ATP7B defective variants will aid in understanding phenotype-genotype correlations especially in the case of severe mutations.

Chapter 2 of this thesis reports my characterization of 21 ATP7B missense variants. The information on these variants is summarized as follows:

The variants p.S657R (hinge), p.T766M (Tm4), p.L795F (Td), p.G1000R (Ph), p.G1176E (ATP loop), p.G1341V (Tm7), p.C1375S (Tm8), are single copy variants that show a defective phenotype in both growth and oxidase assays. Each of those variants expresses ATP7B. Therefore, these seven variants are apparently disease-causing and affect the transport mechanism of ATP7B. This highlights the fact that these residues are located in critical regions of ATP7B.

The variants p.R616Q (hinge) and p.T991M (Ph) were recognized as normal variants in growth and oxidase assays. Both variants express ATP7B. Therefore, these variants have no measurable effect on the transport mechanism of ATP7B. The variants p.R616Q and p.T991M might be non-disease causing variants. Further investigation is required to explore the role of these variants on other functions of ATP7B including trafficking.

The variant p.G1287S (ATP loop) is a variant defective in growth and oxidase assays. A western blot shows no ATP7B band. Therefore, p.G1287S is probably a defective variant, where ATP7B might be mislocalized to an inappropriate cellular fraction.

The variants p.M665I (Tm1) and p.G711R (Tm2) were studied as multiple copy variants, and were found to be defective in growth and oxidase assays. The western blot results suggest that these two variants express ATP7B in its correct size. Therefore, p.M665I and p.G711R are predicted to be disease causing variants. Further analysis using single copy variants would provide more accurate evidence on the functional impact of these two missense variants.

The variants p.N41S (N-ter), p.S744P (Tm3), p.S921N (Td), p.G943C (Tm5), p.A1328T (Tm7), p.G1341S (Tm8), and p.R1415Q (C-ter) were defective in both the growth and oxidase assays. The copy number of these variants is not determined yet, however the PCR results suggest that these *ATP7B* variants were inserted into the yeast genome. These variants are likely to be disease-causing variants.

The two missense variants p.R616Q and p.A604P are located in the N-terminal hinge region. In yeast growth assay, p.R616Q was normal, while A604P was defective. Modeling analysis has shown that side chain of p.R616 is superficial and extending to the exterior of the molecule, suggesting a possible role in interaction with other proteins. The variant p.A604P is embedded in the hinge domain and is associated with a beta-sheet. Therefore, a proline mutation causes disruptive effects on the conformation of the hinge and blocks the transport activity of ATP7B. I have shown that modeling analysis is a useful tool to understand the phenotype of ATP7B missense variants.

Prediction scores have been used to identify putative functional missense variants in several other genes. The functional data available on ATP7B missense variants were used to analyze PolyPhen, SIFT and Align GVGD programs. SIFT (92.5%) and PolyPhen (87.5%) are more sensitive than Align-GVGD (55%) in identifying defective ATP7B variants. The specificity of these programs is still questionable. True normal ATP7B variants are required as gold standards in order to assess the specificity of these programs. The WND mutation database includes missense variants that are classified as suspected non-disease causing variants. These variants were reported in the literature based on several reasons as indicated in the results. A further analysis is needed in order to identify the true normal variants. Prediction

analysis on the suspected non-disease variants has scored 14 variants as defective. Therefore, missense variants that are predicted defective using PolyPhen, and SIFT might require further functional assessment.

ATP7B is involved in various functions that are required for copper homeostasis. Therefore, identifying the effects of ATP7B missense variants on WND is challenging and requires extensive functional testing in various model systems. The yeast assay measures only the transport aspect of ATP7B. Therefore, variants that have normal the function in yeast assay should be investigated in other assays that involve other aspects of ATP7B function including trafficking. A cytotoxicity assay using mammalian cells is under development in our laboratory and will be useful to further assess the function of ATP7B variants. The non-disease causing variants that are reported in our prediction analysis as defective could be studied further, if possible, to obtain additional information from relevant authors regarding frequency.

In summary, the yeast assay was used to study 21 missense variants and their effects on the transport mechanism of ATP7B. The functional data available on these variants will be a useful aid for reliable diagnosis of Wilson disease. My prediction analysis shows that PolyPhen and SIFT are the most useful algorithms for predicting ATP7B defective mutations, although further evaluation is needed. Align-GVGD is less useful for ATP7B diagnostic applications. Functional characterization of ATP7B variants presents an important tool to explore significant residues and domains of ATP7B. This will have important implications for understanding ATP7B function and the diagnosis and treatment of Wilson disease.

References

Abkevich, V.A. ZharkikhA.M. DeffenbaughD. FrankY. ChenD. ShattuckM.H. SkolnickA. GutinS.V. Tavtigian. 2004. Analysis of missense variation in human BRCA1 in the context of interspecific sequence variation. *Journal of medical genetics*. 41:492-507.

Achila, D.L. BanciI. BertiniJ. BunceS. Ciofi-BaffoniD.L. Huffman. 2006. Structure of human Wilson protein domains 5 and 6 and their interplay with domain 4 and the copper chaperone HAH1 in copper uptake. *Proceedings of the National Academy of Sciences of the United States of America*. 103:5729-5734.

Anderson, G.J.D.M. Frazer. 2005. Recent advances in intestinal iron transport. *Current gastroenterology reports*. 7:365-372.

Arguello, J.M.E. ErenM. Gonzalez-Guerrero. 2007. The structure and function of heavy metal transport P1B-ATPases. *Biometals*. 20:233-248.

Arnesano, F.L. BanciI. BertiniS. Ciofi-BaffoniE. MolteniD.L. HuffmanT.V. O'Halloran. 2002. Metallochaperones and metal-transporting ATPases: a comparative analysis of sequences and structures. *Genome.Res.2002.Feb;12(2):255-71.* 12:255-271.

Bao, L.Y. Cui. 2005. Prediction of the phenotypic effects of non-synonymous single nucleotide polymorphisms using structural and evolutionary information. *Bioinformatics (Oxford, England)*. 21:2185-2190.

Barna, M.T. MerghoubJ.A. CostoyaD. RuggeroM. BranfordA. BergiaB. SamoriP.P. Pandolfi. 2002. Plzf mediates transcriptional repression of HoxD gene expression through chromatin remodeling. *Developmental cell*. 3:499-510.

Borjigin, J.A.S. PayneJ. DengX. LiM.M. WangB. OvodenkoJ.D. GitlinS.H. Snyder. 1999. A novel pineal night-specific ATPase encoded by the wilson disease gene. *J.Neurosci.* 19:1018-1026.

Bowcock, A.M.L.A. FarrerL.L. Cavalli-SforzaJ.M. HebertK.K. KiddM. FrydmanB. Bonné-Tamir. 1987. Mapping the Wilson disease locus to a cluster of linked polymorphic markers on chromosome 13. *American journal of human genetics*. 41:27-35.

Bowcock, A.M.L.A. FarrerJ.M. HebertM. AggerI. SternliebI.H. ScheinbergC.H.C.M. BuysH. SchefferM. FrydmanT. Chajek-SaulB. Bonné-TamirL.L. Cavalli-Sforza. 1988. Eight closely linked loci place the Wilson disease locus within 13q14-q21. *American journal of human genetics*. 43:664-674.

Brewer, G.J.R.D. DickV.D. JohnsonJ.A. BrunbergK.J. KluinJ.K. Fink. 1998. Treatment of Wilson's disease with zinc: XV long-term follow-up studies. *J.Lab.Clin.Med.* 132:264-278.

Brewer, G.J.P. HederaK.J. KluinM. CarlsonF. AskariR.B. DickJ. SitterlyJ.K. Fink. 2003. Treatment of Wilson disease with ammonium tetrathiomolybdate: III. Initial therapy in a total of 55 neurologically affected patients and follow-up with zinc therapy. *Archives of neurology*. 60:379-385.

Brewer, G.J.V. Yuzbasiyan-Gurkan. 1992. Wilson Disease. *Medicine*. 71:139-164.

Bull, P.C.D.W. Cox. 1994. Wilson disease and Menkes disease: new handles on heavy-metal transport. *Trends Genet.* 10:246-252.

Bull, P.C.G.R. ThomasJ.M. RommensJ.R. ForbesD.W. Cox. 1993. The Wilson disease gene is a putative copper transporting P-type ATPase similar to the Menkes gene. *Nature Genetics*. 5:327-337.

Cater, M.A.J. ForbesS. La FontaineD. CoxJ.F. Mercer. 2004. Intracellular trafficking of the human Wilson protein: the role of the six N-terminal metal-binding sites. *The Biochemical journal*. 380:805-813.

Cater, M.A.S. La FontaineK. ShieldY. DealJ.F. Mercer. 2006. ATP7B mediates vesicular sequestration of copper: insight into biliary copper excretion. *Gastroenterology*. 130:493-506.

Cauza, E.T. Maier-DobersbergerC. PolliK. KasererL. KramerP. Ferenci. 1997. Screening for Wilson's disease in patients with liver diseases by serum. *Journal of hepatology*. 27:358-362.

Chan, P.A.S. DuraisamyP.J. MillerJ.A. NewellC. McBrideJ.P. BondT. RaevaaraS. OllilaM. NystromA.J. GrimmJ. ChristodoulouW.S. OettingM.S. Greenblatt. 2007. Interpreting missense variants: comparing computational methods in human disease genes CDKN2A, MLH1, MSH2, MECP2, and tyrosinase (TYR). *Human mutation*. 28:683-693.

Chasman, D.R.M. Adams. 2001. Predicting the functional consequences of non-synonymous single nucleotide polymorphisms: structure-based assessment of amino acid variation. *Journal of molecular biology*. 307:683-706.

Chelly, J.Z. TumerT. TonnesenA. PettersonY. Ishikawa-BrushN. TommerupN. HornA.P. Monaco. 1993. Isolation of a candidate gene for Menkes disease that encodes a potential heavy metal binding protein. *Nature Genetics*. 3:14-19.

Chuang, L.M.H.P. WuM.H. JangT.R. WangW.C. SueB.J. LinD.W. CoxT.Y. Tai. 1996. High frequency of two mutations in codon 778 in exon 8 of the ATP7B gene in Taiwanese families with Wilson disease. *Journal of medical genetics*. 33:521-523.

Coronado, V.M. NanjiD.W. Cox. 2001. The Jackson toxic milk mouse as a model for copper loading. *Mamm.Genome*. 12:793-775.

Cox, D.W.L. PratJ.M. WalsheJ. HeathcoteD. Gaffney. 2005. Twenty-four novel mutations in Wilson disease patients of predominantly European ancestry. *Human mutation*. 26:280.

Culotta, V.C.L.W. KlompJ. StrainR.L. CasarenoB. KremsJ.D. Gitlin. 1997. The copper chaperone for superoxide dismutase. *Journal of Biological Chemistry*. 272:23469-23472.

Czlonkowska, A.M. RodoJ. GajdaH.K. Ploos van AmstelJ. JuynR.H. Houwen. 1997. Very high frequency of the His1069Gln mutation in Polish Wilson disease patients. *Journal of neurology*. 244:591-592.

de Bie, P.B. van de SluisE. BursteinP.V. van de BergheP. MullerR. BergerJ.D. GitlinC. WijmengaL.W. Klomp. 2007. Distinct Wilson's Disease Mutations in ATP7B Are Associated With Enhanced Binding to COMMD1 and Reduced Stability of ATP7B. *Gastroenterology*. 133:1316-1326.

de Silva, D.S. Davis-KaplanJ. FergestadJ. Kaplan. 1997. Purification and characterization of Fet3 protein, a yeast homologue of ceruloplasmin. *Journal of Biological Chemistry*. 272:14208-14213.

De Silva, D.M.C.C. AskwithD. EideJ. Kaplan. 1995. The FET3 gene product required for high affinity iron transport in yeast is a cell surface ferroxidase. *The Journal of biological chemistry*. 270:1098-1101.

DiDonato, M.S. NarindrasorasakJ.R. ForbesD.W. CoxB. Sarkar. 1997. Expression, purification and metal binding properties of the N-terminal domain from the Wilson Disease putative Cu-transporting ATPase (ATP7B). *Journal of Biological Chemistry*. 272:32279-32282.

DiDonato, M.J. ZhangL.J. QueB. Sarkar. 2002. Zinc binding to the NH2-terminal domain of the Wilson disease copper-transporting ATPase: implications for in vivo metal ion-mediated regulation of ATPase activity. *Journal of Biological Chemistry*. 277:13409-13414.

Dmitriev, O.R. TsivkovskiiF. AbildgaardC.T. MorganJ.L. MarkleyS. Lutsenko. 2006. Solution structure of the N-domain of Wilson disease protein: distinct nucleotide-binding environment and effects of disease mutations. *Proceedings of the National Academy of Sciences of the United States of America*. 103:5302-5307.

Efremov, R.G.Y.A. KosinskyD.E. NoldeR. TsivkovskiiA.S. ArsenievS. Lutsenko. 2004. Molecular modelling of the nucleotide-binding domain of Wilson's disease protein: location of the ATP-binding site, domain dynamics and potential effects of the major disease mutations. *The Biochemical journal*. 382:293-305.

Elble, R. 1992. A simple and efficient procedure for transformation of yeasts. *BioTechniques*. 13:18-20.

Fan, Y.R. YangL. YuM. WuS. ShiM. RenY. HanJ. HuS. Zhao. 1997. Identification of a novel missense mutation in Wilson's disease gene. *Chin.Med.J (Engl)*. 110:887-890.

Fatemi, N.B. Sarkar. 2002. Structural and functional insights of Wilson disease copper-transporting ATPase. *Journal of Bioenergetics and Biomembranes*. 34:339-349.

Ferenci, P. 2004. Review article: diagnosis and current therapy of Wilson's disease. *Alimentary pharmacology & therapeutics*. 19:157-165.

Ferenci, P. 2005. Wilson's Disease. *Clin Gastroenterol Hepatol*. 3:726-733.

Ferenci, P.K. CacaG. LoudianosG. Mieli-VerganiS. TannerI. SternliebM. SchilskyD. CoxF. Berr. 2003. Diagnosis and phenotypic classification of Wilson disease. *Liver.Int*. 23:139-142.

Figus, A.A. AngiusG. LoudianosC. BertiniV. DessiA. LoiA. Deiana. 1996. Molecular pathology and haplotype analysis of Wilson disease in Mediterranean populations. *American journal of human genetics*. 57:1318-1324.

Figus, A.A. AngiusG. LoudianosC. BertiniV. DessiA. LoiM. DeianaM. LovicuN. OllaG. Soleet al. 1995. Molecular pathology and haplotype analysis of Wilson disease in Mediterranean populations. *Am J Hum Genet*. 57:1318-1324.

Forbes, J.R.D.W. Cox. 1998. Functional characterization of missense mutations in ATP7B: Wilson disease mutation or normal variant? *American journal of human genetics*. 63:1663-1674.

Forbes, J.R.D.W. Cox. 2000. Copper-dependent trafficking of Wilson disease mutant ATP7B proteins. *Human molecular genetics*. 9:1927-1935.

Forbes, J.R.G. HsiD.W. Cox. 1999. Role of the copper-binding domain in the copper transport function of ATP7B, the P-type ATPase defective in Wilson disease *Journal of Biological Chemistry*. 274:12408-12413.

Ganesh, L.E. BursteinA. Guha-NiyogiM.K. LouderJ.R. MascolaL.W. KlompC. WijmengaC.S. DuckettG.J. Nabel. 2003. The gene product Murr1 restricts HIV-1 replication in resting CD4+ lymphocytes. *Nature*. 426:853-857.

Garcia-Rio, I.P.F. PenasA. Garcia-DiezW.H. McLeanF.J. Smith. 2005. A severe case of pachyonychia congenita type I due to a novel proline mutation in keratin 6a. *The British journal of dermatology*. 152:800-802.

Gitlin, J.D. 2003. Wilson disease. *Gastroenterology*. 125:1868-1877.

Gollan, J.L.T.J. Gollan. 1998. Wilson disease in 1998: genetic, diagnostic and therapeutic aspects. *Journal of hepatology*. 28 Suppl 1:28-36.

Gow, P.J.R.A. SmallwoodP.W. AngusA.L. SmithA.J. WallR.B. Sewell. 2000. Diagnosis of Wilson's disease: an experience over three decades. *Gut*. 46:415-419.

Grantham, R. 1974. Amino acid difference formula to help explain protein evolution. *Science (New York, N.Y.* 185:862-864.

Greenblatt, M.S.J.G. BeaudetJ.R. GumpK.S. GodinL. TrombleyJ. KohJ.P. Bond. 2003. Detailed computational study of p53 and p16: using evolutionary sequence analysis and disease-associated mutations to predict the functional consequences of allelic variants. *Oncogene*. 22:1150-1163.

Gu, Y.H.H. KodamaS.L. DuQ.J. GuH.J. SunH. Ushijima. 2003. Mutation spectrum and polymorphisms in ATP7B identified on direct sequencing of all exons in Chinese Han and Hui ethnic patients with Wilson's disease. *Clin.Genet.* 64:479-484.

Ha-Hao, D.H. HefterW. StremmelC. Castaneda-GuillotA.H. HernandezD.W. CoxG. Auburger. 1998. His1069Gln and six novel Wilson disease mutations: analysis of relevance for early diagnosis and phenotype *Eur.J.Hum.Genet.* 6:616-623.

Halliwell, B.J.M. Gutteridge. 1984. Oxygen toxicity, oxygen radicals, transition metals and disease. *Biochemical Journal*. 219:1-14.

Halliwell, B.J.M. Gutteridge. 1990. Role of free radicals and catalytic metal ions in human disease: an overview. *Methods Enzymol.* 186:1-85.

Hamza, I.J. ProhaskaJ.D. Gitlin. 2003. Essential role for Atox1 in the copper-mediated intracellular trafficking of the Menkes ATPase. *Proceedings of the National Academy of Sciences, USA*. 100:1215-1220.

Hamza, I:M. SchaeferL.W. KlompJ.D. Gitlin. 1999. Interaction of the copper chaperone HAH1 with the Wilson disease protein is essential for copper homeostasis. *Proceedings of the National Academy of Sciences, USA*. 96:13363-13368.

Healy, J.K. Tipton. 2007. Ceruloplasmin and what it might do. *J Neural Transm.* 114:777-781.

Henikoff, S.J.G. Henikoff. 1992. Amino acid substitution matrices from protein blocks. *Proceedings of the National Academy of Sciences of the United States of America*. 89:10915-10919.

Hsi, G.L.M. CullenD. Moira GlerumD.W. Cox. 2004. Functional assessment of the carboxy-terminus of the Wilson disease copper-transporting ATPase, ATP7B. *Genomics*. 83:473-481.

Huffman, D.L.T.V. O'Halloran. 2001. Function, structure, and mechanism of intracellular copper trafficking proteins. *Annu.Rev.Biochem.2001;70:677-701.* 70:677-701.

Hung, I.H.M. SuzukiY. YamaguchiD.S. YuanR.D. KlausnerJ.D. Gitlin. 1997. Biochemical characterization of the wilson disease protein and functional expression in the yeast Saccharomyces cerevisiae. *Journal of Biological Chemistry.* 272:21461-21466.

Huster, D.M. HoppertS. LutsenkoJ. ZinkeC. LehmannJ. MossnerF. BerrK. Caca. 2003. Defective cellular localization of mutant ATP7B in Wilson's disease patients and hepatoma cell lines. *Gastroenterology.* 124:335-345.

Huster, D.S. Lutsenko. 2003. The distinct roles of the N-terminal copper-binding sites in regulation of catalytic activity of the Wilson's disease protein. *Journal of Biological Chemistry.* 278:32212-32218.

Iida, M.K. TeradaY. SambongiT. WakabayashiN. MiuraK. KoyamaM. FutaiT. Sugiyama. 1998. Analysis of functional domains of Wilson disease protein (ATP7B) in Saccharomyces cerevisiae. *FEBS Letters.* 428:281-285.

Kaiser C, M.S., Mitchell A. 1994. Methods in Yeast Genetics. Vol. Cold Spring Harbor Laboratory, New York.

Kaler, S.G. 1998. Diagnosis and therapy of Menkes syndrome, a genetic form of copper deficiency. *Am.J.Clin.Nutr.* 67:1029S-1034S.

Kalinsky, H.A. FunesA. ZeldinY. Pel-OrM. KorostishevskyR. Gershoni-BaruchL.A. FarrerB. Bonne-Tamir. 1998. Novel ATP7B mutations causing Wilson disease in several Israeli ethnic groups. *Hum.Mutat.* 11:145-151.

Kaminker, J.S.Y. ZhangA. WaughP.M. HavertyB. PetersD. SebisanovicJ. StinsonW.F. ForrestJ.F. BazanS. SeshagiriZ. Zhang. 2007. Distinguishing cancer-associated missense mutations from common polymorphisms. *Cancer research.* 67:465-473.

Karchin, R.M. DiekhansL. KellyD.J. ThomasU. PieperN. EswarD. HausslerA. Sali. 2005. LS-SNP: large-scale annotation of coding non-synonymous SNPs based on multiple information sources. *Bioinformatics (Oxford, England).* 21:2814-2820.

Kenney, S.M.D.W. Cox. 2007. Sequence variation database for the Wilson disease copper transporter, ATP7B. *Hum Mutat.*

Kim, E.K.O.J. YooK.Y. SongH.W. YooS.Y. ChoiS.W. ChoS.H. Hahn. 1998. Identification of three novel mutations and a high frequency of the Arg778Leu mutation in Korean patients with Wilson disease. *Hum.Mutat.* 11:275-278.

Kitzberger, R.C. MadlP. Ferenci. 2005. Wilson disease. *Metabolic brain disease.* 20:295-302.

Knopfel, M.C. SmithM. Solioz. 2005. ATP-driven copper transport across the intestinal brush border membrane. *Biochemical and biophysical research communications.* 330:645-652.

Knopfel, M.M. Solioz. 2002. Characterization of a cytochrome b(558) ferric/cupric reductase from rabbit duodenal brush border membranes. *Biochemical and biophysical research communications.* 291:220-225.

Ko, J.H.W. SonG.Y. BaeJ.H. KangW. OhO.J. Yoo. 2006. A new hepatocytic isoform of PLZF lacking the BTB domain interacts with ATP7B, the Wilson disease

protein, and positively regulates ERK signal transduction. *J Cell Biochem.* 99:719-734.

Kodama, H.Y. Murata. 1999. Molecular genetics and pathophysiology of Menkes disease. *Pediatr Int.* 41:430-435.

Kodama, H.Y. MurataM. Kobayashi. 1999. Clinical manifestations and treatment of Menkes disease and its variants. *Pediatr Int.* 41:423-429.

Kuo, Y.M.A.A. GybinaJ.W. PyatskowitJ. GitschierJ.R. Prohaska. 2006. Copper transport protein (Ctr1) levels in mice are tissue specific and dependent on copper status. *The Journal of nutrition.* 136:21-26.

Kusuda, Y.K. HamaguchiT. MoriR. ShinM. SeikeT. Sakata. 2000. Novel mutations of the ATP7B gene in Japanese patients with Wilson disease. *J.Hum.Genet.* 45:86-91.

Kyte, J.R.F. Doolittle. 1982. A simple method for displaying the hydropathic character of a protein. *Journal of molecular biology.* 157:105-132.

Langner, C.H. Denk. 2004. Wilson disease. *Virchows Arch.* 445:111-118.

Larin, D.C. MekiosK. DasB. RossA.S. YangT.C. Gilliam. 1999. Characterization of the interaction between the Wilson and Menkes disease proteins and the cytoplasmic copper chaperone, HAH1p. *Journal of Biological Chemistry.* 274:28497-28504.

Li, J.Y.M.A. EnglishH.J. BallP.L. YeyatiS. WaxmanJ.D. Licht. 1997. Sequence-specific DNA binding and transcriptional regulation by the promyelocytic leukemia zinc finger protein. *The Journal of biological chemistry.* 272:22447-22455.

Li, X.S. ChenQ. WangD.J. ZackS.H. SnyderJ. Borjigin. 1998. A pineal regulatory element (PIRE) mediates transactivation by the pineal/retina-specific transcription factor CRX. *Proceedings of the National Academy of Sciences, USA.* 95:1876-1881.

Lim, C.M.M.A. CaterJ.F. MercerS. La Fontaine. 2006. Copper-dependent interaction of dynactin subunit p62 with the N terminus of ATP7B but not ATP7A. *The Journal of biological chemistry.* 281:14006-14014.

Liu, X.Q.Y.F. ZhangT.T. LiuK.J. HsiaoJ.M. ZhangX.F. GuK.R. BaoL.H. YuM.X. Wang. 2004. Correlation of ATP7B genotype with phenotype in Chinese patients with Wilson disease. *World J.Gastroenterol.* 10:590-593.

Loudianos, G.V. DessiA. AngiusM. LovicuA. LoiM. DeianaN. AkarP. VajroA. FigusA. CaoM. Pirastu. 1996. Wilson disease mutations associated with uncommon haplotypes in Mediterranean patients. *Hum.Genet.* 98:640-642.

Loudianos, G.V. DessiM. LovicuA. AngiusB. AltuntasR. GiacchinoM. MarazziM. MarcelliniM.R. SartorelliG.C. SturnioloN. KocakA. YuceN. AkarM. PirastuA. Cao. 1999a. Mutation analysis in patients of Mediterranean descent with Wilson disease: identification of 19 novel mutations. *Journal of medical genetics.* 36:833-836.

Loudianos, G.V. DessiM. LovicuA. AngiusA. FigusF. LilliuS. De VirgiliisA.M. NurchiA. DeplanoP. MoiM. PirastuA. Cao. 1999b. Molecular characterization of Wilson disease in the Sardinian population--evidence of a founder effect. *Hum.Mutat.* 14:294-303.

Loudianos, G.V. DessiM. LovicuA. AngiusE. KanavakisM. TzetisC. KattamisN. ManolakiG. VassilikiT. KarpathiosA. CaoM. Pirastu. 1998. Haplotype and

mutation analysis in Greek patients with Wilson disease. *Eur.J.Hum.Genet.* 6:487-491.

Lutsenko, S.N.L. BarnesM.Y. BarteeO.Y. Dmitriev. 2007a. Function and regulation of human copper-transporting ATPases. *Physiological reviews.* 87:1011-1046.

Lutsenko, S.M.J. Cooper. 1998. Localization of the Wilson's disease protein product to mitochondria. *Proceedings of the National Academy of Sciences,USA.* 95:6004-6009.

Lutsenko, S.E.S. LeShaneU. Shinde. 2007b. Biochemical basis of regulation of human copper-transporting ATPases. *Archives of biochemistry and biophysics.* 463:134-148.

Lutsenko, S.K. PetrukhinM.J. CooperC.T. GilliamJ.H. Kaplan. 1997. N-terminal domains of human copper-transporting adenosine triphosphatases (the Wilson's and menkes disease proteins) bind copper selectively in vivo and in vitro with stoichiometry of one copper per metal-binding repeat. *Journal of Biological Chemistry.* 272:18939-18944.

Maier-Dobersberger, T.P. FerenciC. PolliP. BalacH.P. DienesK. KasererC. DatzW. VogelA. Gangl. 1997. Detection of the His1069Gln mutation in Wilson disease by rapid polymerase chain reaction. *Ann.Intern.Med.* 127:21-26.

Mann, J.R.J. CamakarisD.M. Danks. 1979. Copper metabolism in mottled mouse mutants: distribution of 64Cu in brindled (Mobr) mice. *The Biochemical journal.* 180:613-619.

Mathe, E.M. OlivierS. KatoC. IshiokaP. HainautS.V. Tavtigian. 2006. Computational approaches for predicting the biological effect of p53 missense mutations: a comparison of three sequence analysis based methods. *Nucleic acids research.* 34:1317-1325.

Matthews, B.W. 1995. Studies on protein stability with T4 lysozyme. *Advances in protein chemistry.* 46:249-278.

Mercer, J.F.R.M. Llanos. 2003. Molecular and cellular aspects of copper transport in developing mammals. *J Nutr.2003.May;133(5.Suppl.1):1481S-4S.* 133:1481S-1144S.

Mercer, J.F.B.J. LivingstoneB. HallJ.A. PaynterC. BegyS. ChandrasekharappaP. LockhartA. GrimesM. BhaveD. SiemieniakT.W. Glover. 1993. Isolation of a partial candidate gene for Menkes disease by positional cloning. *Nature Genetics.* 3:20-25.

Meyer, L.A.A.P. DurleyJ.R. ProhaskaZ.L. Harris. 2001. Copper transport and metabolism are normal in aceruloplasminemic mice. *The Journal of biological chemistry.* 276:36857-36861.

Monty, J.F.R.M. LlanosJ.F. MercerD.R. Kramer. 2005. Copper exposure induces trafficking of the menkes protein in intestinal epithelium of ATP7A transgenic mice. *The Journal of nutrition.* 135:2762-2766.

Morgan, C.T.R. TsivkovskiiY.A. KosinskyR.G. EfremovS. Lutsenko. 2004. The distinct functional properties of the nucleotide-binding domain of ATP7B, the human copper-transporting ATPase: analysis of the Wilson disease mutations E1064A, H1069Q, R1151H, and C1104F. *Journal of Biological Chemistry.* 279:36363-36371.

Nakken, S.I. AlsethT. Rognes. 2007. Computational prediction of the effects of non-synonymous single nucleotide polymorphisms in human DNA repair genes. *Neuroscience*. 145:1273-1279.

Nanji, M.S.V.T. NguyenJ.H. KawasoeK. InuiF. EndoT. NakajimaT. AnezakiD.W. Cox. 1997. Haplotype and mutation analysis in Japanese patients with Wilson disease. *American journal of human genetics*. 60:1423-1429.

Ng, P.C.S. Henikoff. 2003. SIFT: Predicting amino acid changes that affect protein function. *Nucleic Acids Res.* 31:3812-3384.

Nose, Y.B.E. KimD.J. Thiele. 2006. Ctr1 drives intestinal copper absorption and is essential for growth, iron metabolism, and neonatal cardiac function. *Cell metabolism*. 4:235-244.

Okada, T.Y. ShionoH. HayashiH. SatohT. SawadaA. SuzukiY. TakedaM. YanoK. MichitakaM. OnjiH. Mabuchi. 2000. Mutational analysis of ATP7B and genotype-phenotype correlation in Japanese with Wilson's disease. *Hum.Mutat.* 15:454-462.

Okkeri, J.E. BencomoM. PietilaT. Haltia. 2002. Introducing Wilson disease mutations into the zinc-transporting P-type ATPase of Escherichia coli. The mutation P634L in the 'hinge' motif (GDGXNDXP) perturbs the formation of the E2P state. *Eur.J.Biochem.* 269:1579-1586.

Orru, S.G. ThomasA. LoizeddaD.W. CoxL. Contu. 1997. 24 bp deletion and Ala1278 to Val mutation of the ATP7B gene in a Sardinian family with Wilson disease *Hum.Mutat.* 10:84-85.

Panagiotakaki, E.M. TzetisN. ManolakiG. LoudianosA. PapatheodorouE. ManesisS. Nousia-ArvanitakisV. SyriopoulouE. Kanavakis. 2004. Genotype-phenotype correlations for a wide spectrum of mutations in the Wilson disease gene (ATP7B). *American Journal of Medical Genetics A*. 131A:168-173.

Payne, A.S.J.D. Gitlin. 1998. Functional expression of the Menkes disease protein reveals common biochemical mechanisms among the copper-transporting p-type atpases. *Journal of Biological Chemistry*. 273:3765-3770.

Pena, M.M.J. LeeD.J. Thiele. 1999. A delicate balance: homeostatic control of copper uptake and distribution. *J.Nutr.* 129:1251-1260.

Petris, M.J.J. CamakarisM. GreenoughS. LaFontaineJ.F.B. Mercer. 1998. A C-terminal di-leucine is required for localization of the Menkes protein in the trans-Golgi network. *Human molecular genetics*. 7:2063-2071.

Petris, M.J.J.F. MercerJ.G. CulvenorP. LockhartP.A. GleesonJ. Camakaris. 1996. Ligand-regulated transport of the Menkes copper P-type ATPase efflux pump from the Golgi apparatus to the plasma membrane: a novel mechanism of regulated trafficking. *EMBO J.* 15:6084-6095.

Petrukhin, K.S. LutsenkoI. ChernovB.M. RossJ.H. KaplanT.C. Gilliam. 1994. Characterization of the Wilson disease gene encoding a P-type copper transporting ATPase: genomic organization, alternative splicing, and structure/function predictions. *Human molecular genetics*. 3:1647-1656.

Prohaska, J.R.A.A. Gybina. 2004. Intracellular copper transport in mammals. *The Journal of nutrition*. 134:1003-1006.

Punter, F.A.D.M. Glerum. 2003. Mutagenesis reveals a specific role for Cox17p in copper transport to cytochrome oxidase. *The Journal of biological chemistry.* 278:30875-30880.

Qian, Y.Y. ZhengK.S. RamosE. Tiffany-Castiglioni. 2005. The involvement of copper transporter in lead-induced oxidative stress in astroglia. *Neurochemical research.* 30:429-438.

Ramensky, V.P. BorkS. Sunyaev. 2002. Human non-synonymous SNPs: server and survey. *Nucleic acids research.* 30:3894-3900.

Rensing, C.B. FanR. SharmaB. MitraB.P. Rosen. 2000. CopA: An Escherichia coli Cu(I)-translocating P-type ATPase. *Proceedings of the National Academy of Sciences,USA.* 97:652-656.

Rensing, C.B. MitraB.P. Rosen. 1997. The zntA gene of Escherichia coli encodes a Zn(II)-translocating P-type ATPase. *Proceedings of the National Academy of Sciences of the United States of America.* 94:14326-14331.

Rice, W.J.A. KovalishinD.L. Stokes. 2006. Role of metal-binding domains of the copper pump from Archaeoglobus fulgidus. *Biochemical and biophysical research communications.* 348:124-131.

Riordan, S.M.R. Williams. 2001. The Wilson's disease gene and phenotypic diversity. *Journal of hepatology.* 34:165-171.

Roberts, E.A.D.W. Cox. 1998. Wilson disease. In Bailliere's Clinical Gastroenterology. Hereditary Diseases of the Liver Vol. L. Powell, editor Bailliere Tindall Ltd., London, U.K. 237-256.

Roberts, E.A.D.W. Cox. 2006. Wilson Disease. In Zakim and Boyer's Hepatology. Vol. T. Boyer, M. Manns, and T. Wright, editors. Elsevier, Philadelphia.

Roberts, E.A.M.L. Schilsky. 2003. A practice guideline on Wilson disease. *Hepatology.* 37:1475-1492.

Schaefer, M.R.G. HopkinsM.L. FaillaJ.D. Gitlin. 1999a. Hepatocyte-specific localization and copper-dependent trafficking of the Wilson's disease protein in the liver. *Am.J.Physiol.* 276:G639-G646.

Schaefer, M.H. RoelofsenH. WoltersW.J. HofmannM. MullerF. KuipersW. StremmelR.J. Vonk. 1999b. Localization of the Wilson's disease protein in human liver. *Gastroenterology.* 117:1380-1135.

Scheinberg, I.H.D. Gitlin. 1952. Deficiency of ceruloplasmin in patients with hepatolenticular degeneration (Wilson's disease). *Science (New York, N.Y.* 116:484-485.

Scheinberg, I.H.I. Sternlieb. 1984. Wilson's disease. Vol. WB Saunders Company, Philadelphia.

Schena, M.D. PicardK.R. Yamamoto. 1991. Vectors for constitutive and inducible gene expression in yeast. *Methods in enzymology.* 194:389-398.

Schilsky, M.L. 2002. Diagnosis and treatment of Wilson's disease. *Pediatr.Transplant.* 6:15-19.

Schumacher, G.K.P. PlatzA.R. MuellerR. NeuhausT. SteinmullerW.O. BechsteinM. BeckerW. LuckM. SchuelkeP. Neuhaus. 1997. Liver transplantation: treatment of choice for hepatic and neurological manifestation of Wilson's disease. *Clin.Transplant.* 11:217-224.

Shah, A.B.I. ChernovH.T. ZhangB.M. RossK. DasS. LutsenkoE. ParanoL. PavoneO. EvgrafovI.A. Ivanova-SmolenskayaG. AnnerenK. WestermarkF.H. UrrutiaG.K. PenchaszadehI. SternliebI.H. ScheinbergT.C. GilliamK. Petrukhin. 1997a. Identification and analysis of mutations in the wilson disease gene (atp7b): population frequencies, genotype-phenotype correlation, and functional analyses. *American journal of human genetics*. 61:317-328.

Shah, A.B.I. ChernovH.T. ZhangB.M. RossK. DasS. LutsenkoE. ParanoL. PavoneO. EvgrafovI.A. Ivanova-SmolenskayaG. AnnerenK. WestermarkF.H. UrrutiaG.K. PenchaszadehI. SternliebI.H. ScheinbergT.C. GilliamK. Petrukhin. 1997b. Identification and analysis of mutations in the Wilson disease gene (ATP7B): population frequencies, genotype-phenotype correlation, and functional analyses. *Am.J Hum.Genet.* 61:317-328.

Shah, N.D. Kumar. 1997. Wilson's disease, psychosis, and ECT [letter]. *Convuls.Ther.* 13:278-279.

Sham, R.L.C.Y. OuJ. CappuccioC. BragginsK. DunniganP.D. Phatak. 1997. Correlation between genotype and phenotype in hereditary hemochromatosis: analysis of 61 cases. *Blood.Cells.Mol Dis.* 23:314-320.

Shim, H.Z.L. Harris. 2003. Genetic defects in copper metabolism. *J Nutr.2003.May;133(5.Suppl.1):1527S-31S.* 133:1527S-1131S.

Singh, A.S. SeveranceN. KaurW. WiltsieD.J. Kosman. 2006. Assembly, activation, and trafficking of the Fet3p.Ftr1p high affinity iron permease complex in Saccharomyces cerevisiae. *The Journal of biological chemistry*. 281:13355-13364.

Solioz, M.C. Vulpe. 1996. CPx-type ATPases: a class of P-type ATPases that pump heavy metals. *Trends Biochem.Sci.* 21:237-241.

Stapelbroek, J.M.C.W. BollenJ.K. van AmstelK.J. van ErpecumJ. van HattumL.H. van den BergL.W. KlompR.H. Houwen. 2004. The H1069Q mutation in ATP7B is associated with late and neurologic presentation in Wilson disease: results of a meta-analysis. *Journal of hepatology*. 41:758-763.

Steindl, P.P. FerenciH.P. DienesG. GrimmI. PabingerC. MadlT. Maier-DobersbergerA. HernethB. DragosicsS. MerynP. KnoflachG. GranditschA. Gangl. 1997. Wilson's disease in patients presenting with liver disease: a diagnostic challenge. *Gastroenterology*. 113:212-218.

Steindl, P.P. FerenciH.P. DienesG. GrimmI. PabingerC. MadlT. Maier-DobersbergerA. HernethB. DragosicsS. MerynP. KnoflachG. GranditschA. Gangl. 1998. Wilson's disease in patients with liver disease: A diagnostic challenge. *Gastroenterology*. 113:212-218.

Sunyaev, S.V. RamenskyI. KochW. Lathe, 3rdA.S. KondrashovP. Bork. 2001. Prediction of deleterious human alleles. *Human molecular genetics*. 10:591-597.

Tanzi, R.E.K.E. PetrukhinI. ChernovJ.L. PellequerW. WascoB. RossD.M. RomanoE. ParanoL. PavoneL.M. BrzustowiczM. DevotoJ. PeppercornA.I. BushI. SternliebM. PirastuJ.F. GusellaO. EvgrafovG.K. PenchaszadehB. HonigI.S. EdelmanM.B. SoaresI.H. ScheinbergT.C. Gilliam. 1993. The Wilson disease gene is a copper transporting ATPase with homology to the Menkes disease gene. *Nature Genetics*. 5:344-350.

Tao, T.Y.F. LiuL. KlompC. WijmengaJ.D. Gitlin. 2003. The copper toxicosis gene product Murr1 directly interacts with the Wilson disease protein. *Journal of Biological Chemistry*. 278:41593-41596.

Tapiero, H.D.M. TownsendK.D. Tew. 2003. Trace elements in human physiology and pathology. Copper. *Biomedicine & pharmacotherapy = Biomedecine & pharmacotherapie*. 57:386-398.

Tavtigian, S.V.A.M. DeffenbaughL. YinT. JudkinsT. SchollP.B. SamollowD. de SilvaA. ZharkikhA. Thomas. 2006. Comprehensive statistical study of 452 BRCA1 missense substitutions with classification of eight recurrent substitutions as neutral. *Journal of medical genetics*. 43:295-305.

Theophilos, M.B.D.W. CoxJ.F. Mercer. 1996. The toxic milk mouse is a murine model of Wilson disease. *Human molecular genetics*. 5:1619-1624.

Thomas, G.R.J.R. ForbesE.A. RobertsJ.M. WalsheD.W. Cox. 1995. The Wilson disease gene: spectrum of mutations and their consequences [erratum in Nat Genet 1995 9:451]. *Nature Genetics*. 9:210-217.

Tsai, C.H.F.J. TsaiJ.Y. WuJ.G. ChangC.C. LeeS.P. LinC.F. YangY.J. JongM.C. Lo. 1998. Mutation analysis of Wilson disease in Taiwan and description of six new mutations. *Hum.Mutat.* 12:370-376.

Tsivkovskii, R.J.F. EissesJ.H. KaplanS. Lutsenko. 2002. Functional properties of the copper-transporting ATPase ATP7B (the Wilson's disease protein) expressed in insect cells. *The Journal of biological chemistry*. 277:976-983.

Tsivkovskii, R.B.C. MacArthurS. Lutsenko. 2001. The Lys1010-Lys1325 fragment of the Wilson's disease protein binds nucleotides and interacts with the N-terminal domain of this protein in a copper-dependent manner. *The Journal of biological chemistry*. 276:2234-2242.

Tumer, Z.N. Horn. 1998. Menkes disease: underlying genetic defect and new diagnostic possibilities. *J.Inherit.Metab.Dis.* 21:604-612.

van de Sluis, B.P. MullerK. DuranA. ChenA.J. GrootL.W. KlompP.P. LiuC. Wijmenga. 2007. Increased activity of hypoxia-inducible factor 1 is associated with early embryonic lethality in Commd1 null mice. *Molecular and cellular biology*. 27:4142-4156.

van Dongen, E.M.L.W. KlompM. Merkx. 2004. Copper-dependent protein-protein interactions studied by yeast two-hybrid analysis. *Biochemical and biophysical research communications*. 323:789-795.

Voet D, V.J. 1995. Biochemistry. Vol. John Wiley and Sons Inc, New York.

Voskoboinik, I.J. MarD. StrausakJ. Camakaris. 2001. The regulation of catalytic activity of the menkes copper-translocating P-type ATPase. Role of high affinity copper-binding sites. *The Journal of biological chemistry*. 276:28620-28627.

Vulpe, C.B. LevinsonS. WhitneyS. PackmanJ. Gitschier. 1993a. Isolation of a candidate gene for Menkes disease and evidence that it encodes a copper-transporting ATPase [erratum in Nat Genet 1993;3:273]. *Nature Genetics*. 3:7-13.

Vulpe, C.B. LevinsonS. WhitneyS. PackmanJ. Gitschier. 1993b. Isolation of a candidate gene for Menkes disease and evidence that it encodes a copper-transporting ATPase [published erratum appears in Nat Genet 1993 Mar;3(3):273] [see comments]. *Nature Genetics*. 3:7-13.

Walshe, J.M. 1956. Penicillamine. A new oral therapy for Wilson's disease. *American Journal of Medicine*. 21:487-495.

Walshe, J.M. 1982. Treatment of Wilson's disease with trientine (triethylenetetramine) dihydrochloride. *Lancet*. 1:643-647.

Wang, Z.J. Moult. 2001. SNPs, protein structure, and disease. *Human mutation*. 17:263-270.

Wernimont, A.K.L.A. YatsunykA.C. Rosenzweig. 2004. Binding of copper(I) by the Wilson disease protein and its copper chaperone. *The Journal of biological chemistry*. 279:12269-12276.

Wilson, S.A.K. 1912. Progressive lenticular degeneration: a familial nervous disease associated with cirrhosis of the liver. *Brain*. 34:295-509.

Wu, Z.Y.N. WangM.T. LinL. FangS.X. MurongL. Yu. 2001. Mutation analysis and the correlation between genotype and phenotype of Arg778Leu mutation in chinese patients with Wilson disease. *Archives of neurology*. 58:971-976.

Xi, T.I.M. JonesH.W. Mohrenweiser. 2004. Many amino acid substitution variants identified in DNA repair genes during human population screenings are predicted to impact protein function. *Genomics*. 83:970-979.

Yang, X.L.N. MiuraY. KawaradaK. TeradaK. PetrukhinT. GilliamT. Sugiyama. 1997. Two forms of Wilson disease protein produced by alternative splicing are localized in distinct cellular compartments. *The Biochemical journal*. 326 (Pt 3):897-902.

Yeyati, P.L.R. ShaknovichS. BoterashviliJ. LiH.J. BallS. WaxmanK. Nason-BurchenalE. DmitrovskyA. ZelentJ.D. Licht. 1999. Leukemia translocation protein PLZF inhibits cell growth and expression of cyclin A. *Oncogene*. 18:925-934.

Yuan, D.S.R. StearmanA. DancisT. DunnT. BeelerR.D. Klausner. 1995. The Menkes/Wilson disease gene homologue in yeast provides copper to a ceruloplasmin-like oxidase required for iron uptake. *Proceedings of the National Academy of Sciences,USA*. 92:2632-2636.

Yuce, A.N. KocakH. OzenF. Gurakan. 1999. Wilson's disease patients with normal ceruloplasmin levels. *Turk.J.Pediatr*. 41:99-102.

Yuzbasiyan-Gurkan, V.G.J. BrewerE. BoerwinkleP.J. Venta. 1988. Linkage of the Wilson disease gene to chromosome 13 in North-American pedigrees. *American journal of human genetics*. 42:825-829.

Zubenko, G.S.A.P. MitchellE.W. Jones. 1980. Mapping of the proteinase b structural gene PRB1, in Saccharomyces cerevisiae and identification of nonsense alleles within the locus. *Genetics*. 96:137-146.